A Vibration Study of the Commissary Building at TAMU

Using the Variance Method and the CX1 Accelerometer

John Nichols BE Honours Class I, PhD,
Member Institution of Engineers (Australia),
Chartered Professional Engineer (Australia)

Texas A&M University, College Station Texas

Monday, 2 December 2013

Table of Contents

Table of Figures

List of Tables

Chapter 1. Introduction

IT Infrastructure & Operations, part of the Computing & Information Services at Texas A&M University, requested a vibration study of the Dollar Food Services Commissary[1]. This report has the following sections, Chapter 2, Literature Review, Chapter 3, Methods, Chapter 4, Results, and Chapter 5, Conclusions. Chapter 2 provides a limited summary of the techniques used for the vibration study. Chapter 3 outlines the methods of data collection and analysis. Chapter 4 summarizes the key results for the analysis of the train loading on the slab in *The Building.* Chapter 5 provides a summary of the key findings of the study.

The principal finding of the study is that the adjacent Houston and Texas Central (H&TC) Railroad line induces vibrations in the concrete slab in The Building that can be detected by the SENSR CX1 Accelerometers used for the study. An analysis of the recorded data using Fast Fourier Transforms and the Variance Method provides some indication of the critical frequencies of the vibration. The existing Server room in Computer Services Building was monitored to provide a baseline vibration level for an existing server group.

[1] Dollar Food Services Commissary is tagged at *The Building* in the remainder of the report.

Chapter 2. Literature Review

Vibration has long been recognized to have an impact on the ability of structures to resist load. The Roman Legions traditional broke step so as not to induce excessive vibration in the masonry and timber bridges of the time (Heyman, 1995). The current issue is the impact of vibration on a bank of computer servers used by the Texas A&M University that may be relocated to *The Building.*

Figure 1 shows the location of the building and the adjacent railway lines.

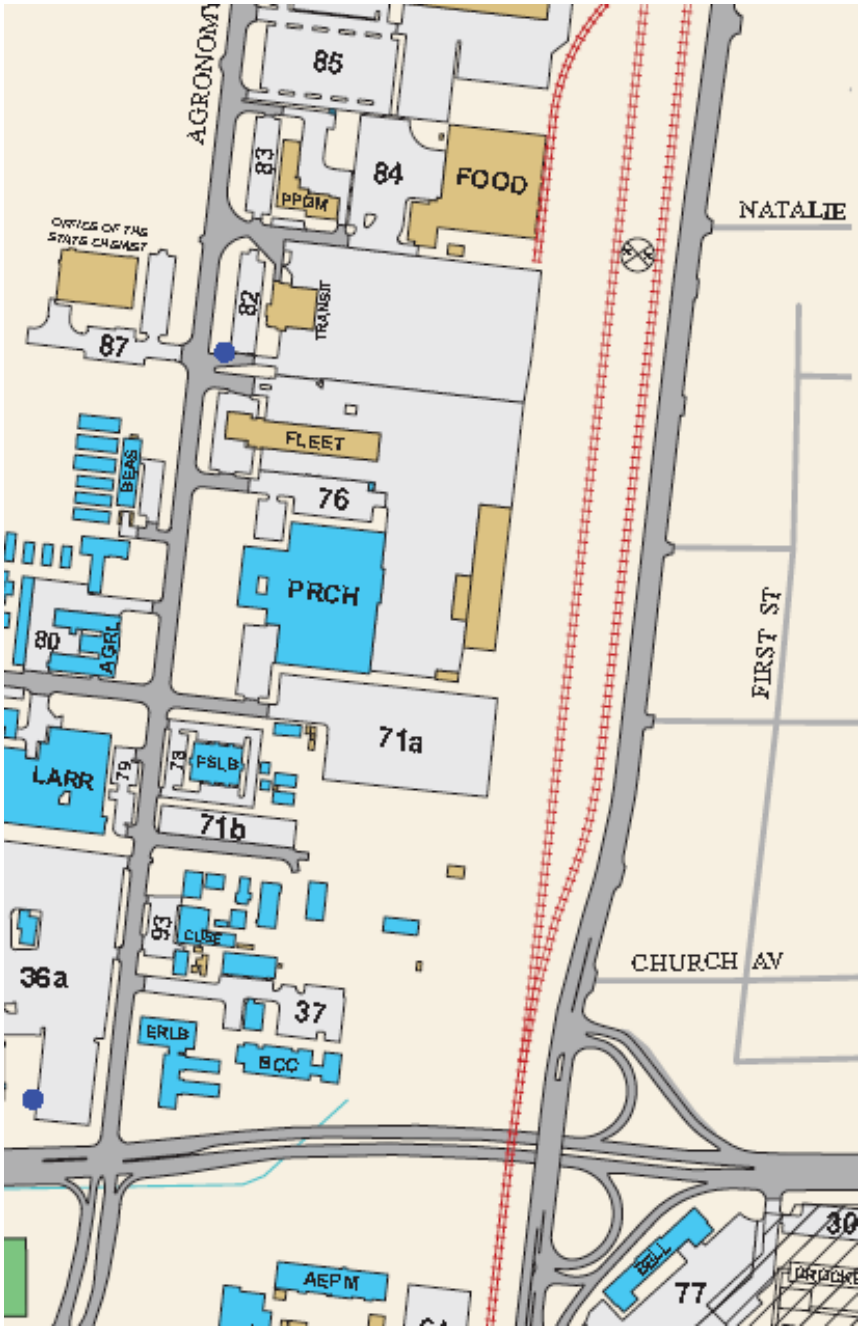

Figure 1 Location of the Dollar Food Services Commissary

The Building is tagged as the Food Building in Figure 1 and is adjacent to the parking lot 84. Figure 1 shows the two adjacent railway lines and the sideline to service *The Building*. This sideline is no longer used, but the mainline was observed to have one to three trains per hour during the study periods.

Figure 2 shows a Google Earth map of the location of the building and the railway lines.

Figure 2 The Building and the adjacent Railway Lines

Figure 2 has two red lines used to measure the length from the railway track to the edge of the building. Line 1[2] is 56 metres and Line 2[3] is 86.9 metres. The building is approximately 68.1 metres in length for the length normal to the railway lines. Figure 3 shows a cross section of the country side located between The Building and the adjacent railway tracks.

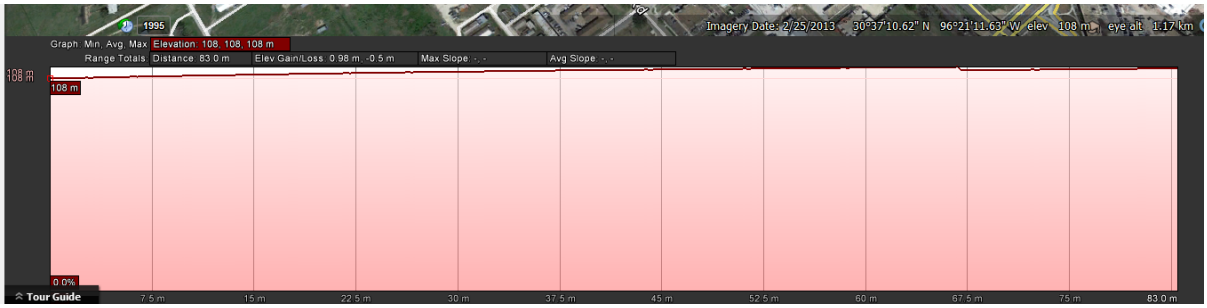

Figure 3 Cross Section of the Route from the Railway Track to the Building

Figure 3 clearly demonstrates the topographical reasons for the location of the food store adjacent to the railway tracks for the development of a spur line. The railway track is about 1 metre lower than the building. Figure 3 shows the railway track at Chainage[4] Zero (Kavanagh, 2004) on the figure.

[2] Shorter red line.
[3] Longer red line.
[4] Chainage is an accepted term for a running length along a centreline.

Figure 4 shows the location of the northern most place, where the record of the time of passage of the trains and the numbers of cars was made by the team.

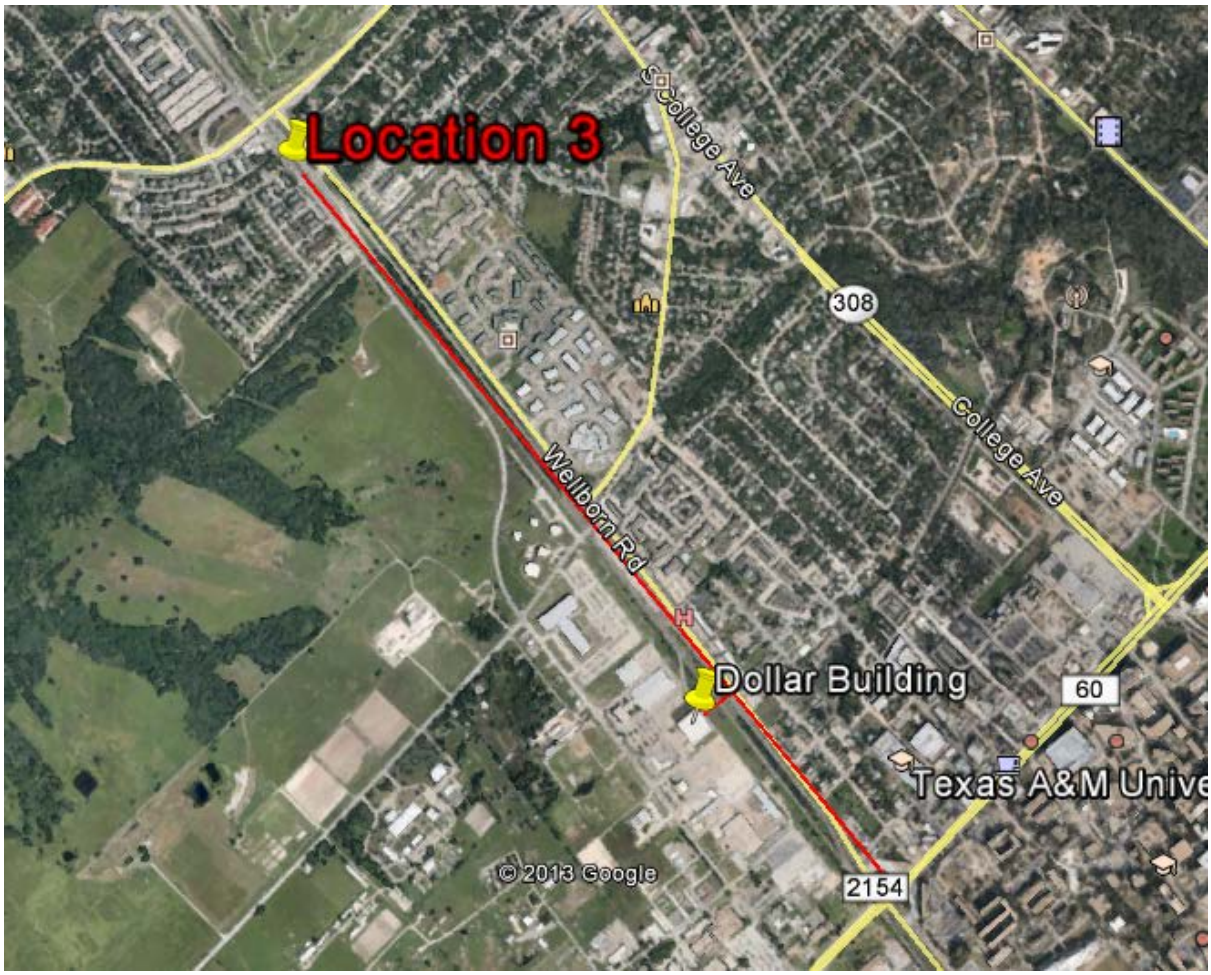

Figure 4 Train Recording Location Three

Location 3 is about 100 metres south of East Villa Maria Avenue in Bryan.

Figure 5 shows the location of the second recording station.

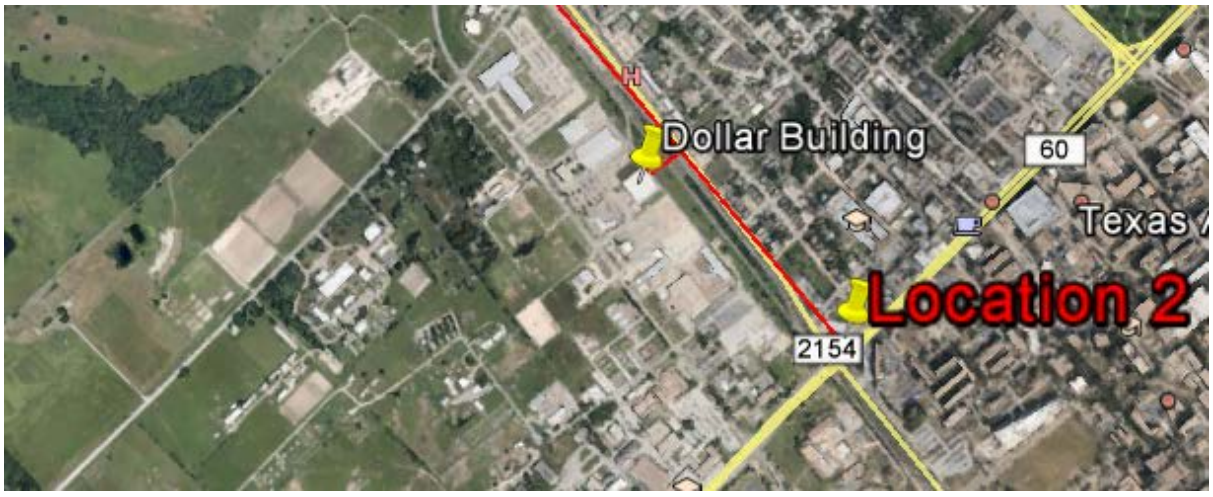

Figure 5 Train Recording Location Two

This station is in the Chimny's Parking Lot as it provides direct visual access to the bridge location over University Drive, College Station.

Figure 6 shows a longitudinal section from Location 3 to Location2. It is derived from Google Earth data and does not represent the centreline of the railway line, but it does show the general topography of the land. The distance from L2 to L3 is 2.43 kilometres.

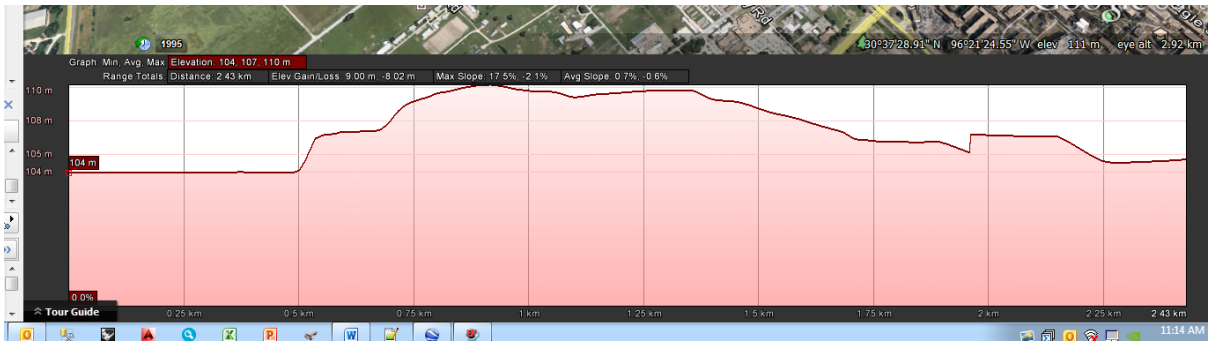

Figure 6 Longitudinal Section for Location 2 to Location 3

The building is located at approximately Chainage 1811 metres from L3.

Figure 7 shows the location of the train recording station L1. This station is in the McDonalds at the corner of Wellborn Drive and George Bush Drive. The distance from L 1 to L2 is 1574 metres.

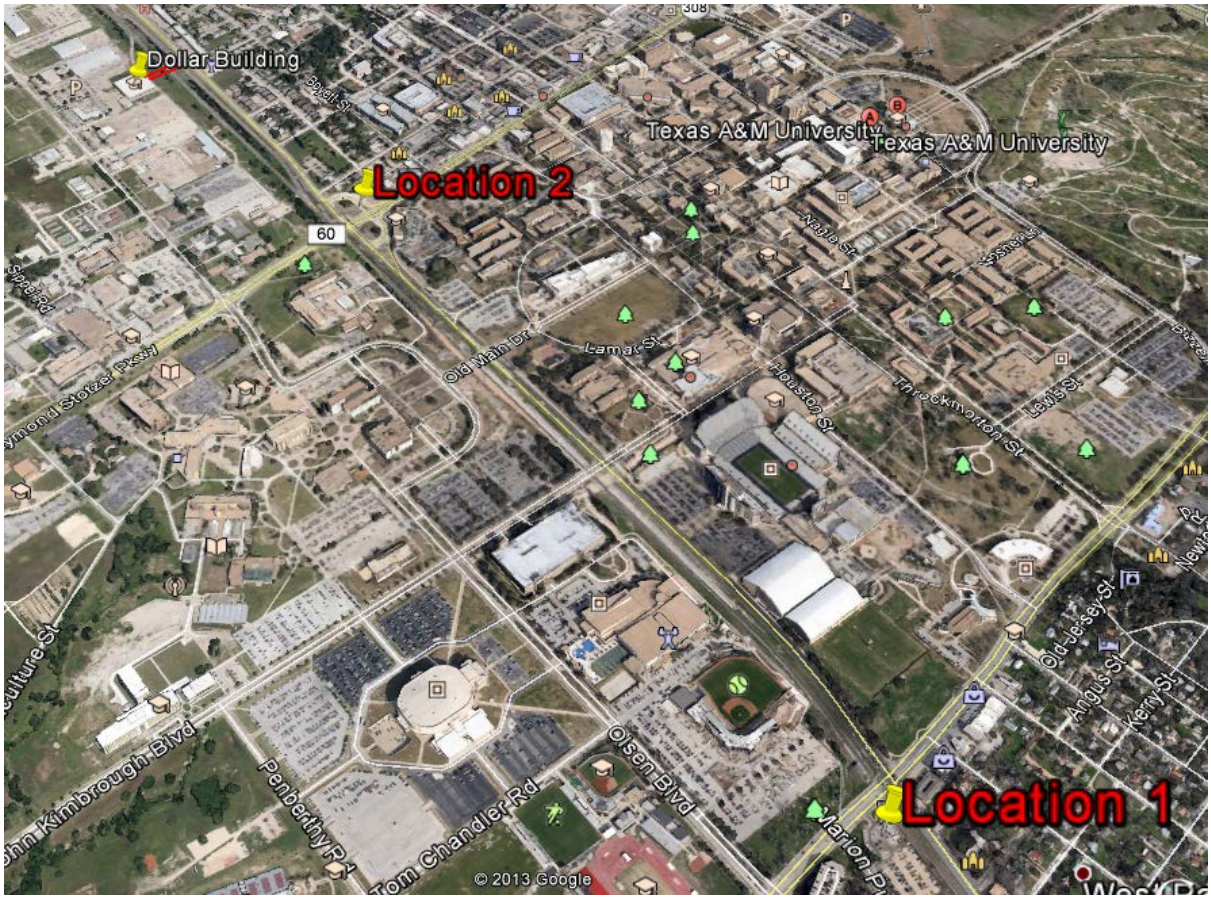

Figure 7 Train Recording Location One

Figure 8 shows a longitudinal section from Location 2 to Location1. It is derived from Google Earth data and does not represent the centreline of the railway line, but it does show the general topography of the land. Location 2 is at Chainage Zero.

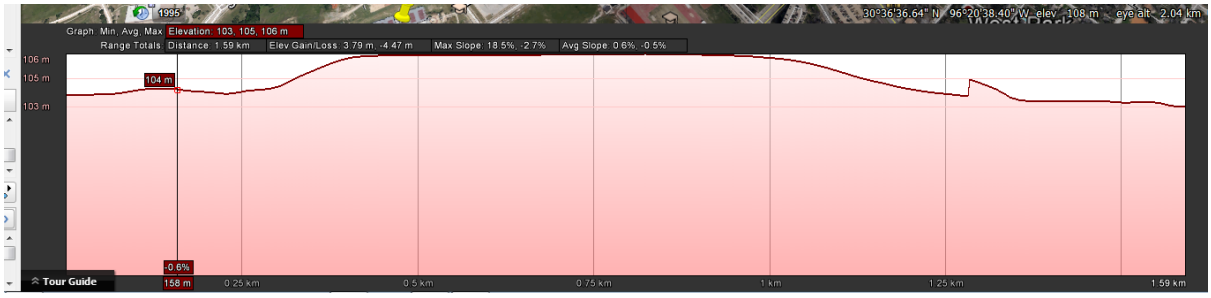

Figure 8 Longitudinal Section for Location 2 to Location 1

Figure 9 shows the travel time in seconds from Location 1 to Location 3 for different travel velocities from 10 to 100 kilometres per hour.

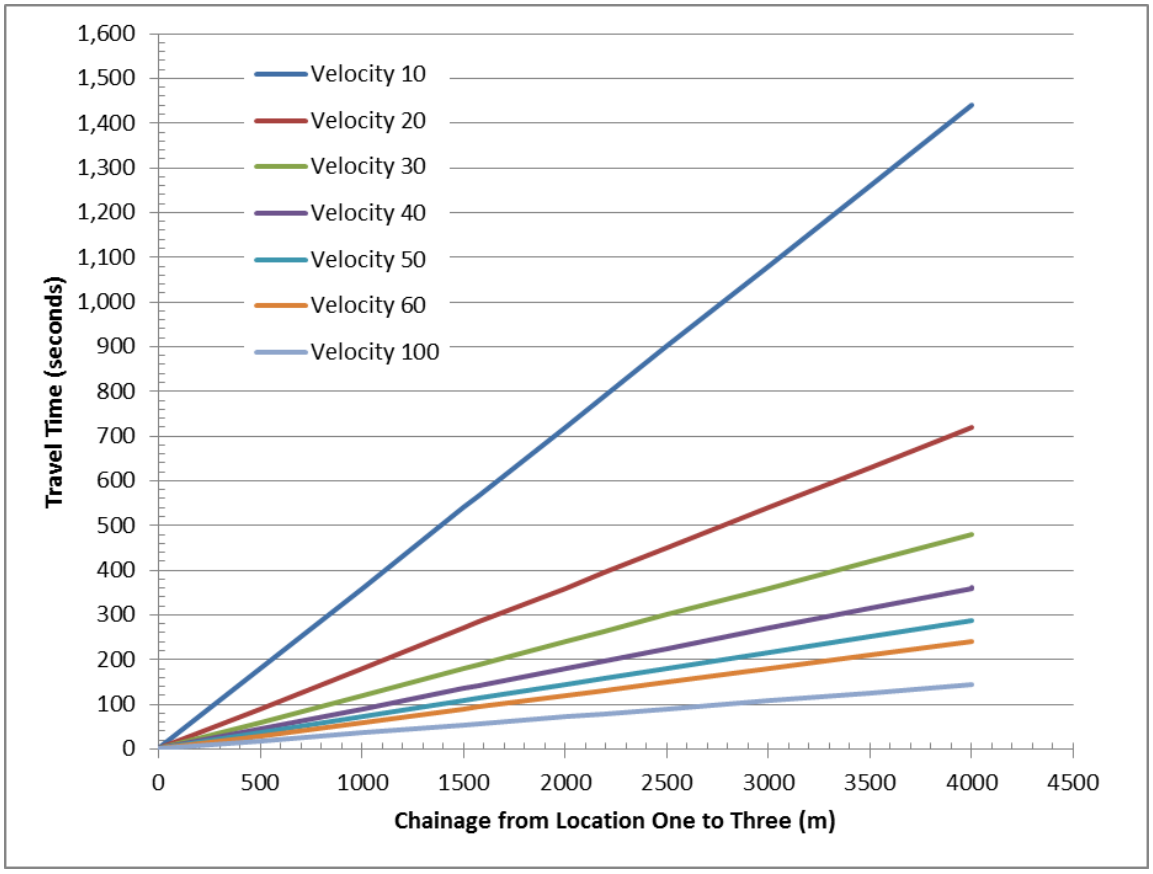

Figure 9 Travel Time from Chainage 0 to 4004 for Different Train Velocities (10 to 100 km/hr)

Table 1 shows the travel times in seconds from the location 1 to location 2 for a speed of 10 kilometres per hour, which is at the low end of the velocity range for the trains passing this building. Train speeds through this built up area are probably constrained by safety concerns for the students at TAMU.

Table 1 Travel Time in Seconds for Different Chainages at ten km/hr

Location	Chainage	Time (seconds)
L 1 McDonalds	0	0.0
	500	180.0
	1000	360.0
	1500	540.0
L2 University Drive	1574	566.6
	2000	720.0
Commissary Building	2193	789.5
	2500	900.0
	3000	1,080.0
	3500	1,260.0
	4000	1,440.0
L3 E. Villa Marie Drive	4004	1,441.4

Travel times for each train was recorded at each of the locations during the survey time.

As simple study of the existing server set in the Computer Services Building[5] was made to determine the ambient vibration levels for an existing installation. Figure 10 shows the location of the recording site for the study of existing server site vibration levels. The location was on the second floor adjacent to the southern wall.

Figure 10 Location 4 - Computer Services Building

Nichols (2003) studied the non-conservative criteria for seismic design spectrum in intraplate regions of the world. Intraplate refers to the seismically more stable region of the world that

[5] TAMU Building number 0516

includes College Station, Texas (Richter, 1958). The concern is the large intraplate earthquake that devastates state sized regions.

Two major intraplate earthquakes triggered this interest, the 1989 Newcastle earthquake (R. E. Melchers, (Editor), 1990; R. E. Melchers & Page, 1992)and the 1985 Nahanni earthquake(D. M. Boore & Atkinson, 1989). The Nahanni earthquake, refer to Figure 11, caused no building damage, but it does point to the very real issue of intraplate events (Cassidy, Rogers, Lamontagne, Halchuk, & Adams, 2010). These types of earthquake whilst rare devastate a large regional area and can be felt over many hundreds of kilometres.

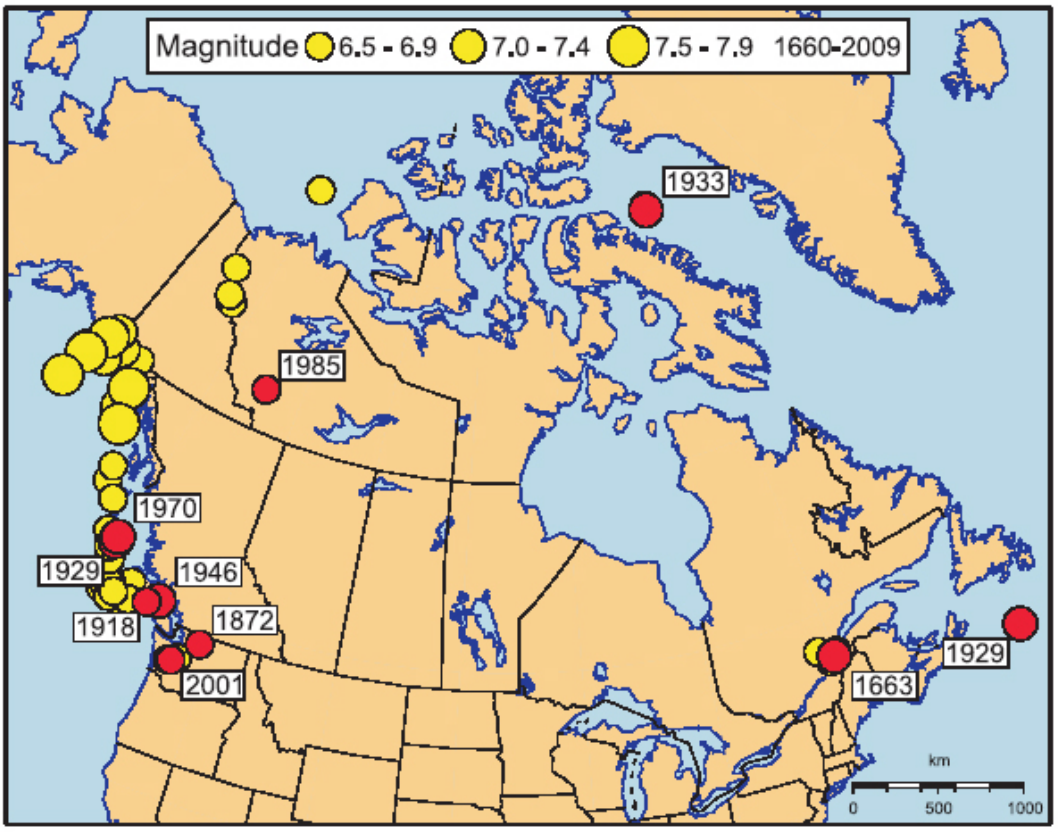

Figure 6. Location of all 'bad' (M 6.5–7.9) earthquakes in Canada (1660–2009). Those highlighted in red are discussed in the text.

Figure 11 Canadian Earthquakes of Concern from 1660 to 2009

Figure 12 shows the time trace for one of the orthonormal axes in the recording taken for the 1985 Nahanni earthquake in the North Western Territories.

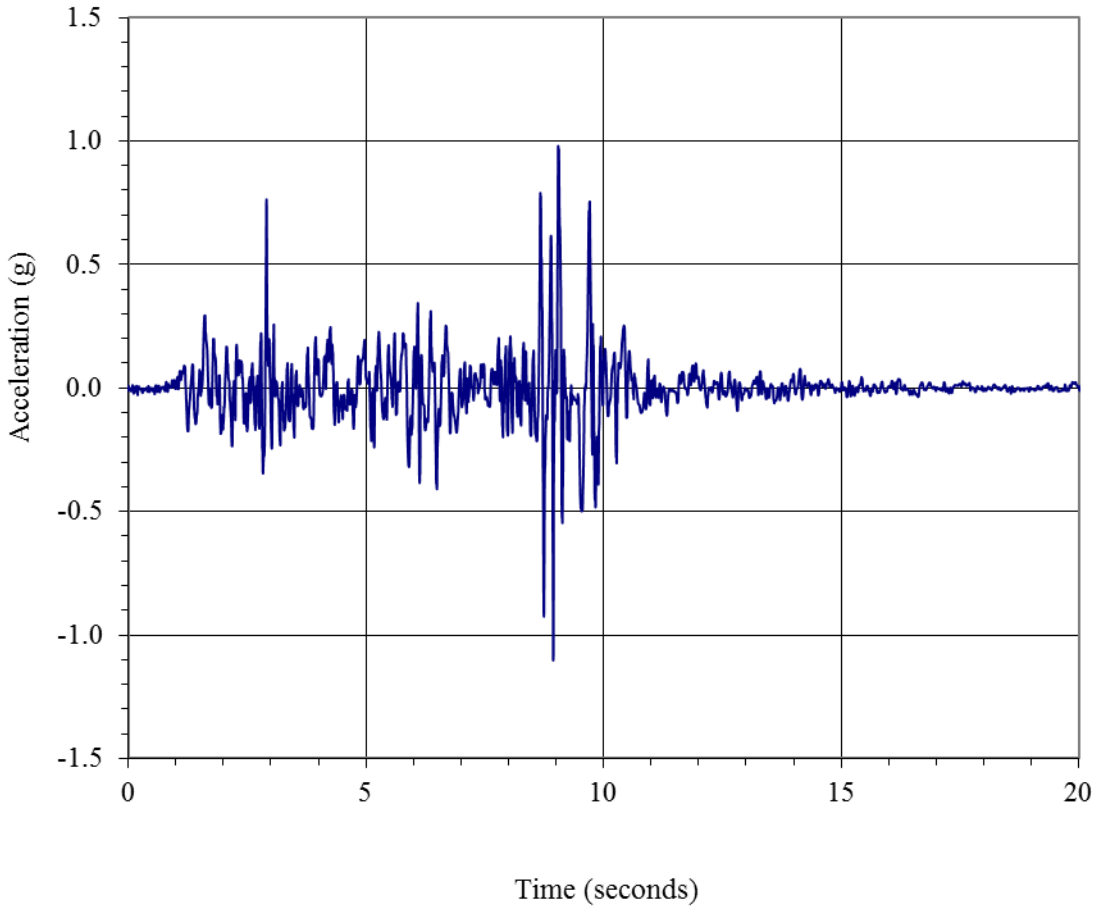

Figure 12 1985 Nahanni Earthquake Acceleration Trace

Whilst the trace is instructive, it does little to provide guidance as to the frequency relationship for the earthquake trace. This is instructive when it is matched with building data and the modal frequencies.

The same trace is transformed using the procedure from Numerical Recipes in Fortran[6] in a program named CONVERT. The discrete Fourier transform programs were validated using the exponential function routine and the square wave routine from Brigham (1988). The results are truncated at the midpoint of the frequencies to avoid confusion with the negative frequencies. In terms of the discontinuity in the data, the midpoints between the upper and lower estimate of the function value were used in the analysis in accordance with normal practice.

Figure 13 shows the Fast Fourier transform for the acceleration trace shown in Figure 12. Figure 14 shows the change in the phase angle for the Fast Fourier transform for the Nahanni earthquake. There are a number of important points to note from these figures.

[6] Press *et al.,* (1994), *Numerical Recipes in Fortran* (Cambridge: Cambridge UP.), DFOUR Routine.

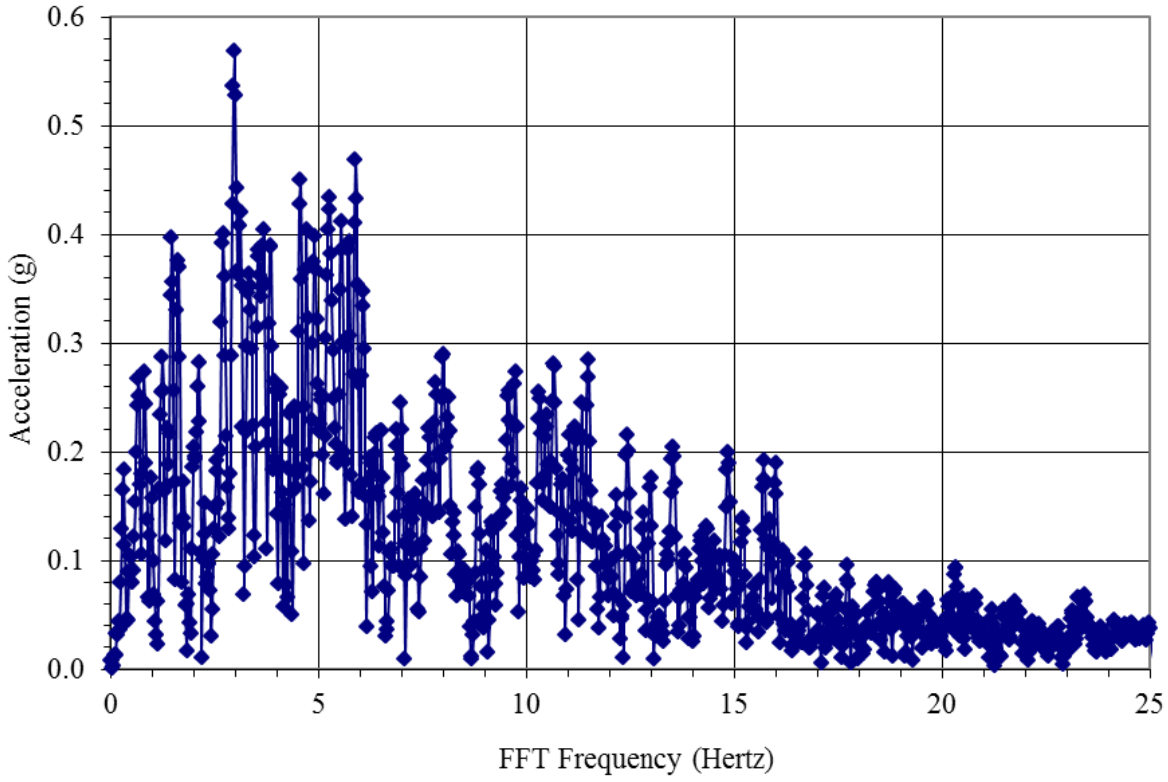

Figure 13 Fast Fourier Transform for the Nahanni Earthquake Trace

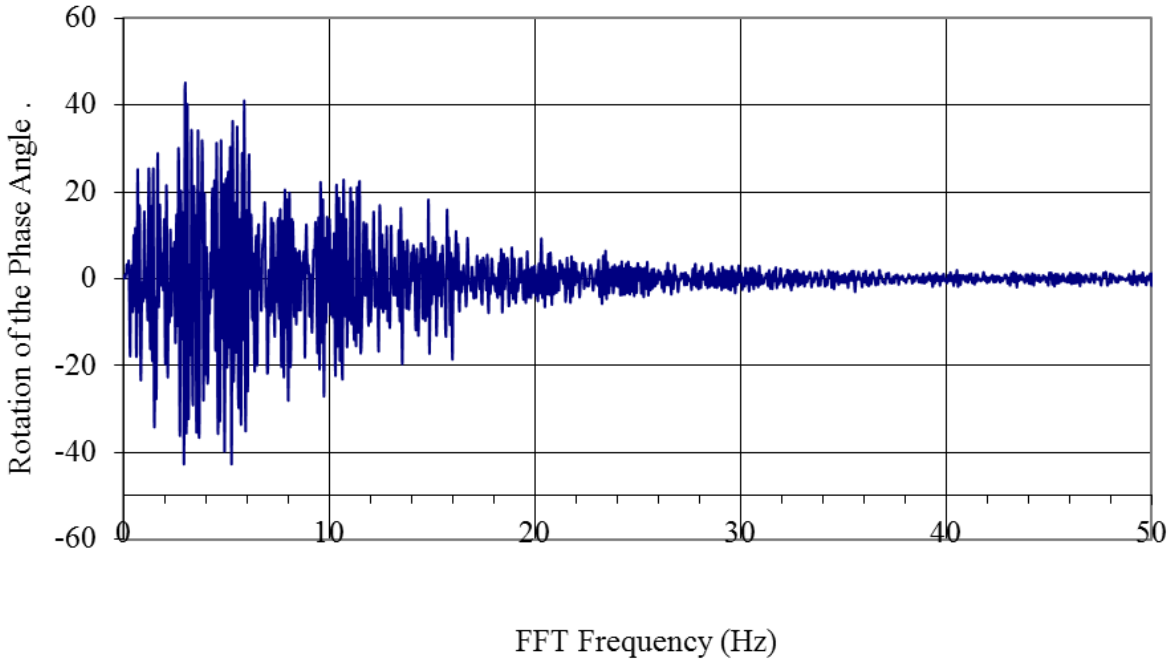

Figure 14 Fast Fourier Transform - Rate of Rotation of the Phase Angle for the Nahanni Earthquake Trace

The points of interest in the figures are

1. In an earthquake load the lower frequencies tend to have higher energy than the higher frequencies
2. As the energy in the spectra increases the energy tends to drift to the lower frequencies at a faster rate than the higher frequencies
3. The rate of rotation of the phase angle is not random as assumed by most theories (Atkinson & Boore, 1995; D. Boore, 1997; David M. Boore, 2005; D. M. Boore & Atkinson, 1989; David M. Boore, Azari Sisi, & Akkar, 2012; Brune, 1970)
4. It is very difficult to compare the responses of different events in the time space and the frequency space provides a good method for comparing earthquakes

Figure 15 shows an alternative method of reviewing the FFT data. The tripart chart makes use of the simple relationships between acceleration, velocity and displacement inherent in Newtons' equations (Halliday & Resnick, 1970). A tripart chart could be prepared for the vibration in *The Building*, but it is beyond the scope of this study.

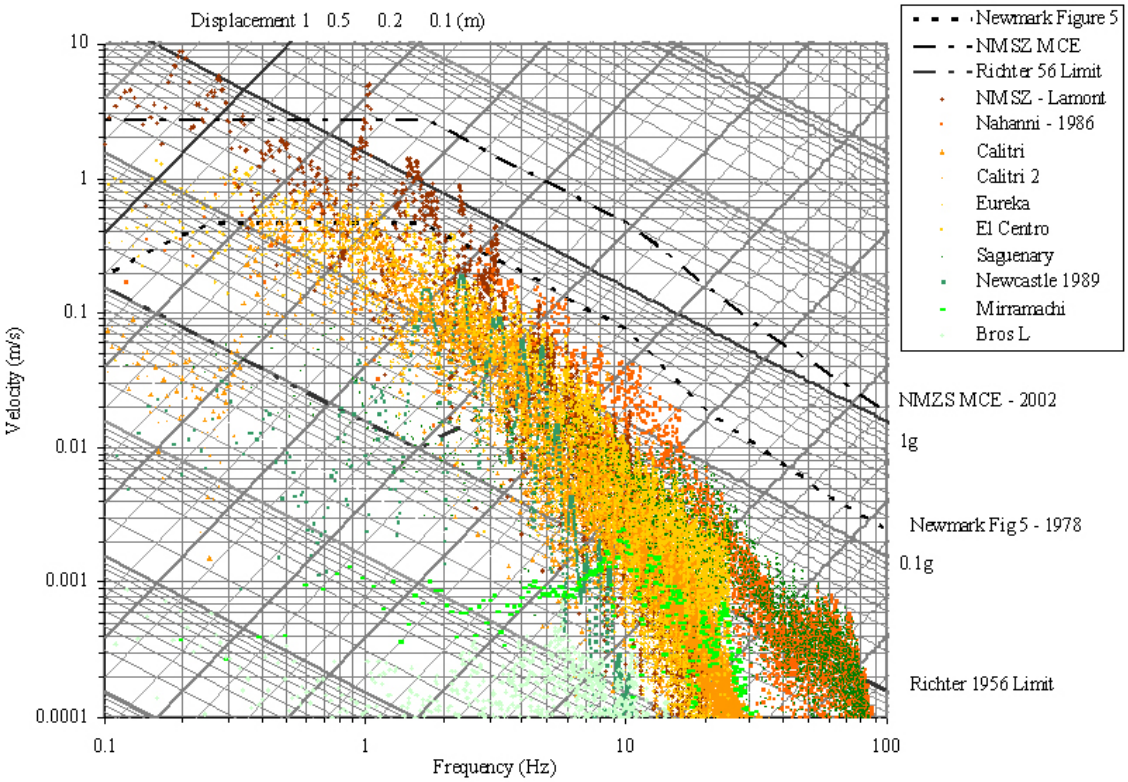

Figure 15 Tri-part Chart of Major Events

The critical point is one of frequency matching. If a frequency from a vibration matches or is close to a natural frequency of a building or a component of the building, then the level damping of the building or component of the building will act as the limit to the development of resonance. Figure 16 shows a classical presentation of the problems inherent in resonance or low levels of damping. Damping is usually expressed as a percentage of the critical damping level. Figure 16

clearly shows the issue of building acceleration, velocity and displacement increasing with a forcing function that is close to the natural frequency of a structure. This is the mathematical representation of resonance. Resonance causes the failure of engineered structures.

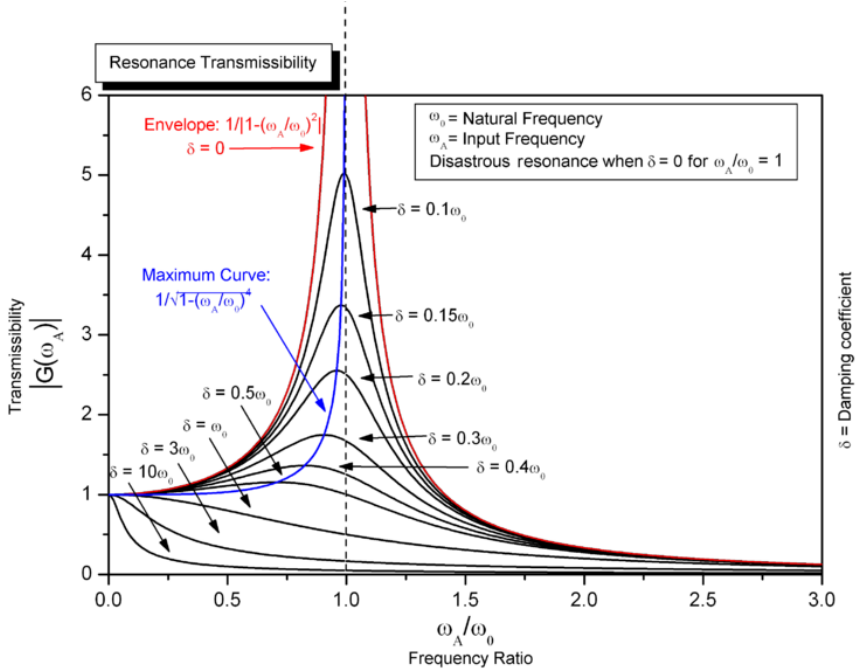

Figure 16 Resonance (From Wikipedia: Resonance, 2009)

Buildings and components tend to resonate at frequencies with a limited range of values. Figure 17 shows a plot of the two standard equations used to estimate the natural frequency of buildings.

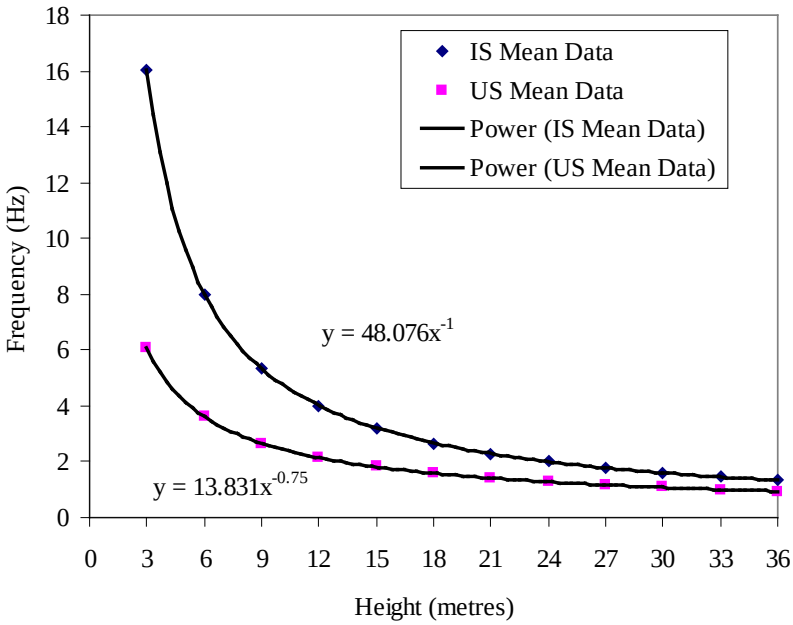

Figure 17 Natural Vibration Frequency Equations

The two equations represent the Indian standard equation(IS 1983, 1984) and the United States standard equation (Hall, 2001). Professor Hall from the University of Illinois at Urbana Champaign noted, in a conversation with the author, that the two equations were originally developed for building data. The US Earthquake Standards Community selected one equation and the Indian Earthquakes Standards Community selected the other equation for the code development. As Hall opined the range is probably about right.

The height of *The Building* is approximately six metres, which suggests a frequency range of 4 to 10 Hz. A train vibration is akin to a small earthquake, although the earthquake duration is usually but not always shorter. A small earthquake has been obtained from the USGS database for a comparison analysis to the reading taken for this study.

This earthquake is the BROS earthquake taken from Tennessee and recorded on the New Madrid Seismic Array[7]. The absolute amplitudes of one of the acceleration components are shown in Figure 18 for this earthquake.

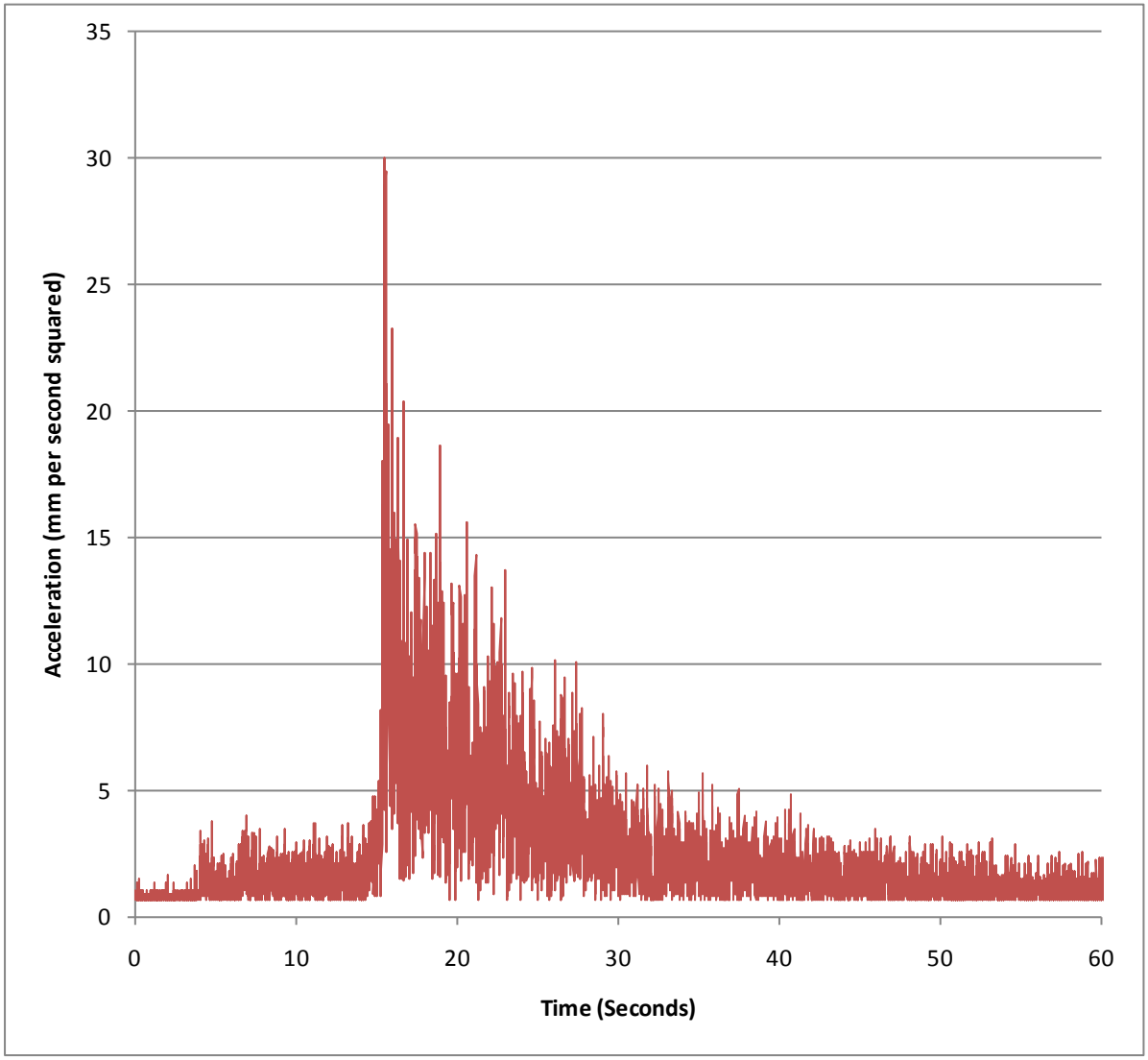

Figure 18 BROS Earthquake Time Trace

[7] May 27, 1995 delta time of 0.005 seconds, # of points= 16128, Station: BROS in TN.

The critical points to note are:

1. the duration of the event, about 15 seconds
2. the peak acceleration of about 30 mm/s^2, which is 3 milli-g', which is within the range of readings taken on the two sites for this study

The BROS earthquake was randomly selected from the database of earthquakes to provide a base line measurement for a previous vibration study. It is used here to illustrate the issues of frequency. The earthquake has a maximum absolute acceleration of 30 mm/s^2, which occurs at the start of the event. The peak velocity at each time step can be calculated using the three components of the acceleration signal, which are then added from vector theory using high school algebra (Kaplan & Lewis, 1971), as shown on Figure 19. The peak velocity is 1 mm/s.

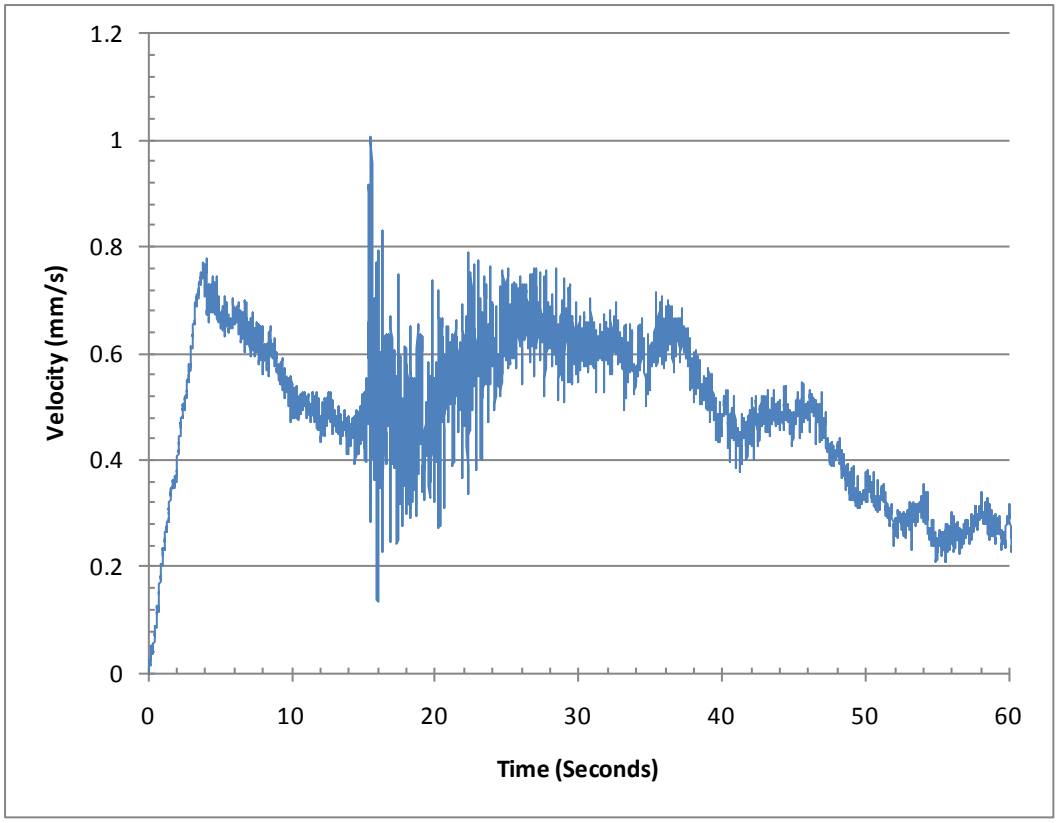

Figure 19 BROS Earthquake Peak Velocity (mm/s)

The data shown on Figure 18 and Figure 19 do not provide any clue as the acceleration or velocity against the frequency. A Fast Fourier Transform analysis of the acceleration data files provides guidance as to the frequency components and amplitudes for the signal. This analysis is shown on Figure 20. Fast Fourier transforms are a standard technique for signal analysis.

The observations that can be made from Figure 20 are:

- The horizontal signals have peaks in the range of 5 to 10 Hz.
- The vertical signal has peaks in the range of 10 to 12 Hz.
- The frequency is a strong component of the signal.

- A ratio of 25 mm/s^2 to the velocity of 1 mm/s shows the low impact of the velocity component that results in damping at low acceleration levels

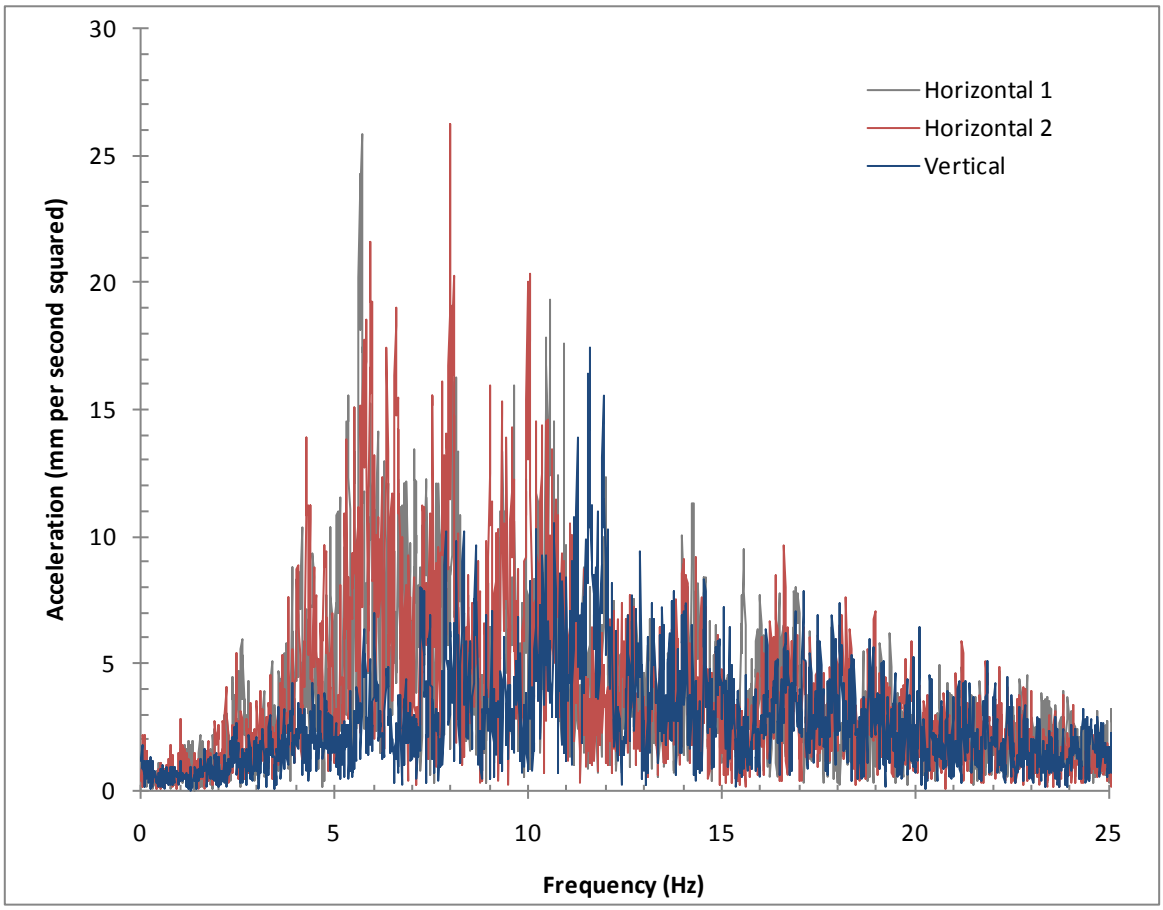

Figure 20 Fast Fourier Transform of Accelerations

A histogram of the count of acceleration amplitudes for the Bros Event from 0 to 100 Hz is shown in Figure 21. This figure is required for a statistical analysis of the likely risk of the damage in a cyclic event.

An approximate equation can be fitted to graph shown in Figure 21.

$$Count = 10^{(3.5548 - 0.147\,acceleration)} \qquad \textbf{Equation 1}$$

One area not so far considered for the development of The Building is the likely need for a backup generator system. A vibration study of a small generator building for the Langford Architectural Complex has occurred over the last few years. This study commenced with the earlier and less sensitive GP2 accelerometers (Guha, 2008). The cracking on the front of the building has increased with time. Figure 23 shows a SENSR GP1, a less sensitive instrument in place to measure vibration in an early study.

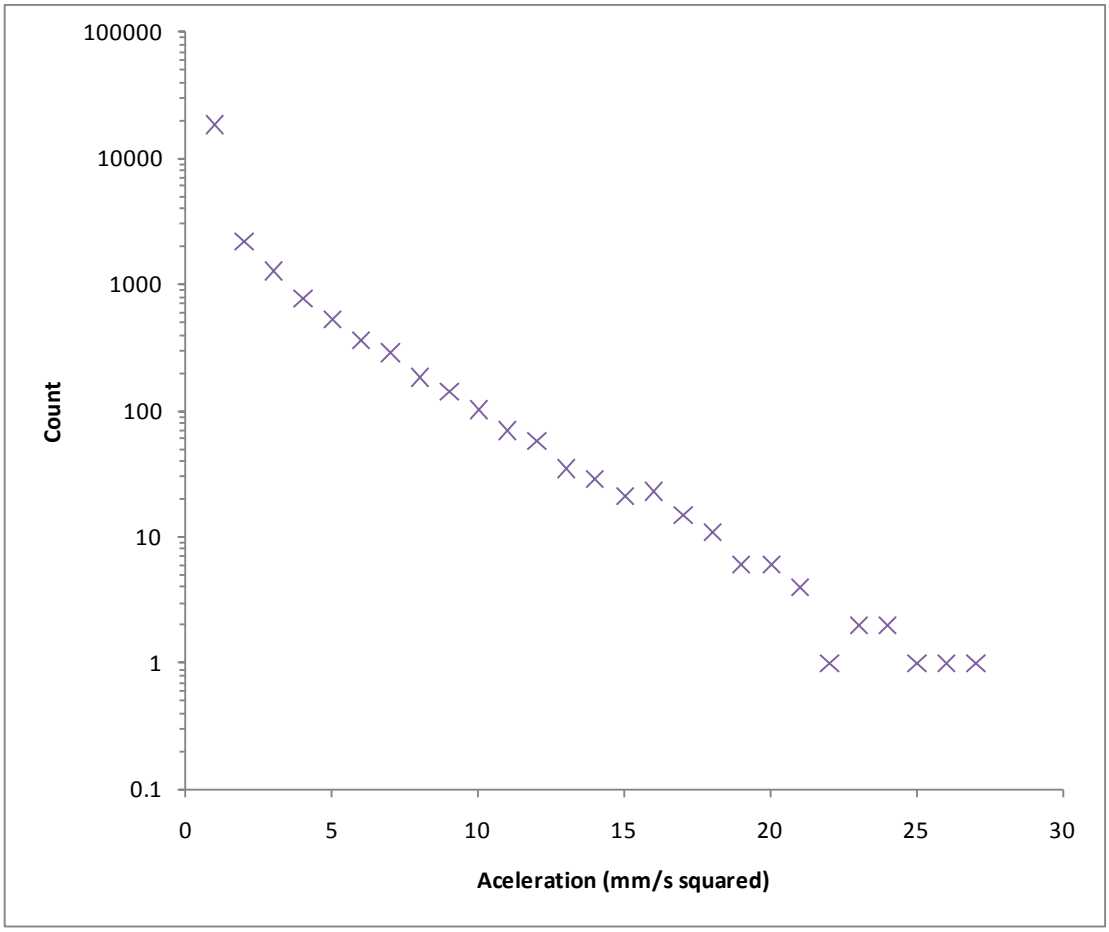

Figure 21 Histogram of the Acceleration Counts from the FFT Analysis

Figure 22 is a generator building near the Langford Building A.

Figure 22 Generator Building - TAMU Campus

Figure 23 Instruments in place to measure vibration

Figure 24 shows a Fast Fourier Transform graph for a Ford F150 falling off a 110 mm kerb, adjacent to the Generator Building The building response at about 8 Hz is evident.

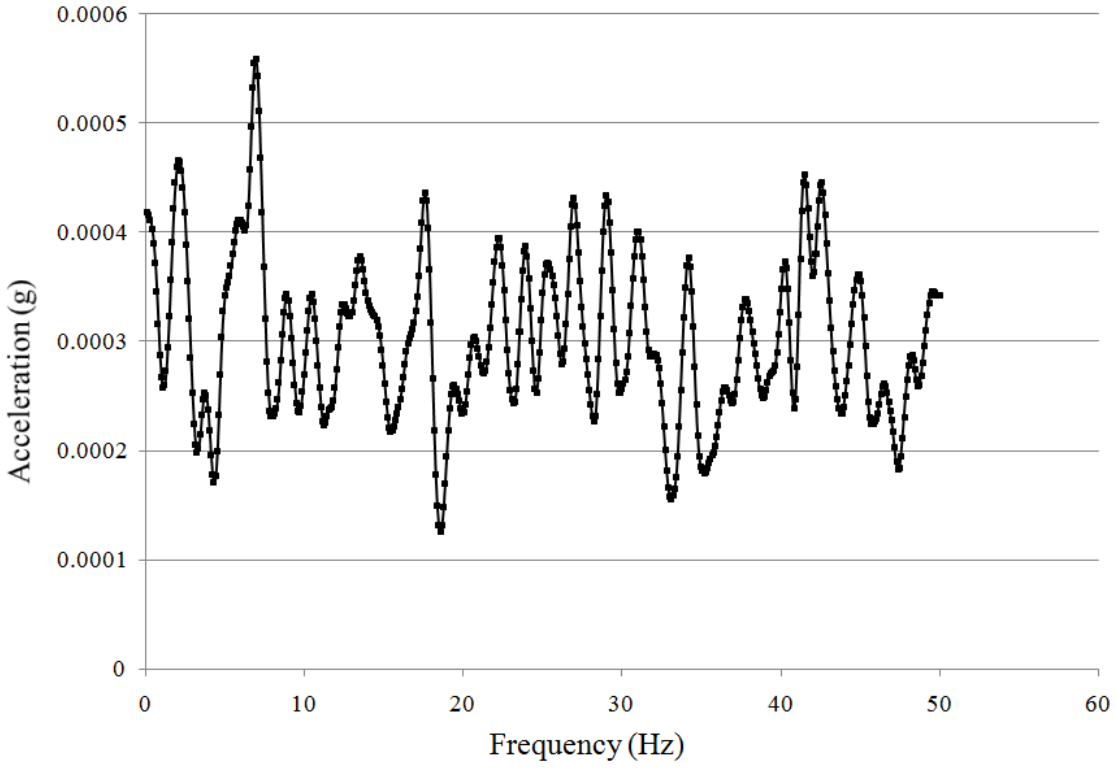

Figure 24 FFT for Truck Movement near Building

Recent measurements with the CX1 Accelerometer are yet to be analysed. The cracking is increasing in the building and this can be attributed to vibration with initial cracking perhaps caused by corroding reinforcing steel. Consideration should be given to the placement and likely impact of a generator building adjacent to *this Building*.

One of the oldest vibration scales in the Modified Mercalli Intensity scale. Figure 25and Figure 26 present the current version of the MM scale.

Earthquake Intensity

Of the two ways to measure earthquake size, magnitude based on instrumental readings and intensity based on qualitative effects of earthquakes, only intensity can be applied to pre-instrumental earthquakes. The 1931 Modified Mercalli scale used in the United States assigns a Roman numeral in the range I - XII to each earthquake effect. The methodology is simple.

- At each location assign a numeral to describe the earthquake effect
- Contour the zones of similar effect
- The earthquake is assumed to have occurred near the region of maximum intensity
- The earthquake may be characterized by the largest Roman numeral assigned to it

The problems with intensity are multifold. First, it is a qualitative assessment that measures different phenomena. The lower values address human response to ground motions, the intermediate values characterize the response of simple structures, and the upper values describe ground failure processes.

Another problem is that incomplete spatial coverage may lead to a mislocation of the earthquake or an underassessment of its size. This is easily visualized for offshore earthquakes or, in the case of the United States, inadequate population distribution at the time of the earthquake.

Modified Mercalli Scale

Average peak velocity (centimeters per second)	Intensity value and description	Average peak acceleration (g is gravity=9.80 meters per second squared)
	I. Not felt except by a very few under especially favorable circumstances. (I Rossi-Forel scale)	
	II. Felt only by a few persons at rest, especially on upper floors of buildings. Delicately suspended objects may swing. (I to II Rossi-Forel scale)	
	III. Felt quite noticeably indoors, especially on upper floors of buildings, but many people do not recognize it as an earthquake. Standing automobiles may rock slightly. Vibration like passing of truck. Duration estimated. (III Rossi-Forel scale)	
1-2	**IV.** During the day felt indoors by many, outdoors by few. At night some awakened. Dishes, windows, doors disturbed; walls make creaking sound. Sensation like heavy truck striking building. Standing automobiles rocked noticeably. (IV to V Rossi-Forel scale)	0.015g-0.02g
2-5	**V.** Felt by nearly everyone, many awakened. Some dishes, windows, and so on broken; cracked plaster in a few places; unstable objects overturned. Disturbances of trees, poles,	0.03g-0.04g

Figure 25 Modified Mercalli Scale - pg 1 (after St Louis University)

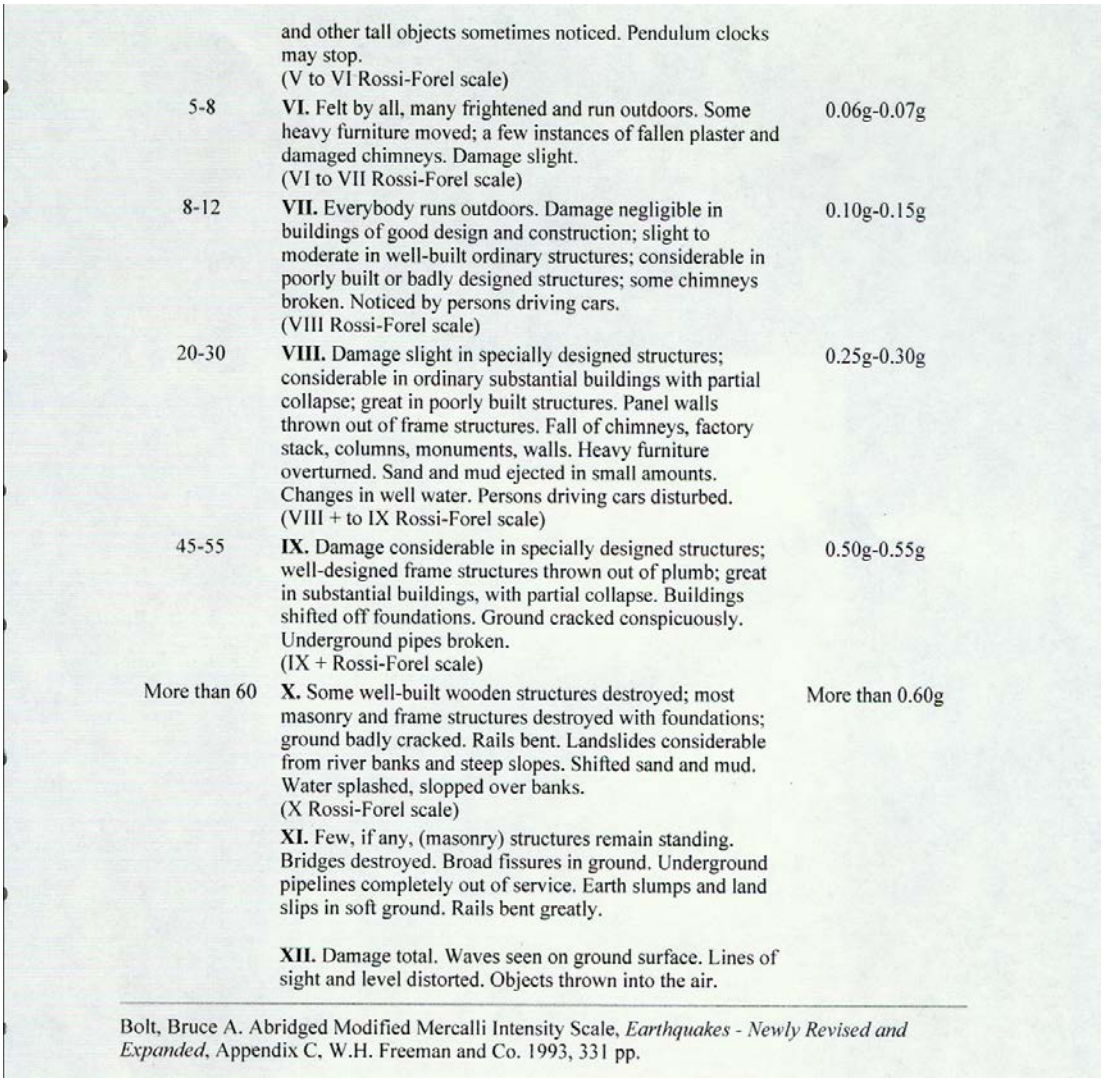

	and other tall objects sometimes noticed. Pendulum clocks may stop. (V to VI Rossi-Forel scale)	
5-8	**VI.** Felt by all, many frightened and run outdoors. Some heavy furniture moved; a few instances of fallen plaster and damaged chimneys. Damage slight. (VI to VII Rossi-Forel scale)	0.06g-0.07g
8-12	**VII.** Everybody runs outdoors. Damage negligible in buildings of good design and construction; slight to moderate in well-built ordinary structures; considerable in poorly built or badly designed structures; some chimneys broken. Noticed by persons driving cars. (VIII Rossi-Forel scale)	0.10g-0.15g
20-30	**VIII.** Damage slight in specially designed structures; considerable in ordinary substantial buildings with partial collapse; great in poorly built structures. Panel walls thrown out of frame structures. Fall of chimneys, factory stack, columns, monuments, walls. Heavy furniture overturned. Sand and mud ejected in small amounts. Changes in well water. Persons driving cars disturbed. (VIII + to IX Rossi-Forel scale)	0.25g-0.30g
45-55	**IX.** Damage considerable in specially designed structures; well-designed frame structures thrown out of plumb; great in substantial buildings, with partial collapse. Buildings shifted off foundations. Ground cracked conspicuously. Underground pipes broken. (IX + Rossi-Forel scale)	0.50g-0.55g
More than 60	**X.** Some well-built wooden structures destroyed; most masonry and frame structures destroyed with foundations; ground badly cracked. Rails bent. Landslides considerable from river banks and steep slopes. Shifted sand and mud. Water splashed, slopped over banks. (X Rossi-Forel scale)	More than 0.60g
	XI. Few, if any, (masonry) structures remain standing. Bridges destroyed. Broad fissures in ground. Underground pipelines completely out of service. Earth slumps and land slips in soft ground. Rails bent greatly.	
	XII. Damage total. Waves seen on ground surface. Lines of sight and level distorted. Objects thrown into the air.	

Bolt, Bruce A. Abridged Modified Mercalli Intensity Scale, *Earthquakes - Newly Revised and Expanded*, Appendix C, W.H. Freeman and Co. 1993, 331 pp.

Figure 26 Modified Mercalli Scale - pg 2 (after St Louis University)

Bolt provides an acceleration range for the MMI Scale as shown in Table 2.

Table 2 MMI Scale Acceleration(after Bolt, 1993)

MM Scale	Acceleration Lower	Acceleration Upper
1	0.0028	0.0029
2	0.0050	0.0055
3	0.0093	0.0105
4	0.0150	0.0200
5	0.0300	0.0400
6	0.0600	0.0800
7	0.1000	0.1500
8	0.1800	0.3000
9	0.3800	0.5500
10	0.6200	0.9200
11	1.1831	1.8986
12	2.1695	3.6346

Bolt's data was plotted and a series of regression analyses showed an exponential fit matched Bolt's data as shown in Figure 27.

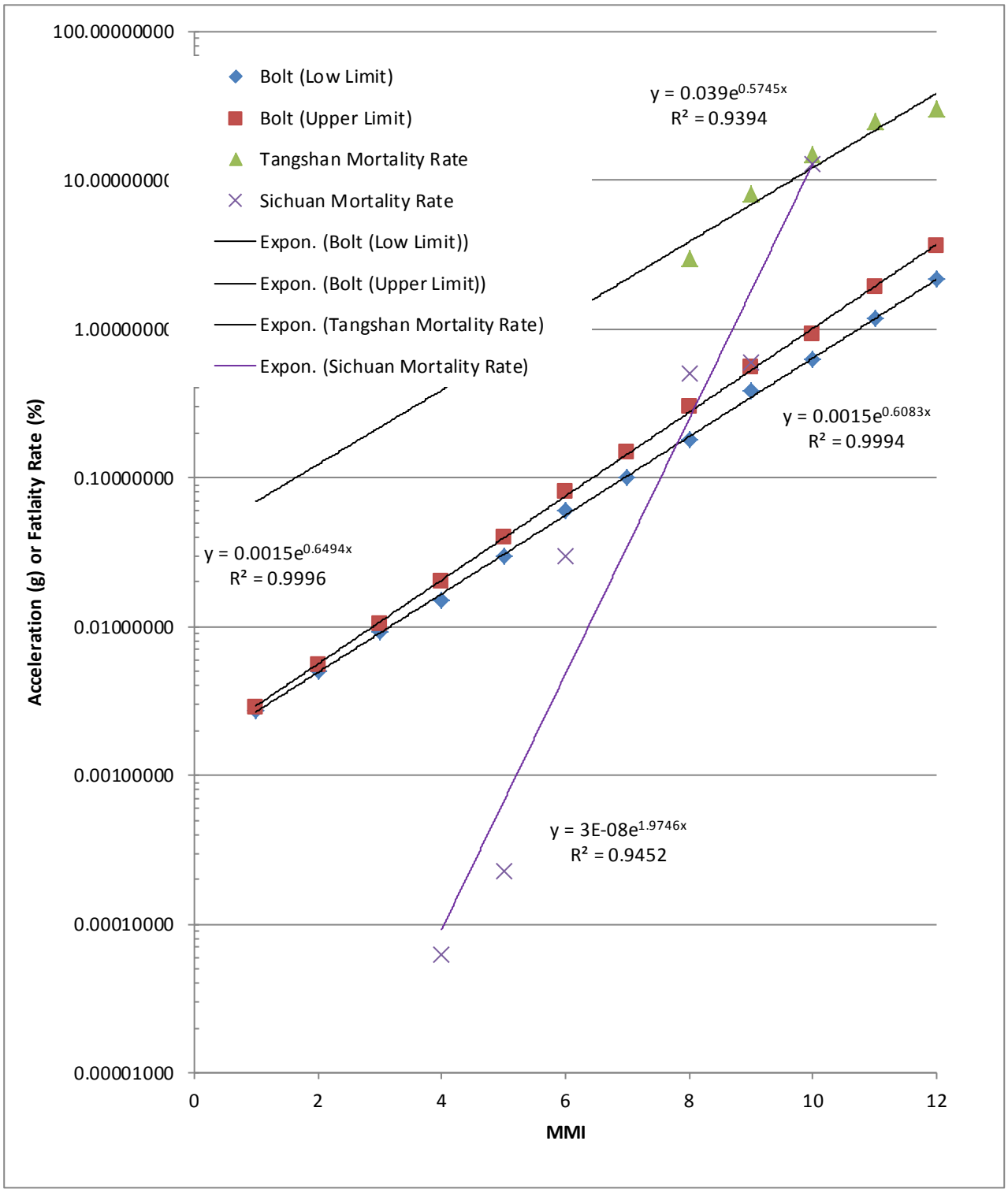

Figure 27 MMI Scale Data

Earthquake data can often be shown to scale using a logarithmic function. In the case of the Bolt data the relationship is exponential. A log to linear scale on the figure provides a linear drawing for the equation. The data can then be simply extrapolated to estimate the acceleration as shown on

the figure. Building damage, collapse and death are related directly to the shaking level. The mortality rate in the 1976 Tangshan and the recent Sichuan earthquakes are plotted against MM Intensity. The Building would have experienced an MMI – I from the trains using the extrapolated equation.

SENSR LLC manufacture the CX1 accelerometer. This research work uses the SENSR CX1 accelerometer, which is able to resolve to about one micro-G in the frequency domain according to the manufacturer (Kavars, 2012). However, a resolution of ten micro G's is acceptable for analysis of the ambient signal noise and resultant vibration present in all structures. The CX1 records 2000 signal points per second and each point contains time, and three acceleration data sets, each data set is orthonormal to the others (Kaplan & Lewis, 1971).

The instruments used are CX1 Serial Number 1002 and Serial Number 1190. CX1 – 1190 is shown in Figure 28.

Figure 28 CX1 Accelerometer

The X axis is left to right, the Y axis is bottom to top and the Z axis is vertical in Figure 28. A recently published paper summarizes the development of an alternative method of recovering the natural frequencies of a building using the Variance Method. This paper is provided with the report.

Table 3 shows a sample of the CSX rail cars used for the traffic count for the train movements on the line.

Table 3 Car Types from CSX Data (courtesy CSX 2013)

Car Picture	Car Type	Number Tag
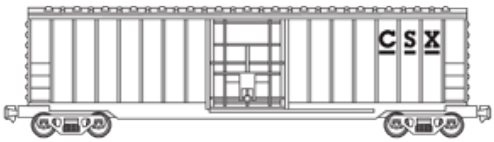	Box Car	1
	Flatcar Empty	2
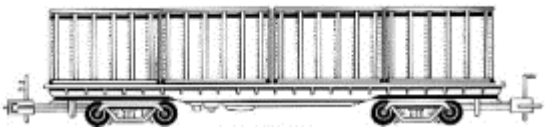	Centre Beam Flat Car	3
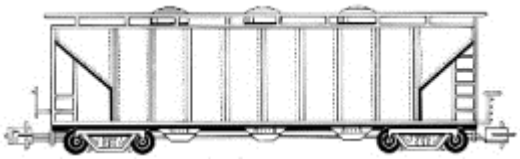	Covered Hopper	4
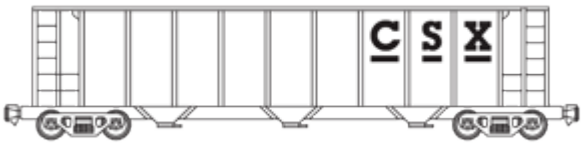	Open Top Hopper	5
	Plain Gondola	6
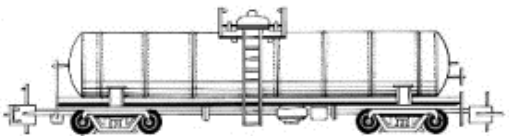	Tank Car	7
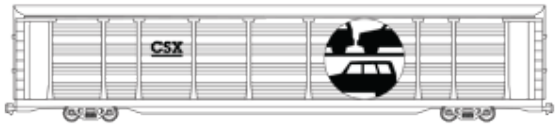	Auto Rack	8

Figure 29 shows a typical example of a set of Union Pacific Locomotives as observed during the study.

Figure 29 Typical Union Pacific Locomotive Engines (after UP, 2013)

UP locomotive 9039 was recorded during the study, this locomotive is a GE C40-8 (Dash 8-40C). The train unit has a mass of 399,000#, with 12 wheels; the mass per wheel is 148 kN. The greatest load occurs at a coupling between cars and assuming a distance between wheel pairs of 7 feet or 2.1 metres, the applied load is about 74 kN per metre over an 8 m length or 1.76 mega Newtons as an equivalent point load.

Figure 30 shows a picture of a locomotive similar to one observed during the study.

Figure 30 Picture of Locomotive similar to the UP 9039 observed in the study

Chapter 3. Methods

1. Introduction

The study periods were on two days, the first day was 17 October 2013 and the second day was 5 November 2013. This chapter on methods outlines the:

1. study locations for the accelerometers on each of the two days
2. details for the train traffic on the line
3. ambient noise levels in the Computer Services Building
4. format of the CX1 Data Records

2. Station Locations

Two different configurations were used for the station locations for the accelerometers inside *The Building*. Figure 31 shows the testing locations for the CX1 accelerometers on the first day of testing. The Y and X coordinate system orientation was maintained for all testing work, refer to Figure 31.

Figure 31 Station Sites on the First Day of Testing

Station 1 is located in the long hallway on the western side of the building. Station 2 is against the eastern wall of the building, about midway into the cooler room.

Figure 32 shows the station sites for the second day of testing. These sites were at the northern edge of the long east west hallway in the cooler room and about 1 metre north of the entrance door to the cooler room on the eastern wall. The north south reference assumes the railway line is aligned north to south.

Figure 32 Station Sites on the Second Day of Testing

3. Train Data

Data recorded for each train was:

1. Start time that train passed the location point
2. Direction of travel
3. Count of the number of carriage units in the train
4. End time of the train
5. On the second day the types of carriages was recorded as set out in Table 2.

The clock times for each data gathering unit was recorded to allow a comparison of the results.

4. Ambient Noise Levels

Ambient noise levels were recorded from the 6 November 2013 until the 11 November 2013. A single device CX1 – Serial Number 1190 was used for this record set.

5. CX1 Record Data

CX1 data is recorded using the standard CX1 Recorder Program. The output is stored in Comma Separated Data Files.

Table 4 shows a sample of the output data from the CX1.

Table 4 CX1 Sample Data Output

Sample Number	Date	Time	Acceleration X	Acceleration Y	Acceleration Z
2000	10/17/2013	3:40:33 PM	-0.00982	0.001609	1.000105
2001	10/17/2013	3:40:33 PM	-0.00988	0.001496	0.999933
2002	10/17/2013	3:40:33 PM	-0.00994	0.001383	0.999819
2003	10/17/2013	3:40:33 PM	-0.00982	0.001383	0.999876
2004	10/17/2013	3:40:33 PM	-0.00965	0.001382	1.000048
2005	10/17/2013	3:40:33 PM	-0.0096	0.001437	1.000219
2006	10/17/2013	3:40:33 PM	-0.00971	0.001493	1.000332
2007	10/17/2013	3:40:33 PM	-0.00988	0.001435	1.000388
2008	10/17/2013	3:40:33 PM	-0.01	0.001434	1.000444
2009	10/17/2013	3:40:33 PM	-0.01	0.00149	1.000501
2010	10/17/2013	3:40:33 PM	-0.01	0.001604	1.000502
2011	10/17/2013	3:40:33 PM	-0.01005	0.001661	1.000502

Table 5 summarizes the data sets used in the different stages of the analysis.

Table 5 Record and Analysis Set Details

Record Type	Number of Records	Time of Records (seconds)
CX1 CSV File	600000	300
FFT Analysis	16384	8.982
FFT Contour Plan	835584	417.792

Data is initially stored in a standard CX1 CSV File with 2000 records per second and a total of 300 seconds stored per file. These are merely temporary files. The CX1 Recorder Program puts the name of the instrument, the serial number and the date of the record in the file name; an example is CX1_1190 - ATC - 20131017_164533.csv.

6. CX1 Analysis Methods

The analysis method is based on the CX Recorder program supplied by the manufacturer. The output is stored as Comma Separated Files. The program CXAPI takes the CSV files and completes a Fast Fourier Transform analysis. The program accumulates the results into 51 FFT traces for use in

the ConRec contouring package. The output from the ConRec is a series of plots of the FFT and analysis results.

The first result is the three contour plots for the X, Y and Z directional data from the CX1 data using ConRec package. Figure 33 shows a sample acceleration plot from the first day of testing for the fourth train. The X results shows a strong set of contour peaks at about 5 Hz. The peak contour point is 0.86 milli g.

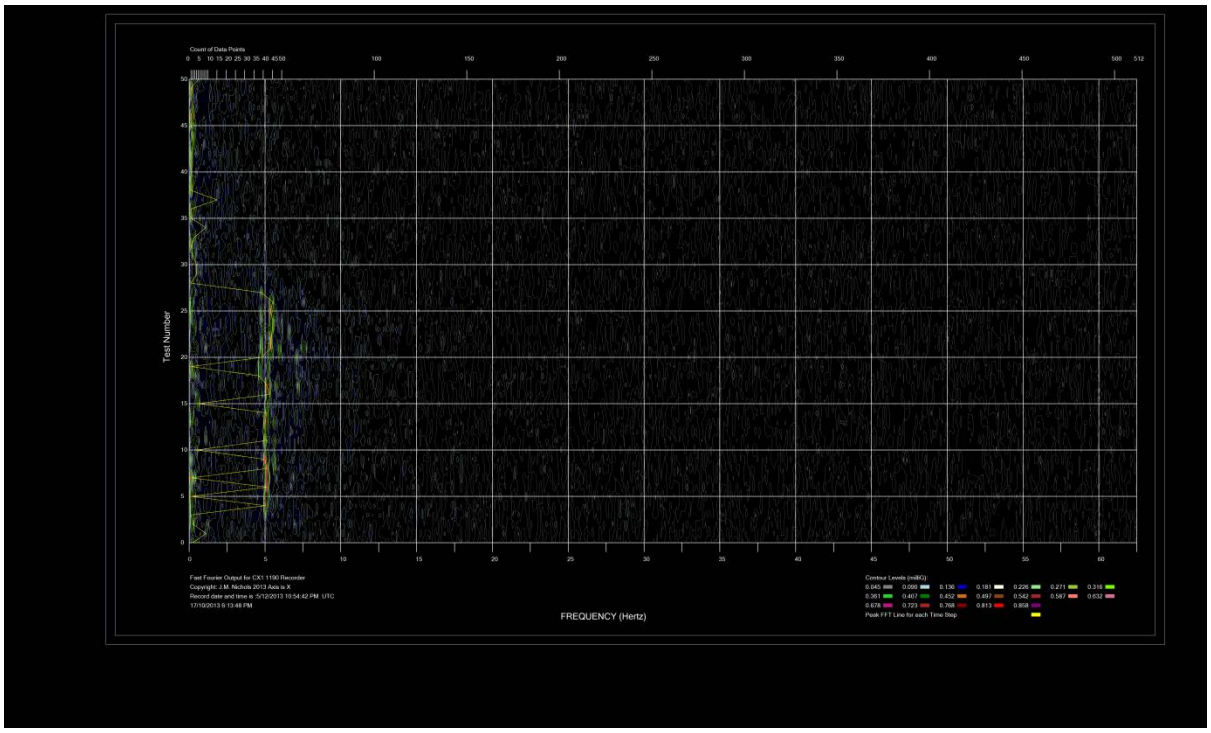

Figure 33 Sample X Acceleration Plot Train 4 Day 1

Figure 34 shows a sample acceleration plot from the first day of testing for the fourth train. The Y results shows a strong set of contour peaks at about 5 Hz. The peak contour point is 1 milli g. The Y direction is normal to the train lines, so the surface waves propagating from the train movement on the earth's surface cause a weak movement in the direction parallel to the train tracks, the X direction in this building and a slightly stronger movement in the Y direction or normal to the tracks.

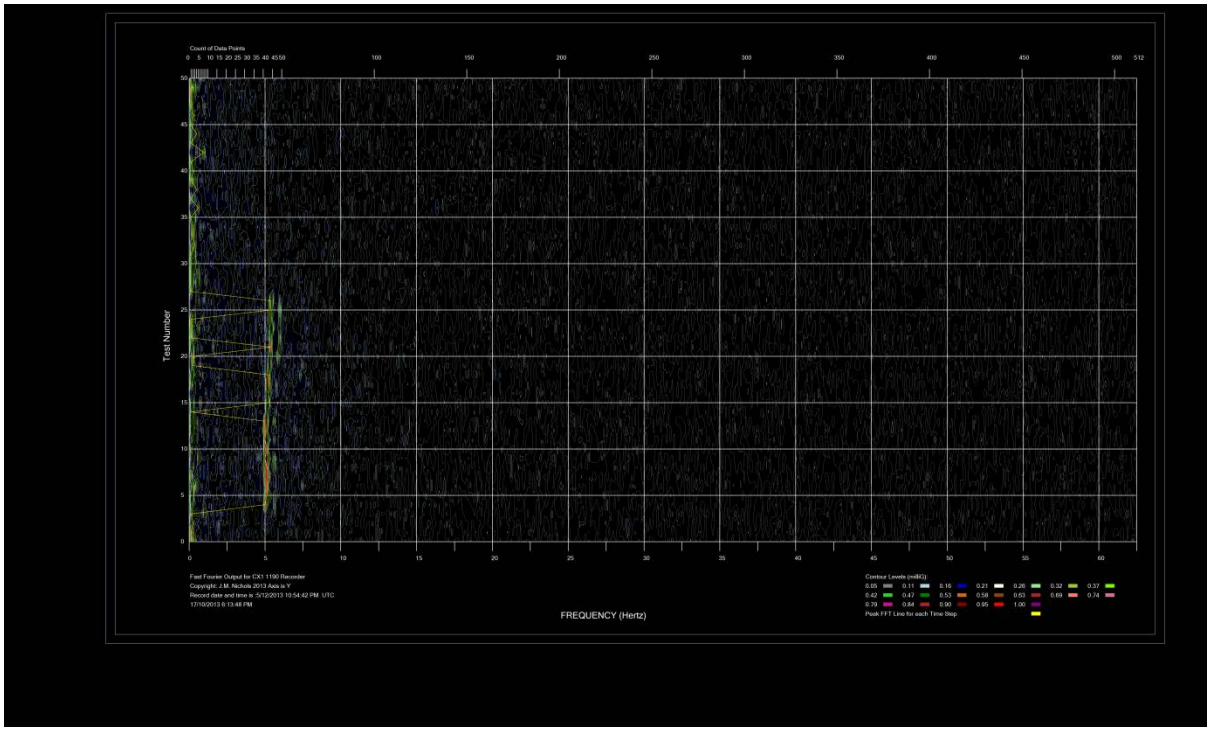

Figure 34 Sample Y Acceleration Plot Train 4 Day 1

Figure 35 shows a sample acceleration plot from the first day of testing for the fourth train. The Z results shows a strong set of contour peaks at about 5 Hz. The peak contour point is 1.71 milli g.

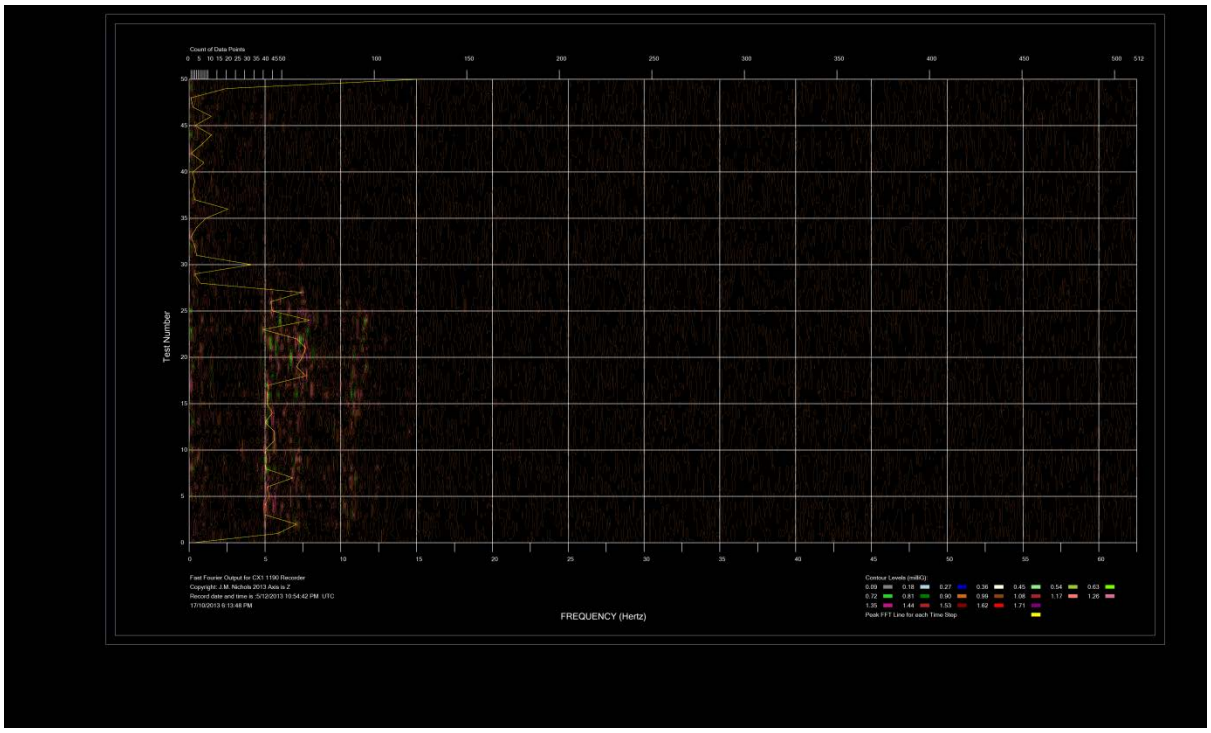

Figure 35 Sample Z Acceleration Plot Train 4 Day 1

The Z direction dominates the frequency component. The Z direction has a frequency component in the range of 5 to 7.5 Hz, so that the expected peak frequency of the combined signal will be in the range of 5 to 7.5 Hz. Figure 36 shows the plot of all of the FFT data points for the fourth train. The peak signal in the five Hz range is evident in the plot. Figure 37 shows the Y Signal.

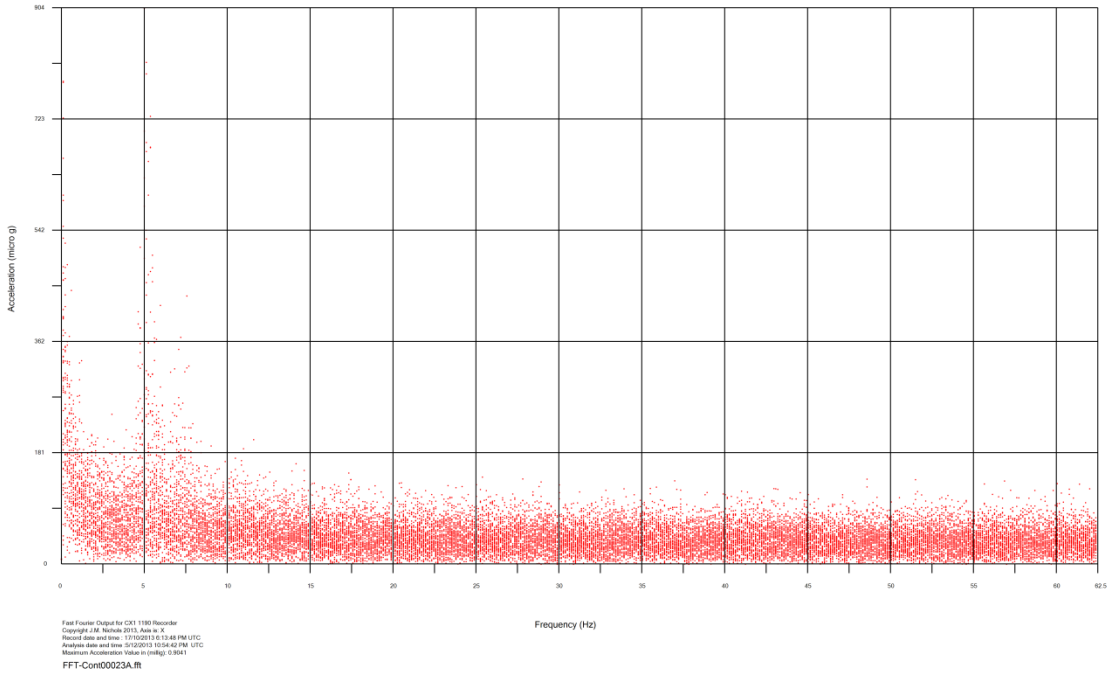

Figure 36 FFT Signal X Direction Day 1 Train Four

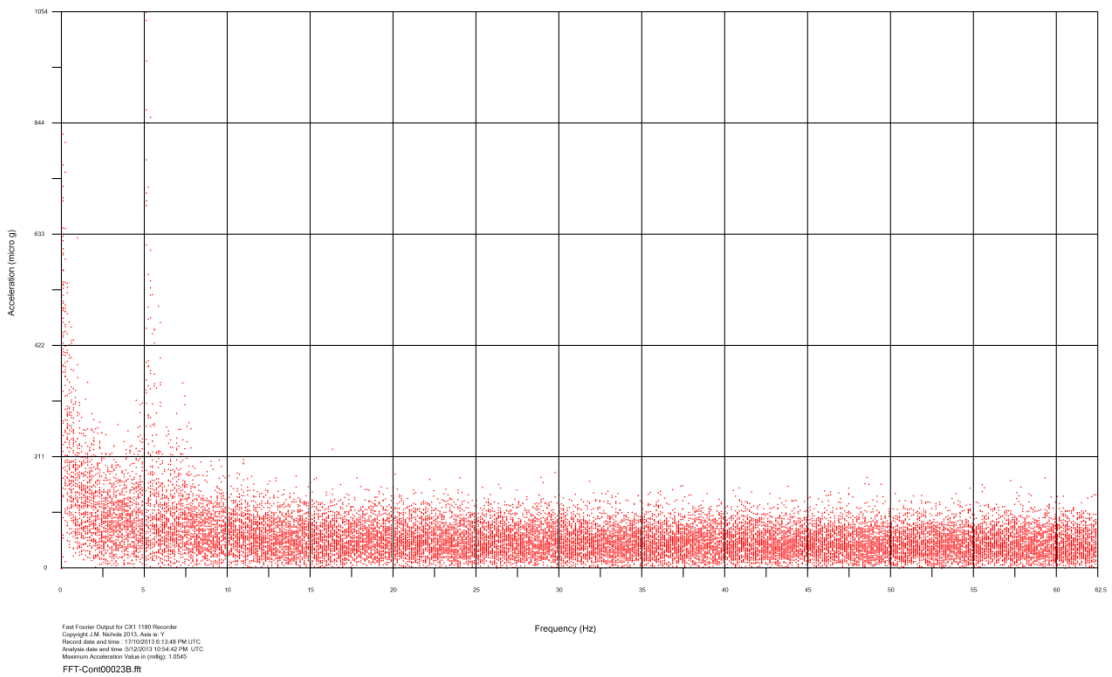

Figure 37 FFT Signal Y Direction Day 1 Train Four

Figure 38 shows the Z signal. This signal has a significant scatter in the region of 50 to 10 Hz.

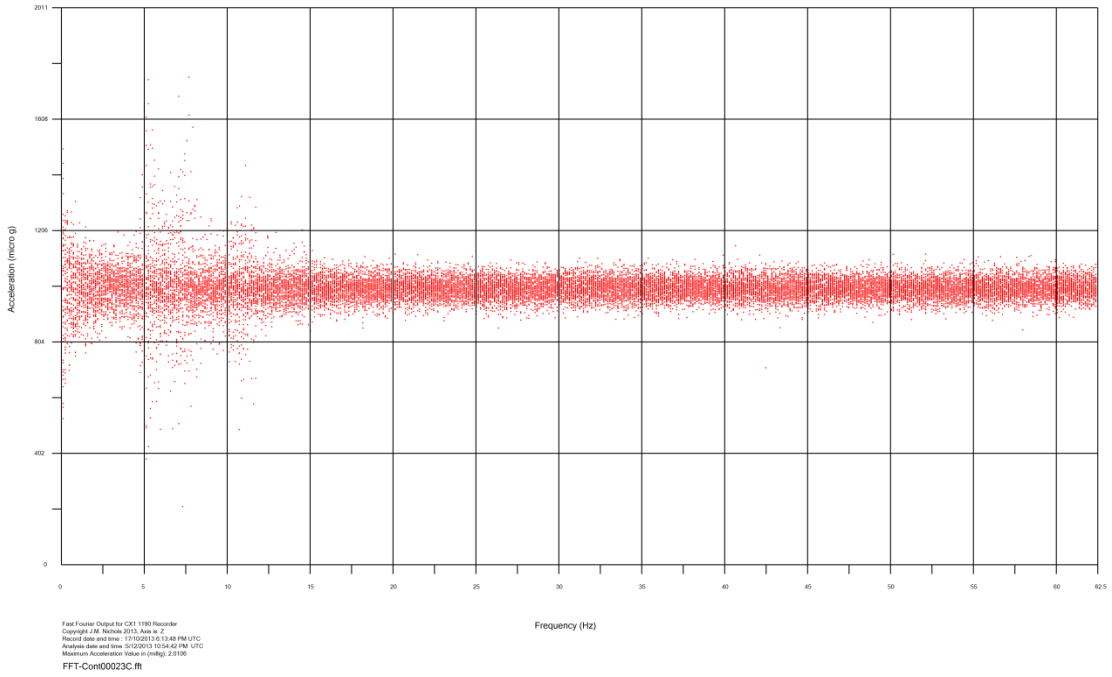

Figure 38 FFT Signal Z Direction Day 1 Train Four

Figure 39 shows the Variance Model analysis of the set of FFT points. The model shows the peak values in the 5 to 7.5 Hz region of the spectrum.

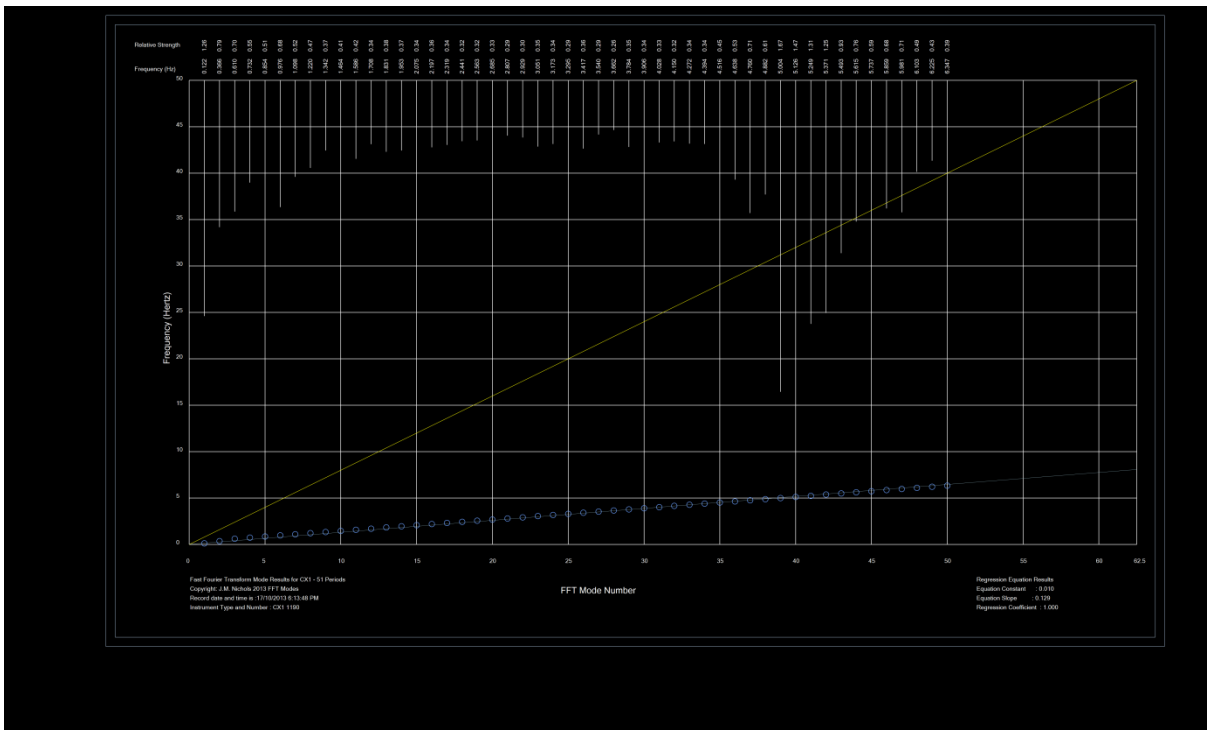

Figure 39 Spectrum Modes - Day 1 Train 4

Figure 40 shows a plot of the raw data used to calculate the modal values shown plotted in Figure 39. The peaks are about 5 and 7.75 Hz are evident on the plot.

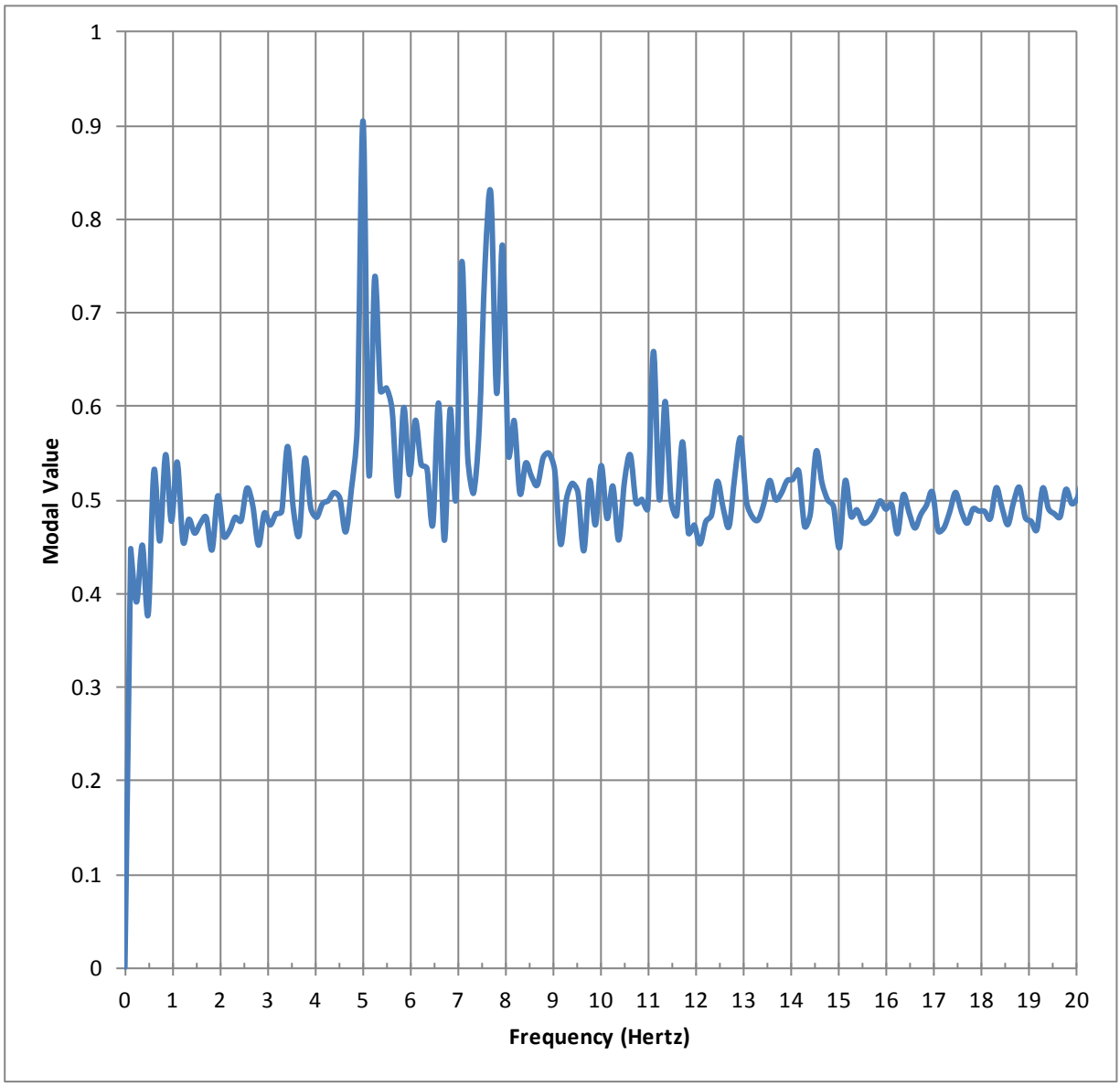

Figure 40 FFT Data for Day 1 Train Four

The Variance Model suggests the location and strength of the major modes of vibration for the building. It is likely the 11 Hz mode is a harmonic frequency caused by the 5.5 Hz mode.

Chapter 4. Results

1. Introduction

The results for the train impacts on the building are presented in Chapter 4. This chapter contains sections on:

1. Site details
2. Clock details
3. Experimental Periods

2. Site Details

Site and station details were summarized in the Literature Review. The critical issue of location for the train counts are:

1. Location 2 used for Day 1
2. Locations 1, 2 and 3 used for Day 2
3. Location 4 used for the period from 6 November 2013 until 11 November 2013

3. Clock Details

The clock details for the first day of the study are shown in Table 6. SENSR LLC uses a system of UTC to record all data from the CX instruments. Table 7 shows the clock timing details for the second day.

Table 6 Day One Clock Timing Details

Time Signal	Standard Time	Difference	Comment
NIST	08: 19: 39	0.1 second delay time	17 October 2013
COMPUTER A Station 1	08: 19: 36	- three seconds	
COMPUTER B Station 2			
CAMERA A	08:34:00	+ fifteen minutes	
ACCELEROMETER 1002	UTC	+ five hours	GMT

Table 7 Day Two Clock Timing Details

Time Signal	Standard Time	Difference	Comment
NIST	08: 19: 39	0.1 second delay time	5 November 2013
COMPUTER A Station 2	08: 19: 36	No delay	
COMPUTER B Station 3		1 minute 11 seconds delay	
ACCELEROMETER 1002	UTC	+ five hours	GMT
ACCELEROMETER 1190	UTC	+ five hours	GMT

Clock timing issues are not relevant to the ambient site study.

4. Experimental Periods

The experimental periods were:

1. Day 1 : 10 am until 2 pm
2. Day 2 : 8 am until 5 pm
3. Calibration Study 6 November 2013 until 11 November 2013

5. Train Arrival Times and Details – Day One

The train arrival times for the first day are summarized in Table 8. A number of pictures taken on the day are listed in the table. The train arrivals are tied to the record number associated with CX1 Serial Number 1002.

Table 8 Day One Train Arrival Times

Train Number	Camera Time	NIST TIME	GMT or UTC	Record Number for 1002	Pictures
One	11:41:20	11:26:20	16:26:20	26	1452, 1453, 1454, 1455, 1456, 1457
Two	12:52:26	12:37:26	17:37:26	40	1458
Three	1:07:43	12:52:00	17:52:00	43	1459, 1460
Four	1:29:28	13:14:28	18:14:28	48	1461,1462

Table 9 provides details of the first train on the first day. Table 10 is for the second train.

Table 9 Day One Train One

Train	Details	
One	Union Pacific Loco	
Direction	Northbound	
Time to pass	268 s	4 minutes 28 seconds
Velocity	18.6 (41.6)	Metres per second (mph)
Number of carriages	184	Assume 27 m long
Mass	Not known	

Table 10 Day One Train Two

Train	Details	
Two	Union Pacific Loco	
Direction	Southbound	
Time to pass	216	3 minutes 36 seconds
Velocity	9.8 (21.9)	Metres per second (mph)
Number of carriages	79	Assume 27 m long
Mass	Not known	

Table 11 provides details for day one with the third train.

Table 11 Day One Train Three

Train	Details	Comments
Three	Union Pacific Loco	
Direction	Southbound	
Time to pass	156	2 minutes 36 seconds
Velocity	7.0 (15.6)	Metres per second (mph)
Number of carriages	41	Assume 27 m long
Mass	Not known	

Table 12 provides details for day one with the fourth train.

Table 12 Day One Train Four

Train	Details	Comments
Four	Union Pacific Loco	
Direction	Southbound	
Time to pass	178	2 minutes 58 seconds
Velocity	10.1 (22.5)	Metres per second (mph)
Number of carriages	105	Assume 17 m long
Mass	Not known	

6. *Train Velocity Results Day One*

Figure 41 shows the estimated train velocity in metres per second

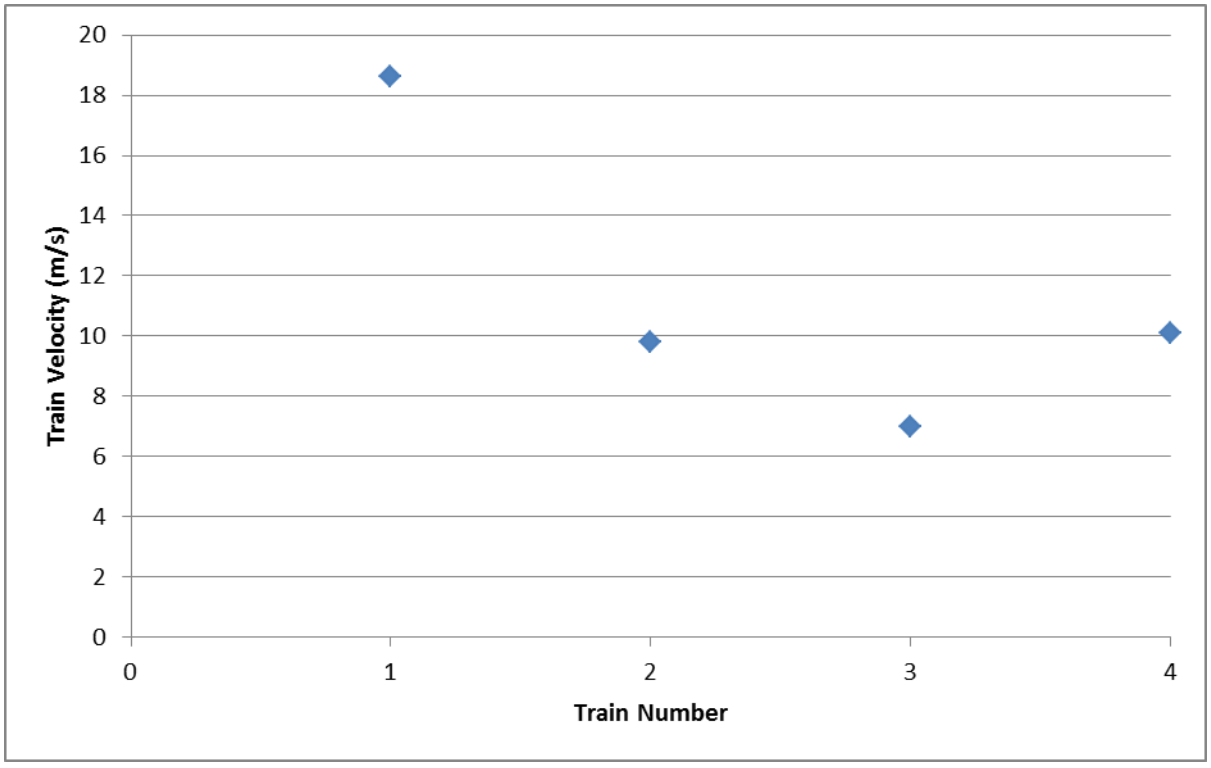

Figure 41 Day One Train Velocity in metres per second

7. *Peak Acceleration Results Day One*

Figure 42 shows the acceleration data for X – max, min and average for CX1002 on the first day. Figure 43 shows the acceleration data for Y – max, min and average for CX1002 on the first day. Figure 44 shows the acceleration data for Z – max, min and average for CX1002 on the first day.

The issues with the readings are:

1. It is not possible to close the building so some readings may be caused by people or equipment insider the building
2. Each record set is 600000 records, or 300 seconds
3. Each FFT analysis set is 16,384 records, with 51 sets per contour group so that 103 data sets from the CX1 are translated to 73 FFT sets to ensure a power of 2 in the analysis

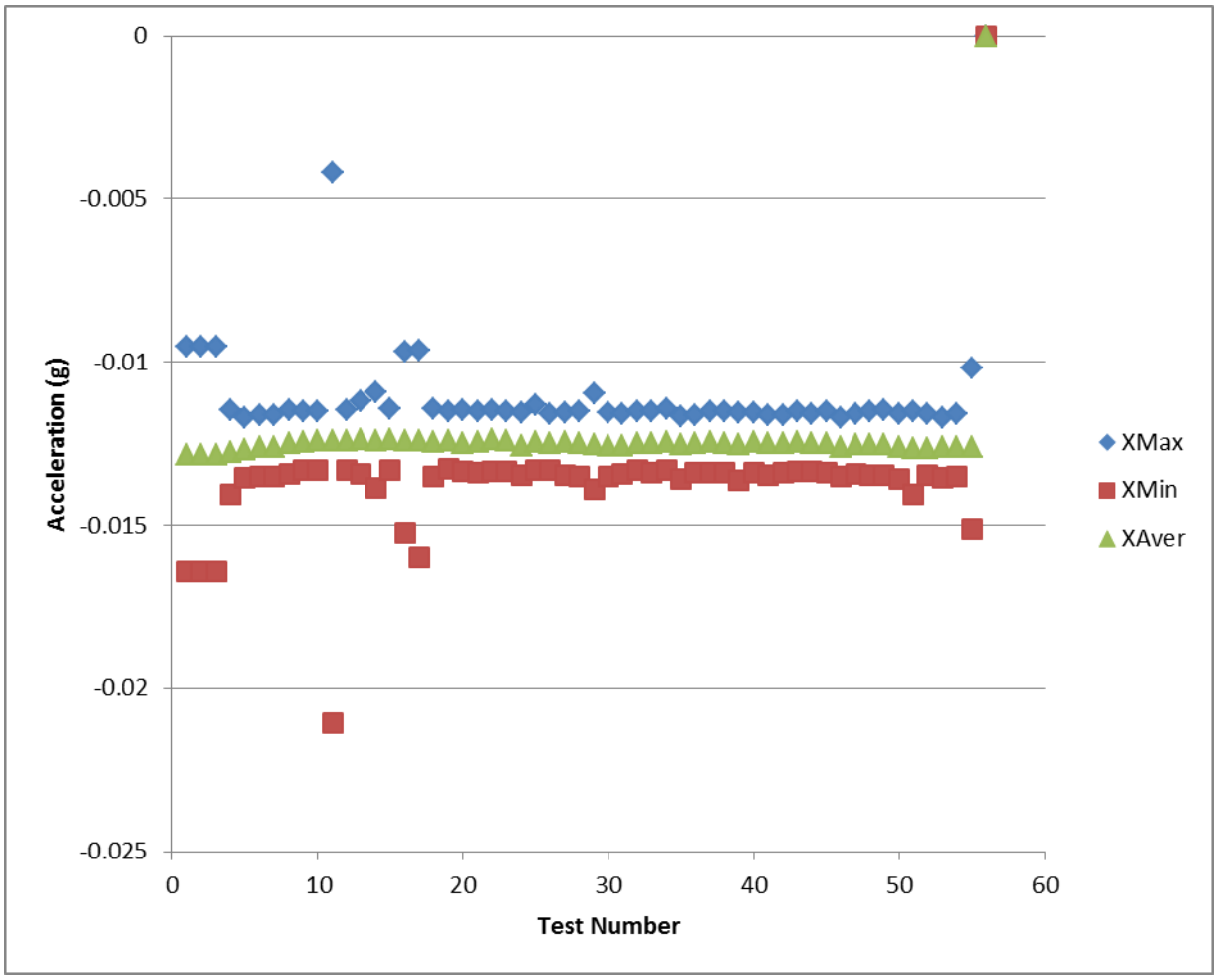

Figure 42 SENSR CX1 1002 X Acceleration Data

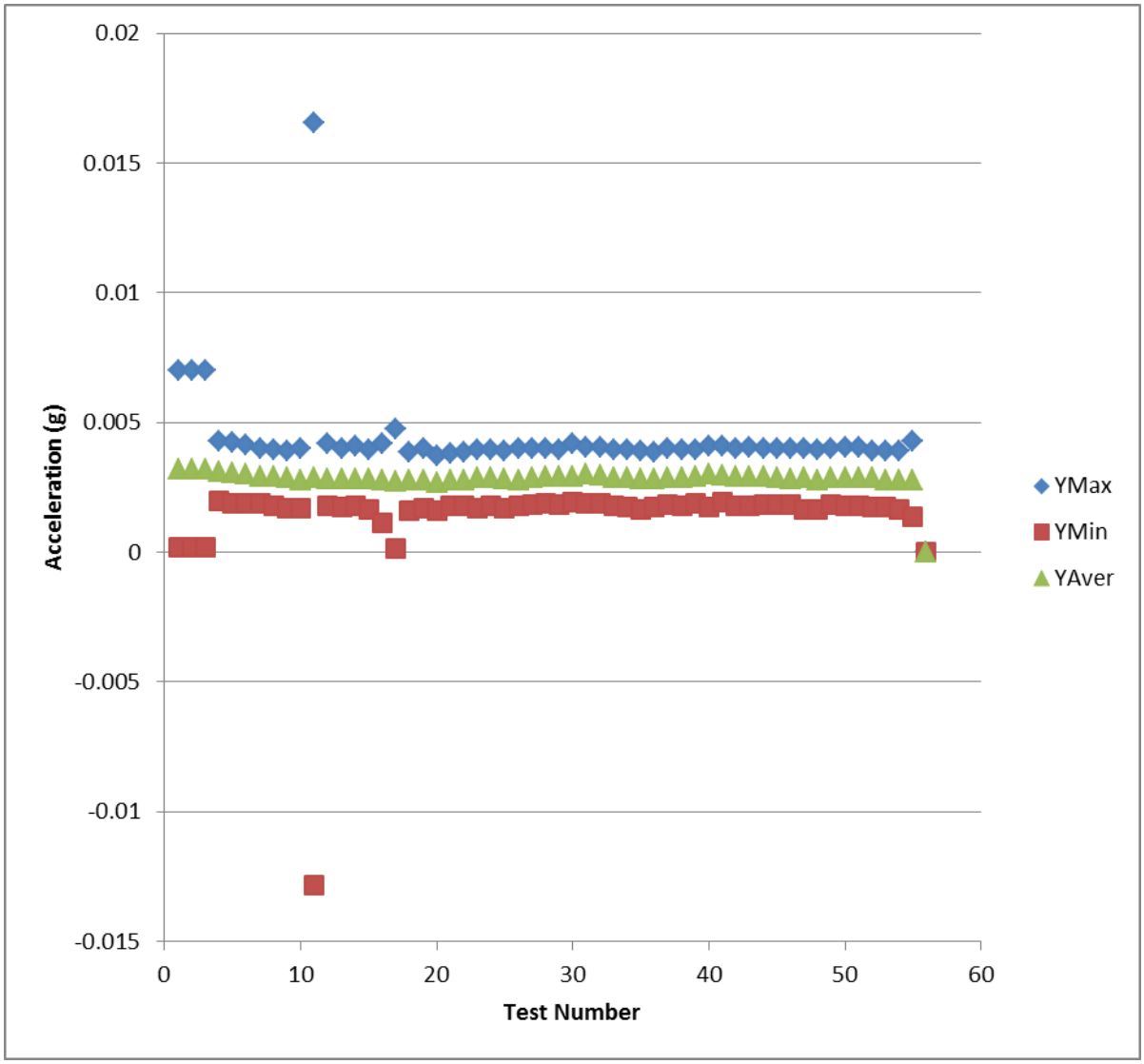

Figure 43 SENSR CX1 1002 Y Acceleration Data

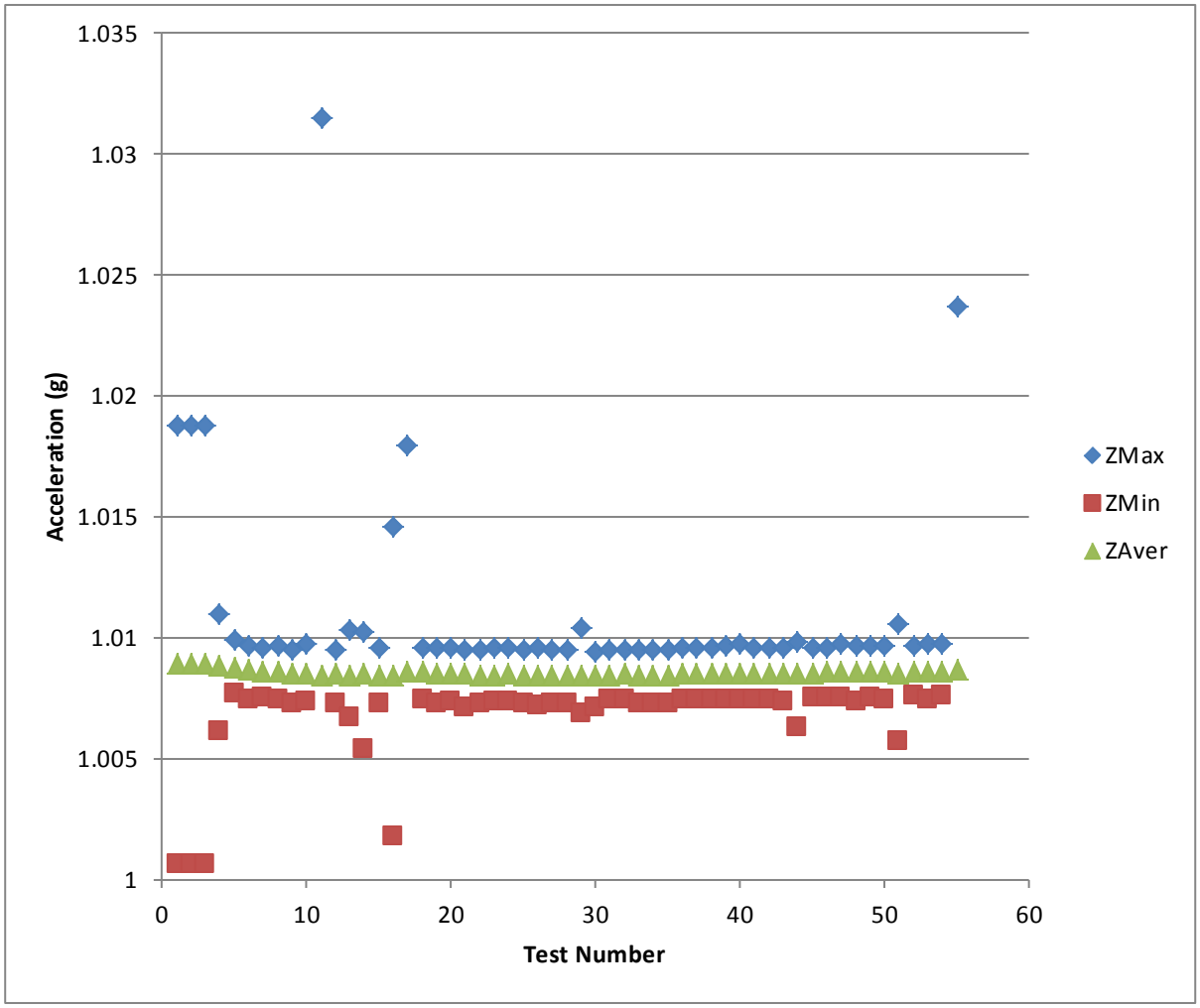

Figure 44 SENSR CX1 1002 Z Acceleration Data

8. *Fast Fourier Results Day One*

A program has been developed in C# to provide a contour plot of the FFT signals with pseudo time. Fifty one FFT records of seconds duration are stacked onto a single plot and contoured using CONREC (Bourke, 1987).

The CX1 records essentially Brownian motion of the surrounding area when there are no applied loads [8]. Figure 58[9] shows a record of essentially Brownian Motion in the Z direction for the period before the train enters the study area. The causes of the few peaks in this data cannot be ascertained, but the overall load is low with a peak of 0.8 milli g's.

Figure 59[10] shows the FFT data for the period in which the train enters the segment from Location 2 to Location 3 in a northbound direction. Figure 60[11] shows the FFT results for the remainder of the train.

[8] add Nelson record
[9] Figure 58 FFT Result 22 from Day One, essentially Brownian Motion is shown on page 53 in the Exhibits section.
[10] Figure 59 FFT Result 26 from Day One, Train onto Bridge shown on page 54 in the Exhibits section.
[11] Figure 60 FFT Result 27 from Day One, Remainder of Train shown on page 55 in the Exhibits section.

The significant spike at about 40 Hz is consistently observed with higher speed trains, this is likely due to the S – Wave in the steel track hitting the steel railway bridge across University Drive. This can of course not be conclusively proven, but the incident is recorded in a number of records. The remaining peaks are in the region of ten Hertz, which is a region of damage evolution in buildings.

Figure 45 shows the FFT data set used to contour the Results Set 27 plotted as a single data set of acceleration level against frequency. It can be considered as looking sideways at a drawing of Figure 60.

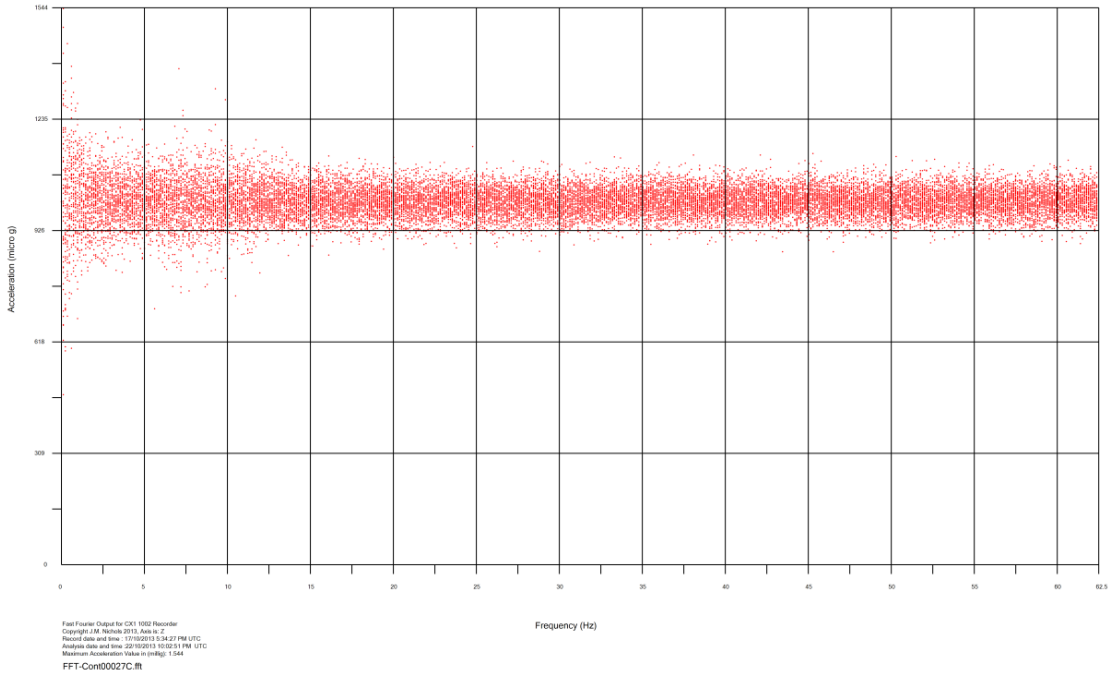

Figure 45 FFT Data as a single data set

The Variance Model uses an algorithm to estimate the peaks in the frequency set. The algorithm searches for points that fit a set of criteria related to their variance level relative to the mean level for each frequency (J. M. Nichols, 2013). Interestingly, the algorithm that matched the vibration data on the Pont y Prydd Bridge lacked the sensitivity to locate any frequencies in these data sets and a revised more sensitive algorithm was developed for this study. Figure 61[12] shows the Variance Model output for Brownian motion. Figure 62[13] shows the train impact on the Variance Model output.

The train tends to shift the energy into lower frequency modes generally in the region of 5 to 10 Hz.

9. *Train Arrival Times and Details – Day Two*

Table 13 summarizes the details of the nine trains that passed the study area on the 5 November 2013. Train number 8 was stopped on the second line whilst the ninth train past.

[12] Figure 61 FFT Spectrum Modal Analysis for the 22nd Data Set shown on page 56 in the Exhibits section.
[13] Figure 62 FFT Spectrum Modal Analysis for the 27th Data Set shown on page 57 in the Exhibits section

Table 13 Train Details for the Second Day

Train	Location	Time	End Time	Pass Duration (seconds)	Unit Total	Direction	Locomotive
1	1	8:48:30	8:53:30	349	46	Up	
	2	8:55:00	8:57:38	158	47		
2	2	8:58:00	9:02:02	242	33	Down	UP 1-9039
	1	9:05:00	9:06:25	85	37		
3	3	9:16:00	9:18:50	170	114	Down	UP 2-7183
	2	9:20:00	9:23:30	195	110		
	1	9:23:00	9:25:34	154	115		
4	1	9:54:00	9:56:13	133	46	Up	UP 3-7916
5	1	10:35:45	10:37:45	120	98	Up	
	2	10:37:00	10:38:35	95[14]	90		
	3	10:40:15	10:43:15	180	90		
6	3	10:46:45	10:49:55	190	46	Down	(Eng. Two)
	2	10:51:00	10:53:12	132	46		
	1	10:56:00	10:57:00	60	45		
7	2	11:23:00	11:26:31	211	92	Down	4388
	1	11:24:00	11:26:30	210	82		
	1	11:26:00	11:28:30	150	80		
8	3	3:12:15	NK	NK	22	Down	(Eng. Three)
	2	3:35:30	3:36:20	50	21		Halted
	1	3:38:10	3:38:51	41	23		
9	2	3:24:38		NK	83	Up	
	1	3:27:00		NK	87		

Table 14 summarizes the estimated train velocities for Day Two.

Table 14 Train Velocity Summary for Day Two

Train	Velocity L1 to L2	Velocity L2 to L3	Velocity L1 to L3
		Metres per second	
1 (↑)[15]	4.04	8.91	6.04
2 (↓)	3.75 (L1: 10.66[16])	NK[17]	NK
3 (↓)	9.53	9.52	9.52
4 (↑)	L1: 9.74	NK	NK
5 (↑)	20.98 (L1: 22.05)	12.46	14.82 (L3: 15)
6 (↓)	8.1	18.5	7.21
7 (↓)	8:74/26.33 (L1: 16.45)	L2: 11.77	NK
8 (↓)	9.83 (L1: 10.91)	L2: 8.94	NK – Halted on Spur
9 (↑)	9.15	L2: 8.32	NK

[14] Time is considered to be unreliable
[15] Northbound Symbol
[16] Instantaneous Velocity from Pass Time
[17] Not Known

Train 7 was counted by two people at Location 1. The time estimate for the arrival at Location is 11:24 for the first counter and 11:26 for the second counter. If the velocity for counter 1 is adopted the train is travelling at 26.33 m/s[18] and for second counter is 8:74 m/s which is probably low. Train 5 appears to have been accelerating once it crossed University Drive.

Figure 46 shows the estimated train speeds based on the timing data collected at the three locations. The direction of the train, either up or northbound or down or southbound is also shown on the figure. The average velocity measured was 9.95 m/s.

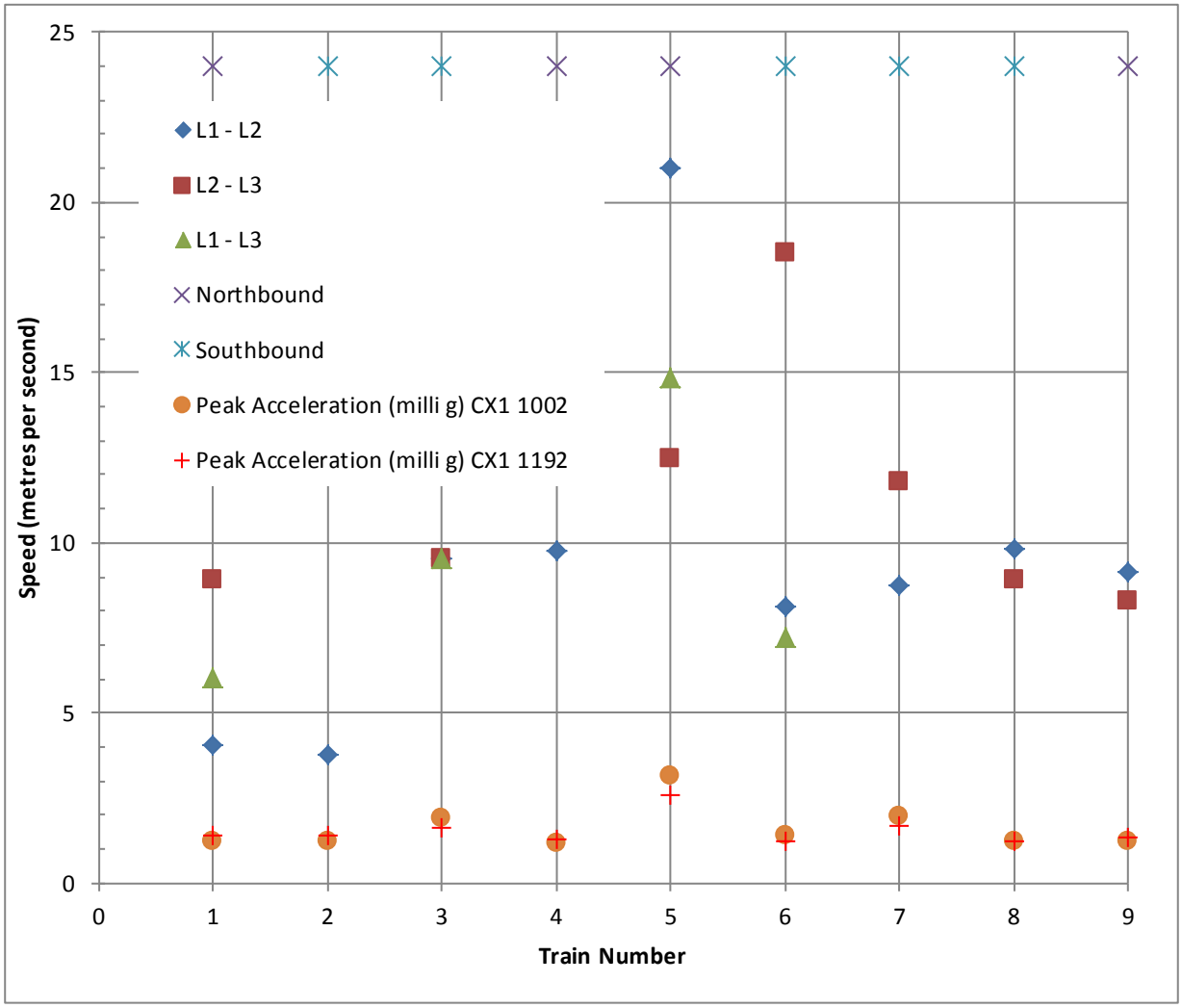

Figure 46 Train Speed and Direction

Train speed appears to be controlled in the section south of University Drive and given the movement of students and traffic across this section of railway line the reasons are self-evident.

Table 15 summarizes the count of the different types of cars on each train. Each train was counted at each location. Discrepancies exist in the counts as the counters were not skilled in differentiating the care types.

[18] 59 miles per hour, which is unlikely.

Table 15 Train Car Types Count

Train				Car Type				
#	1	2	3	4	5	6	7	8
1	0	2	2	18	0	1	23	0
	19	2	0	0	0	2	24	0
2	0	0	0	0	0	0	0	33
	2	0	0	0	0	0	0	35
3	0	0	0	114	0	0	0	0
	0	0	0	110	0	0	0	0
	0	0	0	100	10	0	5	0
4	0	2	2	17	2	0	23	0
5	0	0	0	0	98	0	0	0
	0	0	0	0	90	0	0	0
	0	0	90	0	0	0	0	0
6	0	46	0	0	0	0	0	0
	0	46	0	0	0	0	0	0
	0	45	0	0	0	0	0	0
7								
	1	10	2	0	29	2	30	8
	21	4	4	5	11	0	31	4
8	4	2	1	2	0	3	10	0
9	0	0	83	0	0	0	0	0
	0	0	0	0	87	0	0	0
	0	0	83	0	0	0	0	0
8	7	2	0	0	0	2	10	0
	0	2	2	5	1	2	11	0

10.Peak Acceleration Results – Day Two

Figure 47 shows the peak, average and minimum X accelerations for the CX1 1002 accelerometer on the second day. Figure 48 shows the peak, average and minimum Y accelerations for the CX1 1002 accelerometer on the second day. Figure 49 shows the peak, average and minimum Z accelerations for the CX1 1002 accelerometer on the second day

The negative acceleration in the Figure 47 merely indicates that the instrument was not level. The results show some form of disturbance at about the 100^{th} record set. It is likely this is some form of internal movement or activity in the building near the accelerometers as it is not of the form evident in the movement of trains.

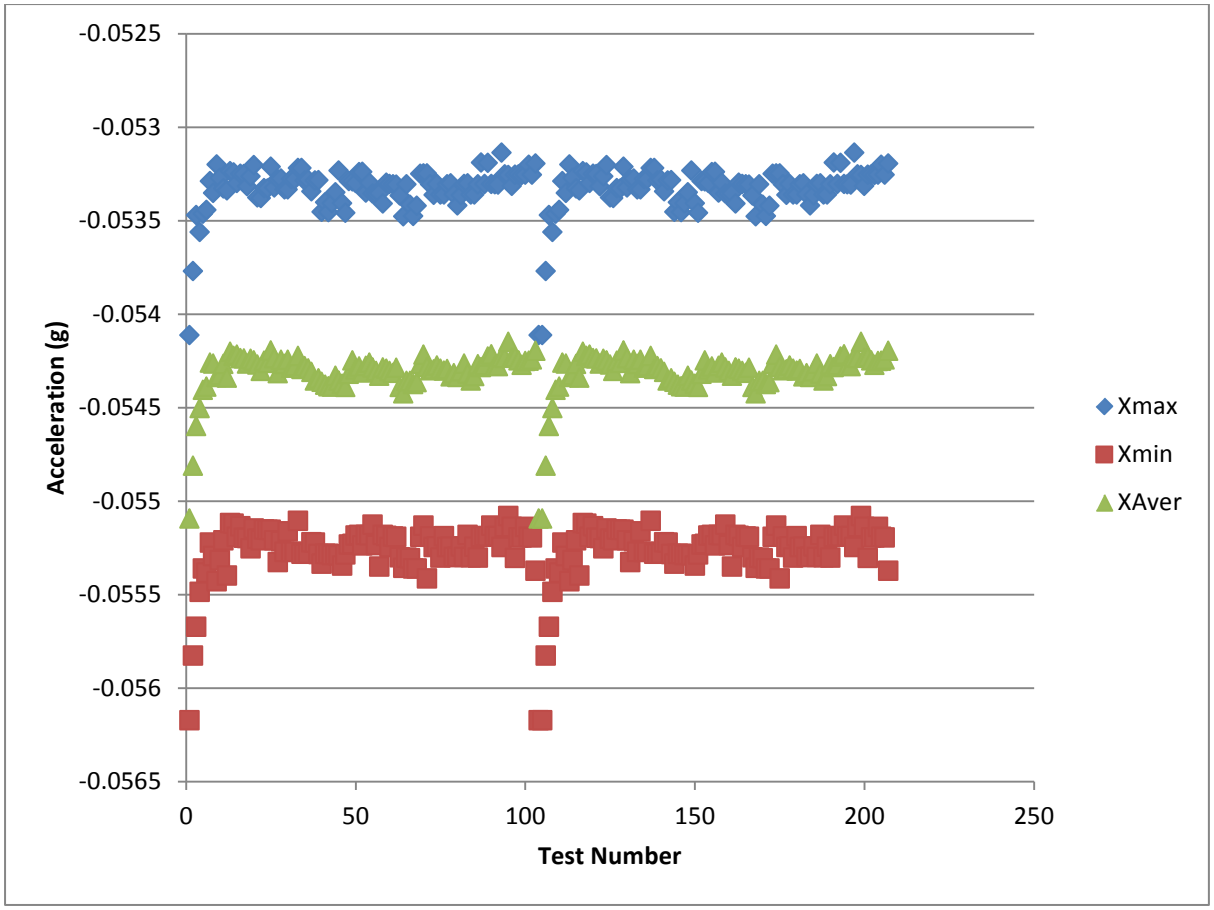

Figure 47 SENSR CX1 1002 X Acceleration Data

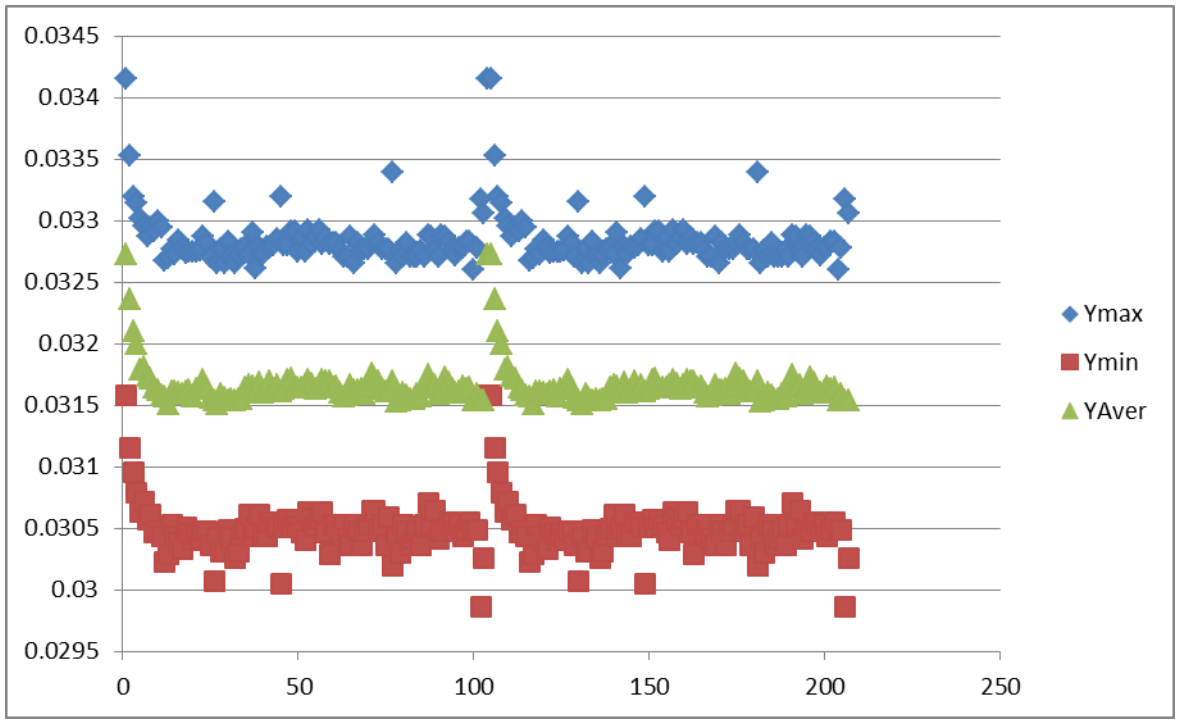

Figure 48 SENSR CX1 1002 Y Acceleration Data

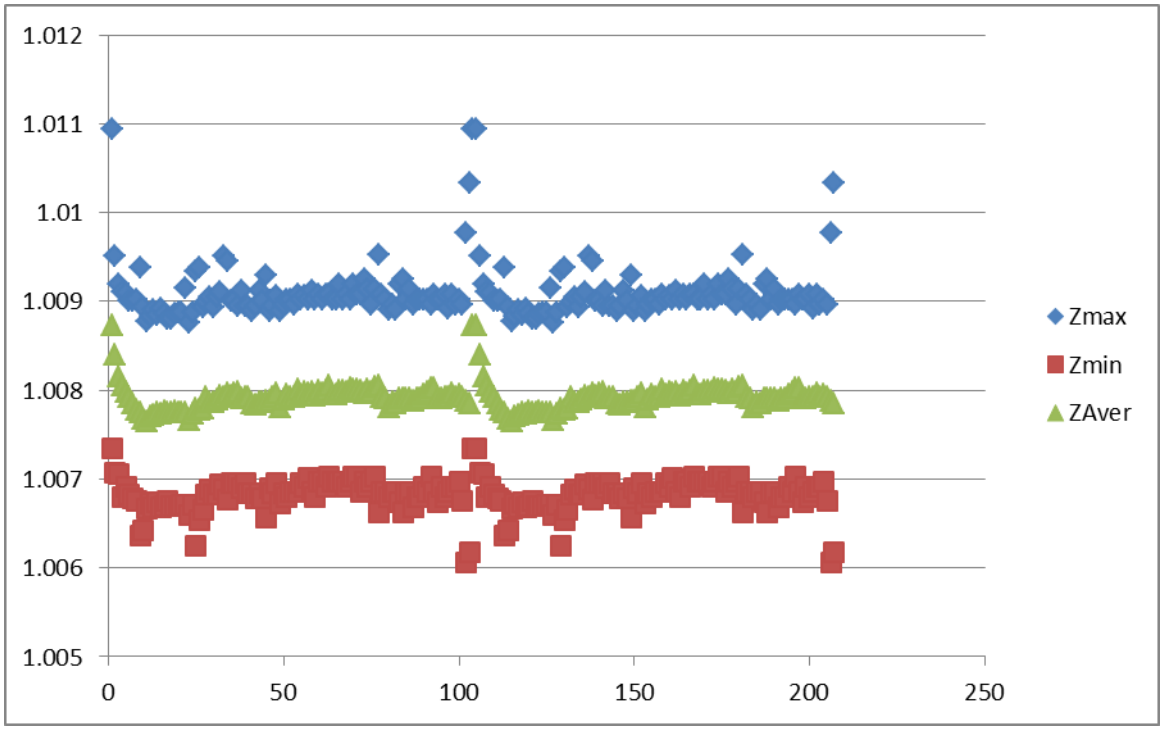

Figure 49 SENSR CX1 1002 Z Acceleration Data

11.Fast Fourier Transform Results – Day Two

Figure 63 shows the FFT data for the period in which the train enters the segment from Location 2 to Location 3 in a northbound[19] direction.

Figure 64 shows the FFT data for the period in which the train enters the segment from Location 2 to Location 3 in a northbound direction. This data is for the X acceleration, which is parallel to the tracks.

Figure 65 shows the FFT data for the period in which the train enters the segment from Location 2 to Location 3 in a northbound direction, being normal to the tracks.

Figure 66 shows the FFT data for the period in which the train enters the segment from Location 2 to Location 3 in a northbound direction, which is the vertical direction.

The results show a peak in the region of 12 Hertz. Figure 50 shows the FFT data set used to contour the Results Set 27 plotted as a single data set of acceleration level against frequency. It can be considered as looking sideways at a drawing of Figure 66.

[19] Confirm direction of movement

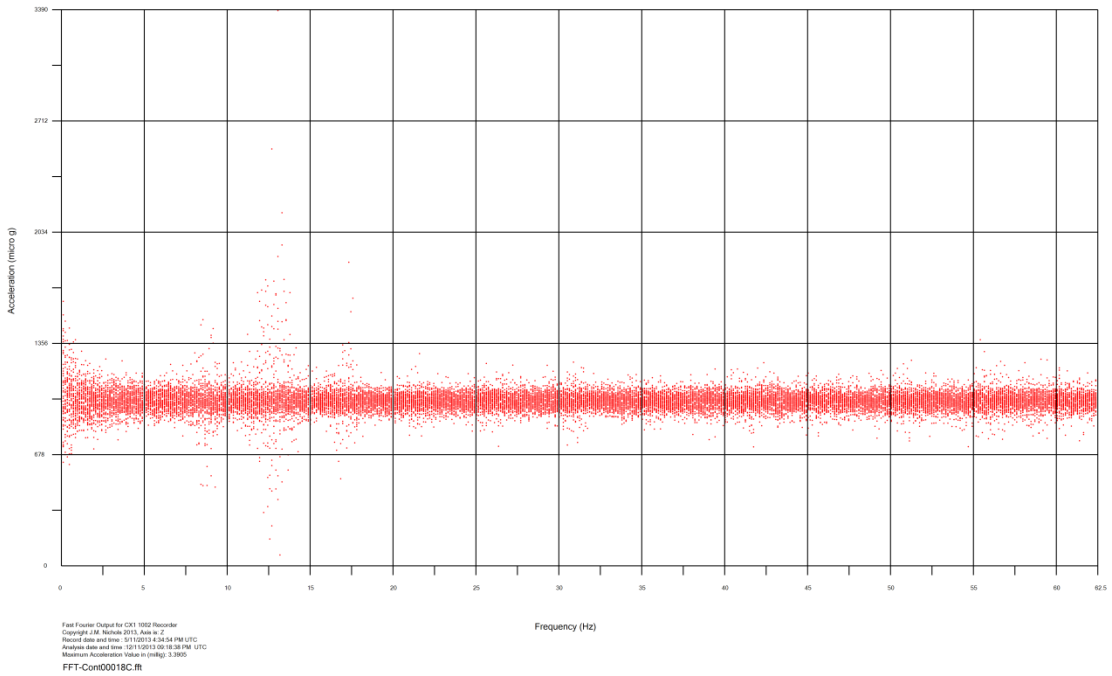

Figure 50 FFT Point Data 27 Z Direction from Day Two, Train onto Bridge

Figure 50 shows the scattered statistical data used in the Variance Model to estimate the FFT spectrum of frequencies of interest in the study. The assumption is these frequencies provide a reasonable representation of the natural frequencies defined by Newtons' equation of motion.

Figure 67 shows the FFT Spectrum data for the 27th data set. The results show three peaks of interest, in the range of 0.5 to 20 Hertz.

Figure 51 shows a plot of the speed of the trains at Location 1 plotted against the maximum accelerations measured at Stations 2 and 3 on Day 2 and Station 2 . The issues with the measurement of the velocity are that:

1. the trains are decelerating as each train approaches College Station
2. the only complete set of velocity measurements on Day 2 occurred at Location 1 due to the issue of rain and changing counters at Location 3
3. no mass is known on the trains and clearly this will have an impact on the loads

The train velocity does have an impact on the peak acceleration measured in the building, the relationship is that an increase of 1 m/s in train speed increases the acceleration by 0.12 milli-g. Beyond that insufficient information exists to determine the impact of the trains.

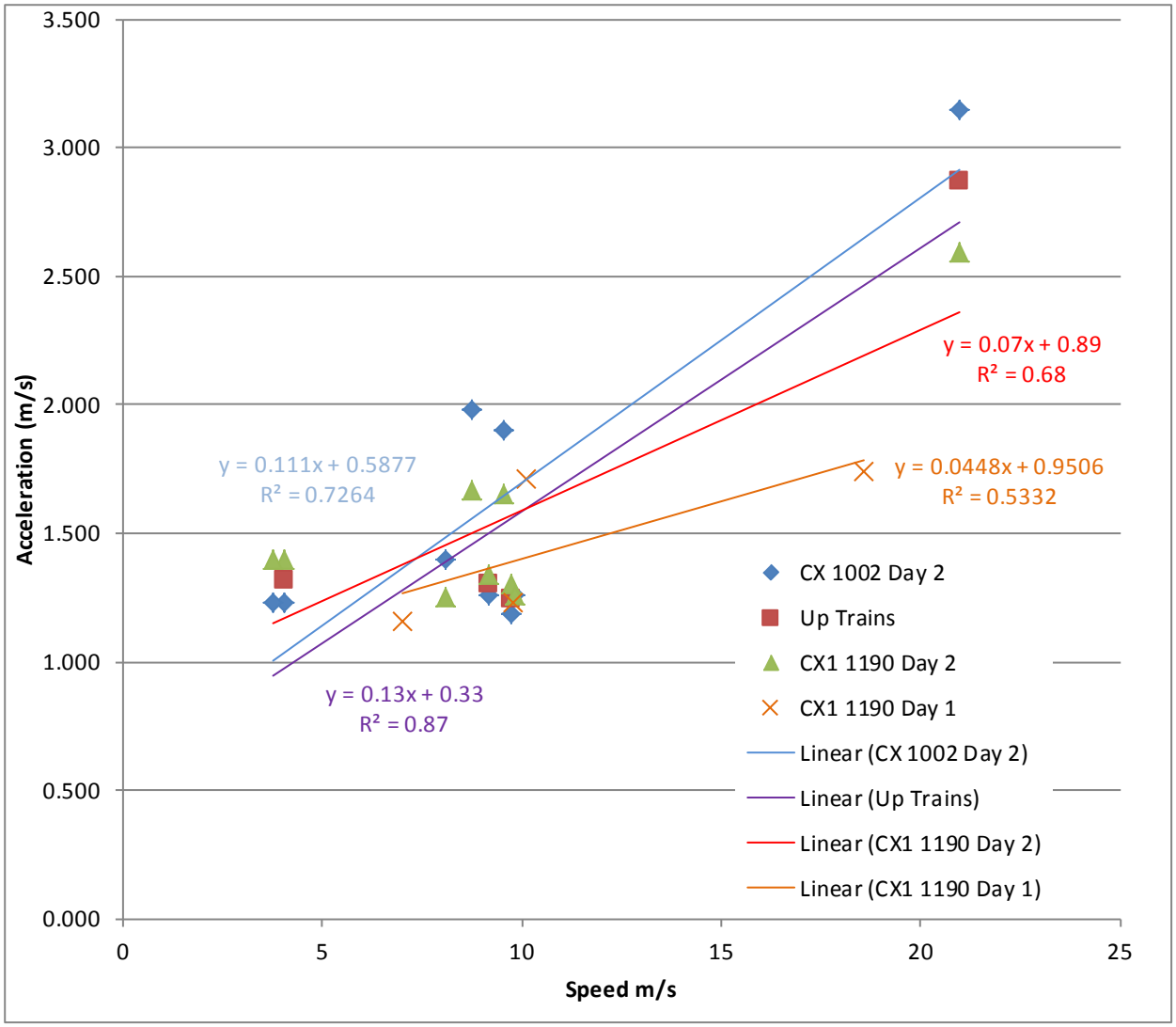

Figure 51 Speed of the Trains against Peak Acceleration

12.Ambient Noise Study Results

The ambient noise study is summarized in this section.

Figure 52 shows the maximum and minimum acceleration levels for the X direction for the first 26 tests.

Figure 53 shows the maximum and minimum acceleration levels for the Y direction for the first 26 tests.

Figure 54 shows the maximum and minimum acceleration levels for the Z direction for the first 26 tests.

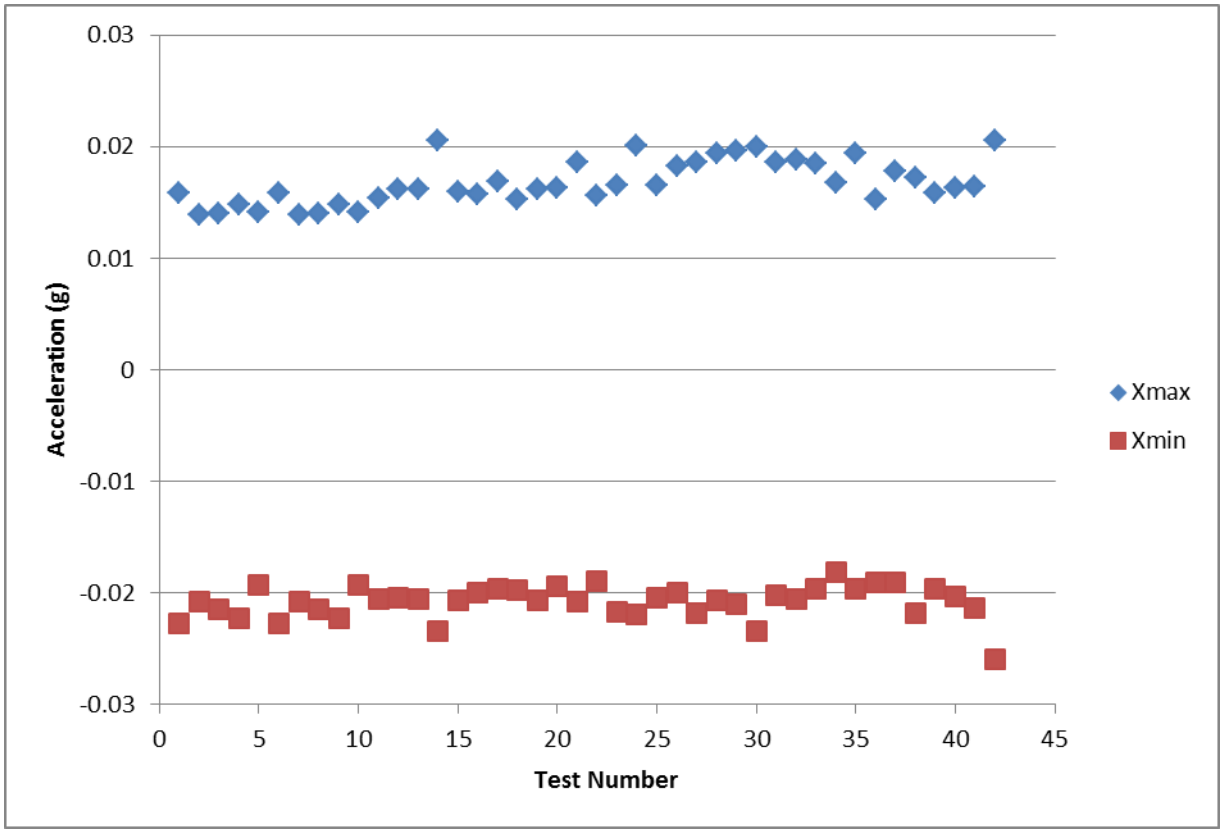

Figure 52 Acceleration Levels for X Direction

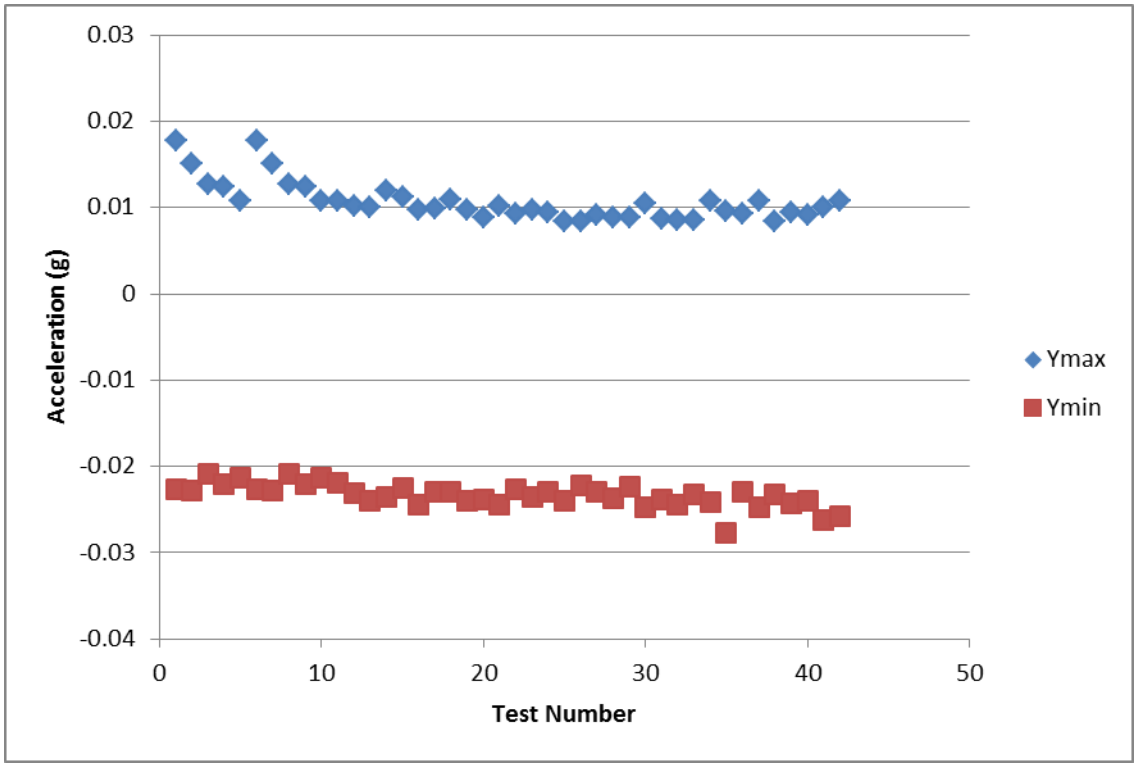

Figure 53 Acceleration Levels for Y Direction

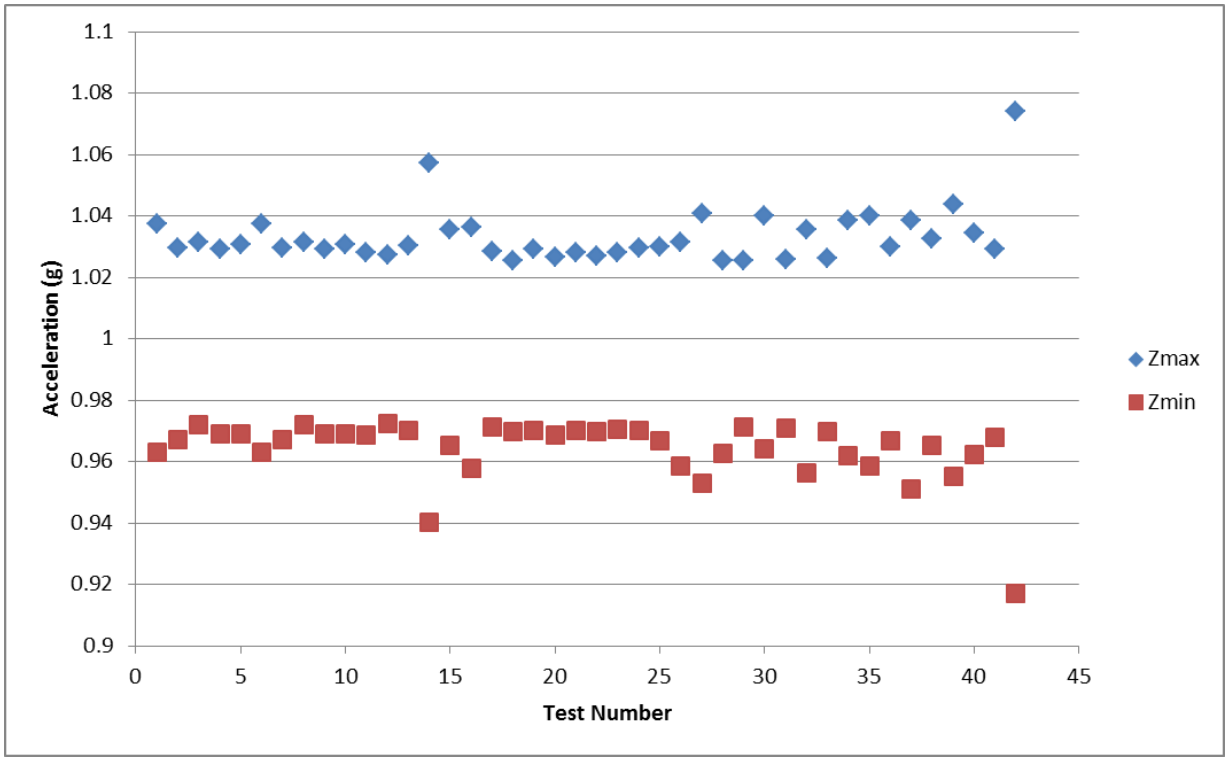

Figure 54 Acceleration Levels for Z Direction

Figure 68 shows the ambient noise level for the X direction for set five of the results.

Figure 69 shows the ambient noise level for the X direction for set nine of the results.

Figure 70 shows the ambient noise level for the Z direction for set five of the results.

Figure 71 shows the ambient noise level for the Z direction for set nine of the results.

Figure 55 shows the FFT data set used to contour the Results Set 5 Z plotted as a single data set of acceleration level against frequency. It can be considered as looking sideways at a drawing of Figure 70.

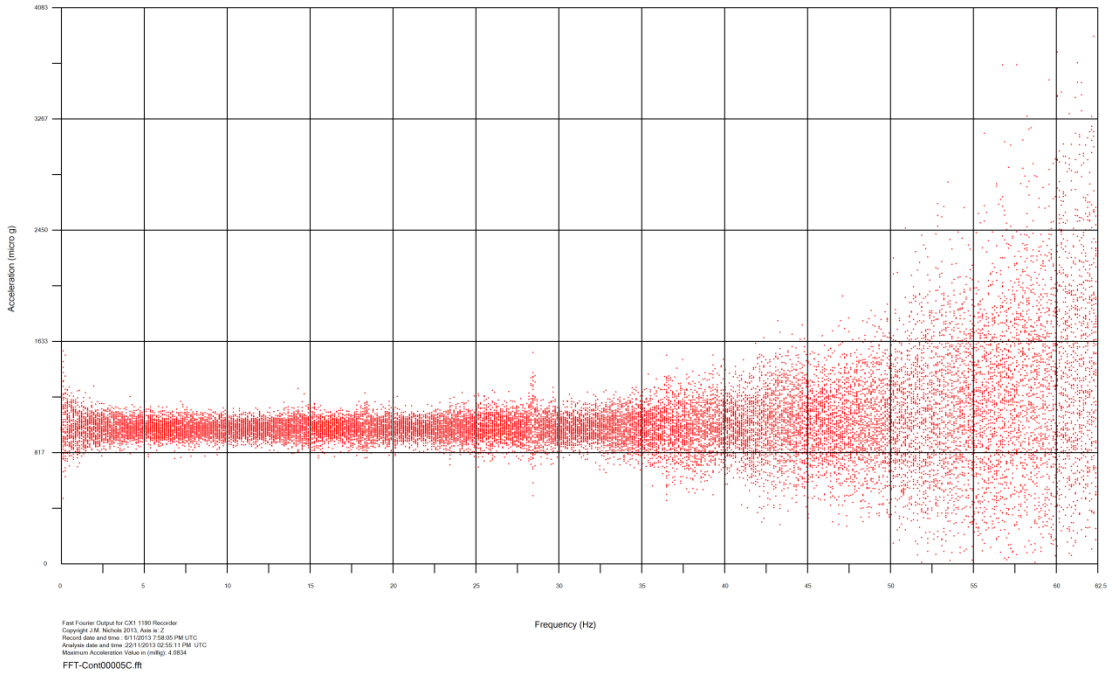

Figure 55 FFT Point Data 5 Z Direction – Ambient Study

Figure 56 shows the FFT data set used to contour the Results Set 27 plotted as a single data set of acceleration level against frequency. It can be considered as looking sideways at a drawing of Figure 71.

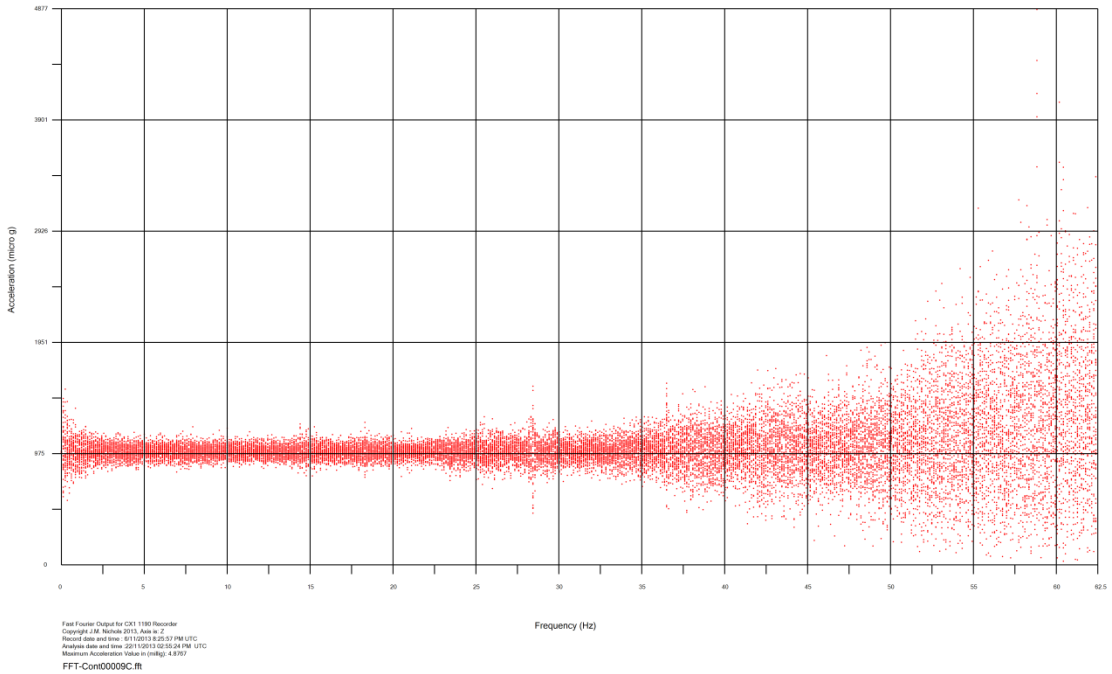

Figure 56 FFT Point Data 9 Z Direction – Ambient Study

Figure 71 shows the FFT Spectrum for the fifth data set.

Figure 73 shows the FFT Spectrum for the ninth data set.

The results for the ambient noise study show that the signal is concentrated in the region about 50 Hz. In the small set reviewed for this draft of the report the peak signal occurred at the 12th data set with a value of 12 milli g. Figure 74 shows the peak signal observed in this small sample of the total data set for the ambient study.

13. Day One Acceleration Contour Plans for Train Movements

Four trains were observed to pass *The Building* on the first day of the experimental work. The acceleration contour plans for the Z direction for the passage of the four trains are shown on Figure 75, Figure 76, Figure 77, Figure 78, Figure 79 and Figure 80for Trains One to Four respectively.

The results show the impact of the trains on the building in the range of 5 to 12 Hertz. Figure 81 and Figure 82 show the Y and X direction acceleration data for the fourth train. Figure 83 shows the Spectrum Frequency Set. The histogram along the top axis of the plot shows the relative strength of the modal points. *The Building* is responding in the range of 5 to 7 Hz for this train loading.

14.Day Attenuation Data

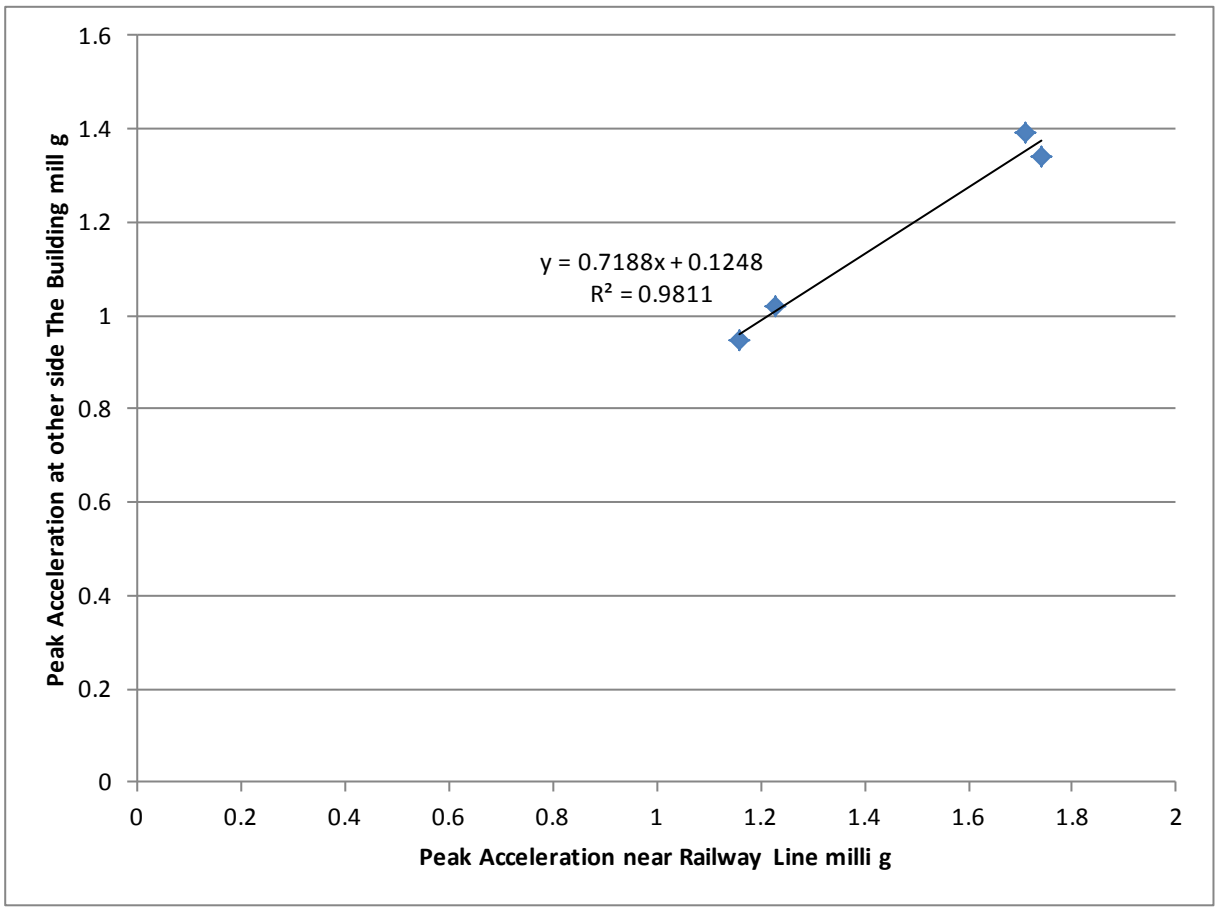

Figure 57 Acceleraton Levels at Front and Back of the Building on Day 1 - Four Trains

Chapter 5. Conclusions

The Building is located on the western side of the adjacent Houston and Texas Central (H&TC) Railroad line which has served the Bryan and College Station regions for more than a century. *The Building* used for the storage of Food for the University Dining System was situated at this location so that a spur line could be provided from the adjacent main trunk line. The spur line geometry requirements clearly limited the locations available for this storage area.

CIS requested a study on the impact of the train movements on the adjacent Houston and Texas Central (H&TC) Railroad line. The study involved collecting vibration data for *The Building* on the 17 October 2013 and 5 November 2013 using two CX1 accelerometers. An ambient noise study involved collecting vibration data for the existing Computer Services Centre on the fourth floor for the period 6 November 2013 until 11 November 2013. The analysis of the ambient noise study for this draft report was limited to a short set of data from the 6 November 2013, due to time constraints.

The study showed that the train traffic does cause a vibration in *The Building*, which can be measured using the SENSR CX1 accelerometer and a standard recording program. Data was collected at three locations in the building over two days, the results show that the average vibration is in the order of 3 to 4 milli-g's when an average train passes. The frequency of the peak movements is in the range of 1 to 15 Hz, which is prototypical for a building and matches the general expectations for this type of construction.

The limitations for this study are:

1. The mass of the trains could not be determined
2. The geology of the local area was not considered for the analysis to determine if this impacts on the vibration levels
3. The study was limited to two days, 17 October 2013 and 5 November 2013, these are deemed to be representative of the typical traffic on the rail track
4. Due to Homeland Security concerns this previous limitation cannot be checked or confirmed
5. No analysis was made of the wave generated in the ground with the passage of the trains
6. No observations were made as the track used for each train in the region of The Building, due to safety restrictions on entering this railway area and undergrowth
7. No information was available on the slab in *The Building* to determine the natural frequencies of the slab, this would be a natural second step to see if the observed frequencies may be a future problem

8. No recording was made of interior movements inside The Building during the study period

9. The occupants of the building or machinery inside the building may have impacted the results, but the problem data sets were reviewed and if warranted discarded

The ambient noise study showed a peak vibration level of 12 milli-g, but at a frequency in excess of 50 Hertz.

The limitations on the ambient noise study are:

1. No observation was made of the movements of the occupants during the study period

2. The study period was considered to be a typical period of use and vibration levels

3. No data was collected on the type of equipment used in the data centre

4. The short data set analysed for this draft report represents the conditions for the centre

Building collapse will occur at about 100 milli g's as has been recently observed in Italy and Australia in two tragic earthquake. The levels of vibration generated by the trains are not likely to cause serious issues with the building over the long term, except for any potential fatigue of steel connections.

The analysis of the experimental data has shown that the building responds to the surface waves generated by the railway track.

Chapter 6. References

Atkinson, G. M., & Boore, D. M. (1995). Ground motion relations for Eastern North America. *Bulletin of the Seismological Society of America, 85*(1), 17-30

Boore, D. (1997). [‘Personal communication late 1997"].

Boore, D. M. (2005). On Pads and Filters: Processing Strong-Motion Data. *Bulletin of the Seismological Society of America, 95*(2), 745-750

Boore, D. M., & Atkinson, G. M. (1989). Spectral scaling of the 1985 to 1988 Nahanni, Northwest Territories, earthquakes. *Bulletin of the Seismological Society of America, 79*(6), 1736-1761

Boore, D. M., Azari Sisi, A., & Akkar, S. (2012). Using Pad-Stripped Acausally Filtered Strong-Motion Data. *Bulletin of the Seismological Society of America, 102*(2), 751-760

Bourke, P. (1987). ConRec - A contouring subroutine. *Byte, 12*(6), 143 - 150

Brigham, E. O. (1988). *The fast Fourier transform and its applications*. Englewood Cliffs: Prentice.

Brune, J. N. (1970). Tectonic Stress and the Spectra of Seismic Shear Waves from Earthquakes. *Journal of Geophysical Research, 75*(26), 4997 - 5009

Cassidy, J. F., Rogers, G. C., Lamontagne, M., Halchuk, S., & Adams, J. (2010). Canada’s Earthquakes: ‘The Good, the Bad, and the Ugly. *Geoscience Canada, 37*(1), 1-20

Guha, P. (2008). *A Study of Traffic Induced Building Vibration.* Master of Science, Texas A&M, College Station.

Hall, W. J. (2001, 26 April 2001). [On the development of the alternative period formula's between the Indian and US Standards.].

Halliday, D., & Resnick, R. (1970). *Fundamentals of Physics*. NY: Wiley.

Heyman, J. (1995). *The Stone Skeleton*. Cambridge: Cambridge University Press.

IS 1983. (1984). *Criteria for the Earthquake Resistant Design of Structures*. New Delhi: Bureau of Indian Standards.

Kaplan, W., & Lewis, D. J. (1971). *Calculus and Linear Algebra*. NY: Wiley.

Kavanagh, B. F. (2004). *Surveying with Construction Applications*. Upper Saddle River: Pearson.

Kavars, C. (2012, 26 March 2012). [Comments on FFT and accelerometers being used for bridge damage evaluation].

Melchers, R. E., (Editor). (1990). *Proceedings of the Conference on the Newcastle Earthquake*, Newcastle. Institution of Engineers (Aust): pg. (1-10)

Melchers, R. E., & Page, A. W. (1992). The Newcastle Earthquake. *Building and Structures, 94*, 143-156

Nichols, J. M. (2003). *A Mathematical Review of the Non-Conservative Criteria Related to the Seismic Design Spectrum used in Intraplate Regions.* Paper presented at the XIV Mexican National Conference on Earthquake Engineering, Leon Mexico. Sociedad Mexicana de Ingeniería Sísmica, A. C.: pg.

Nichols, J. M. (2013). A Modal Study of the Pont-Y-Prydd Bridge using the Variance Method. *Masonry International*

Richter, C. F. (1958). *Elementary Seismology*. San Francisco: Freeman.

Exhibits

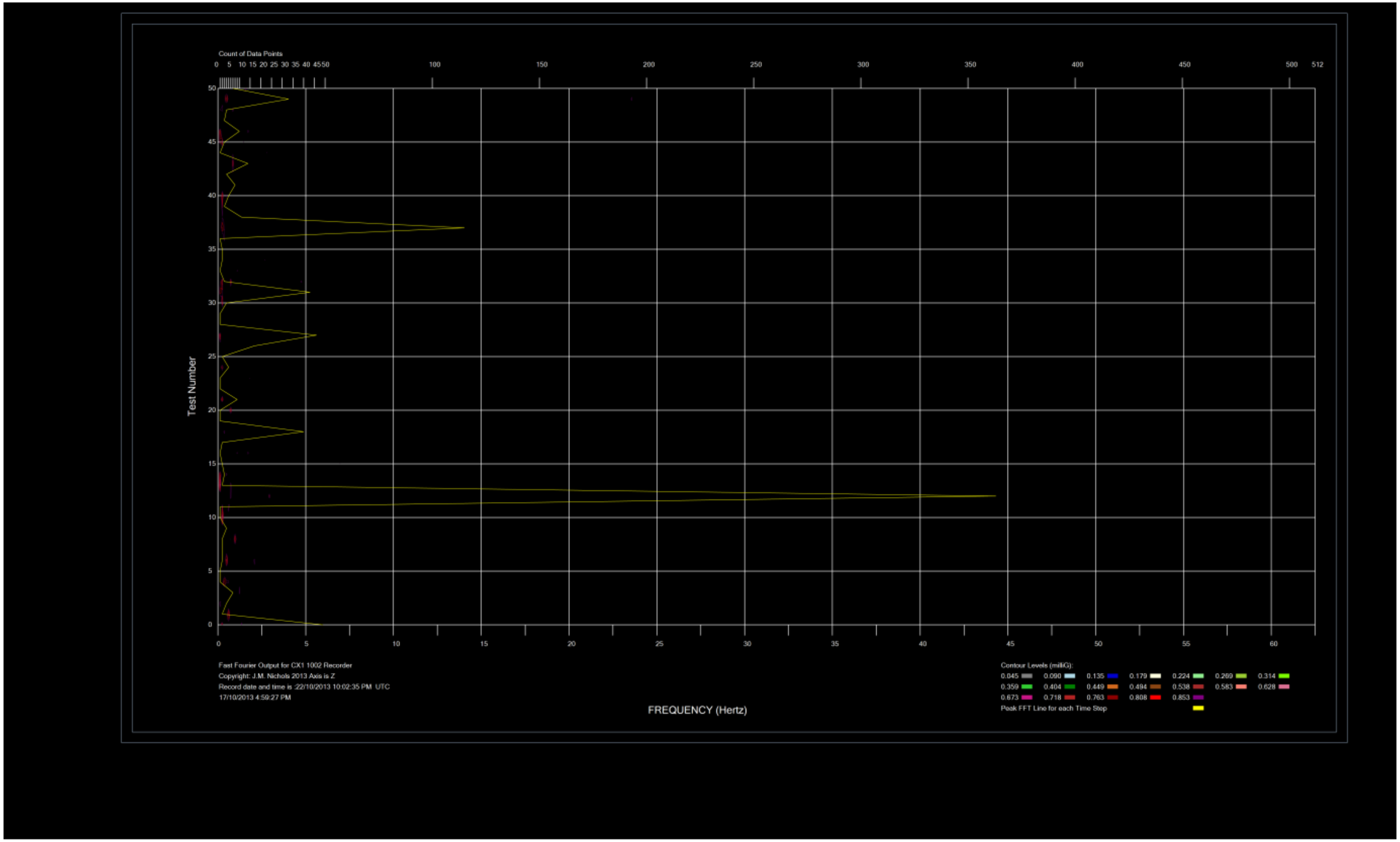

Figure 58 FFT Result 22 from Day One, essentially Brownian Motion

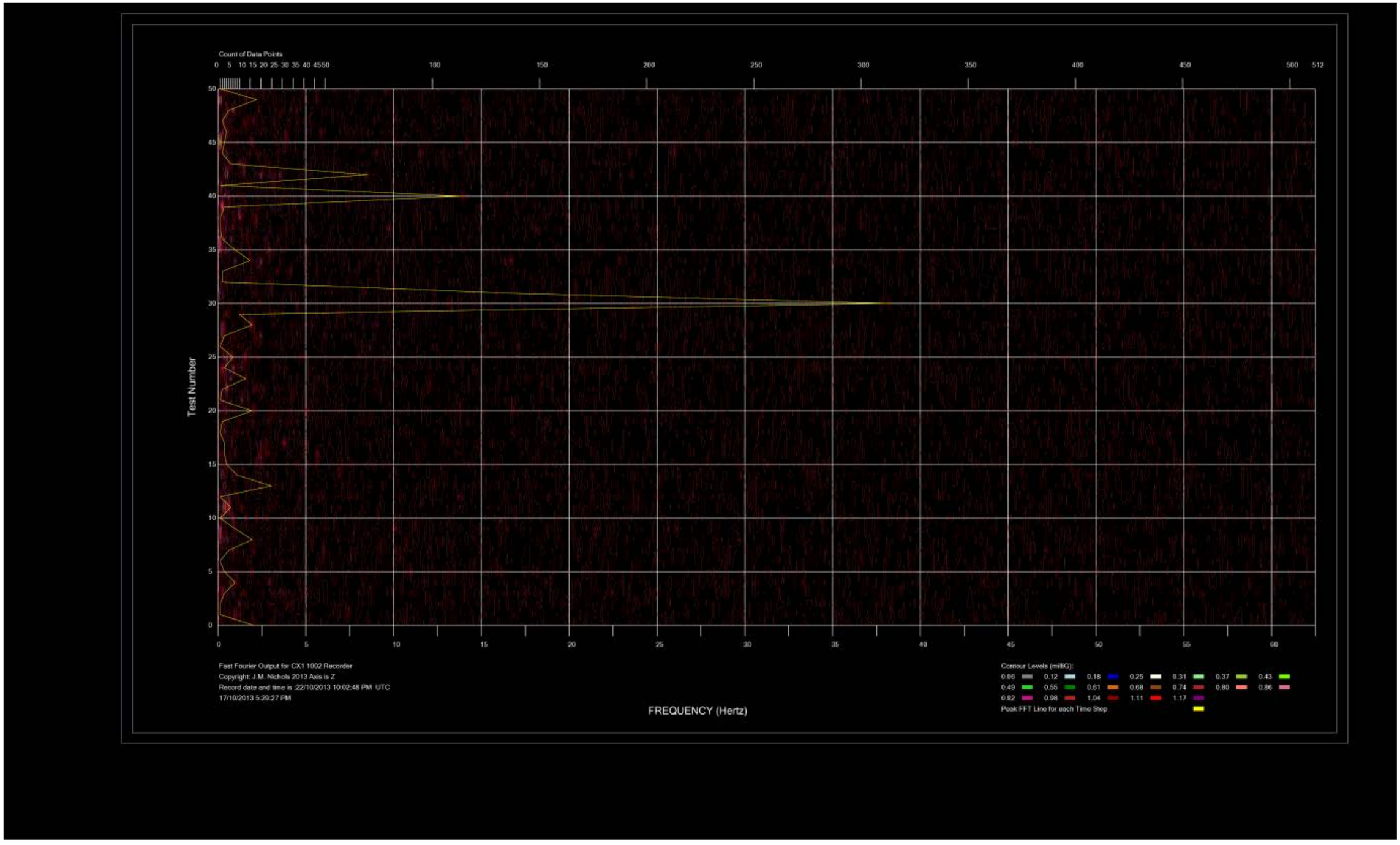

Figure 59 FFT Result 26 from Day One, Train onto Bridge

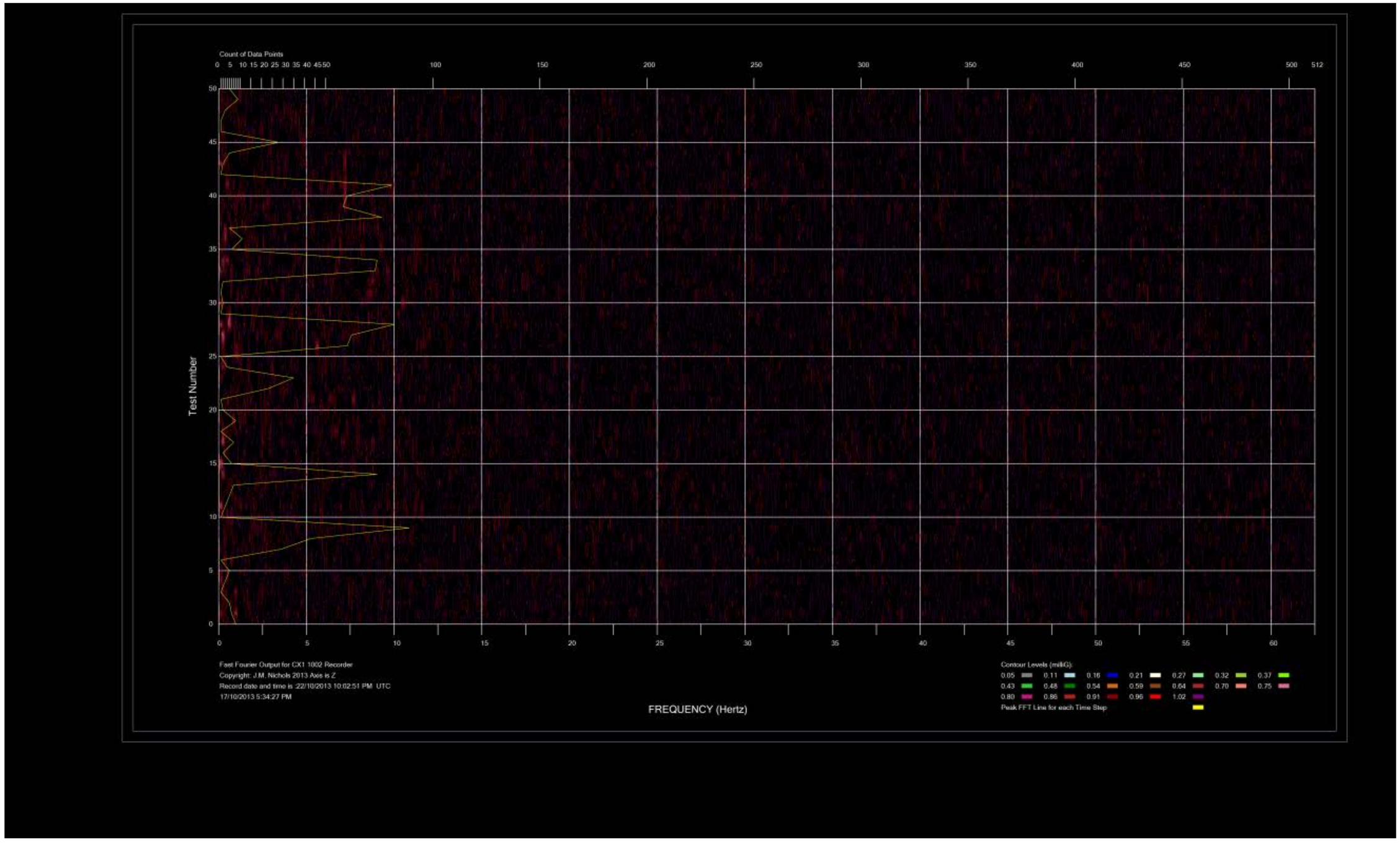

Figure 60 FFT Result 27 from Day One, Remainder of Train

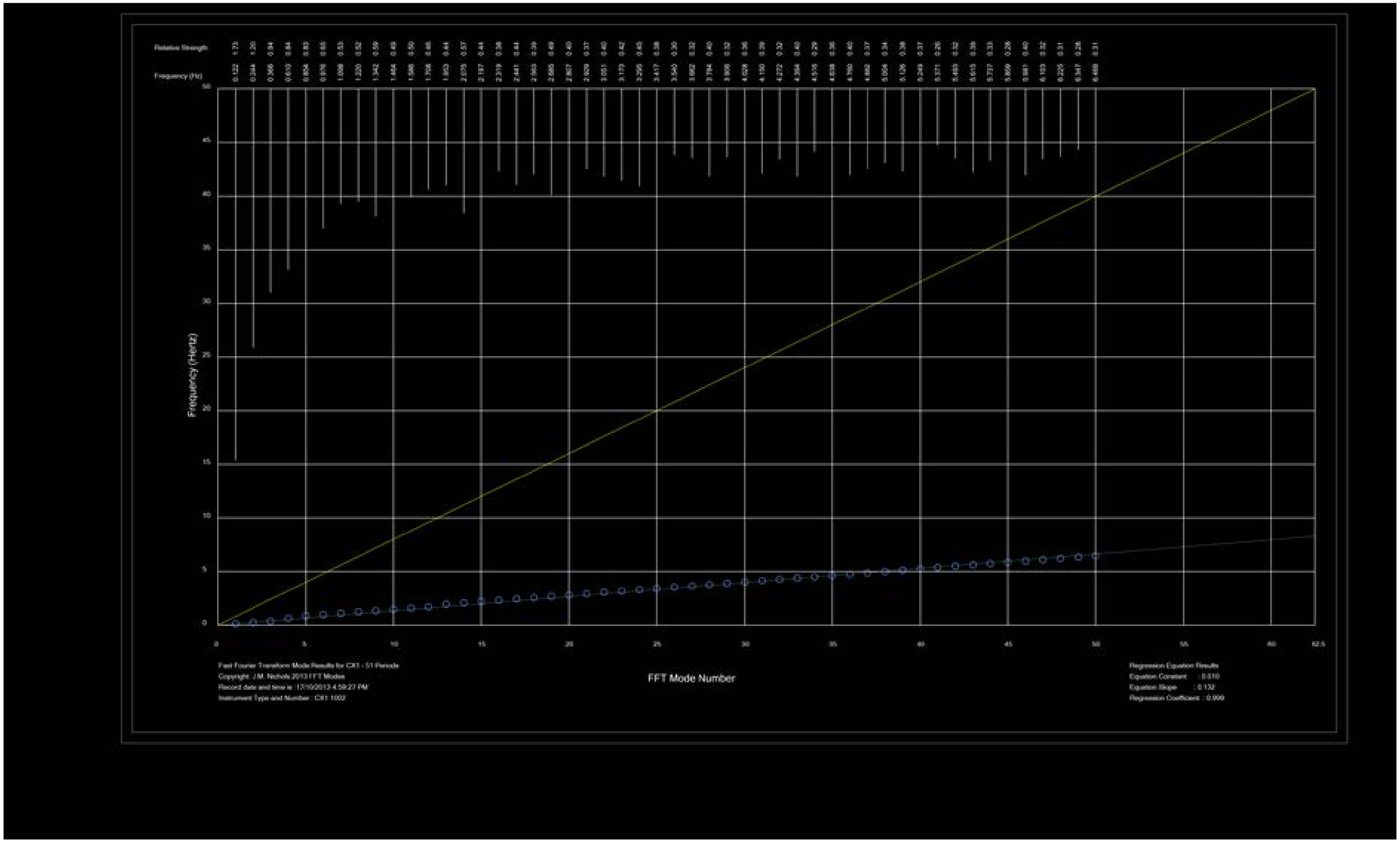

Figure 61 FFT Spectrum Modal Analysis for the 22nd Data Set

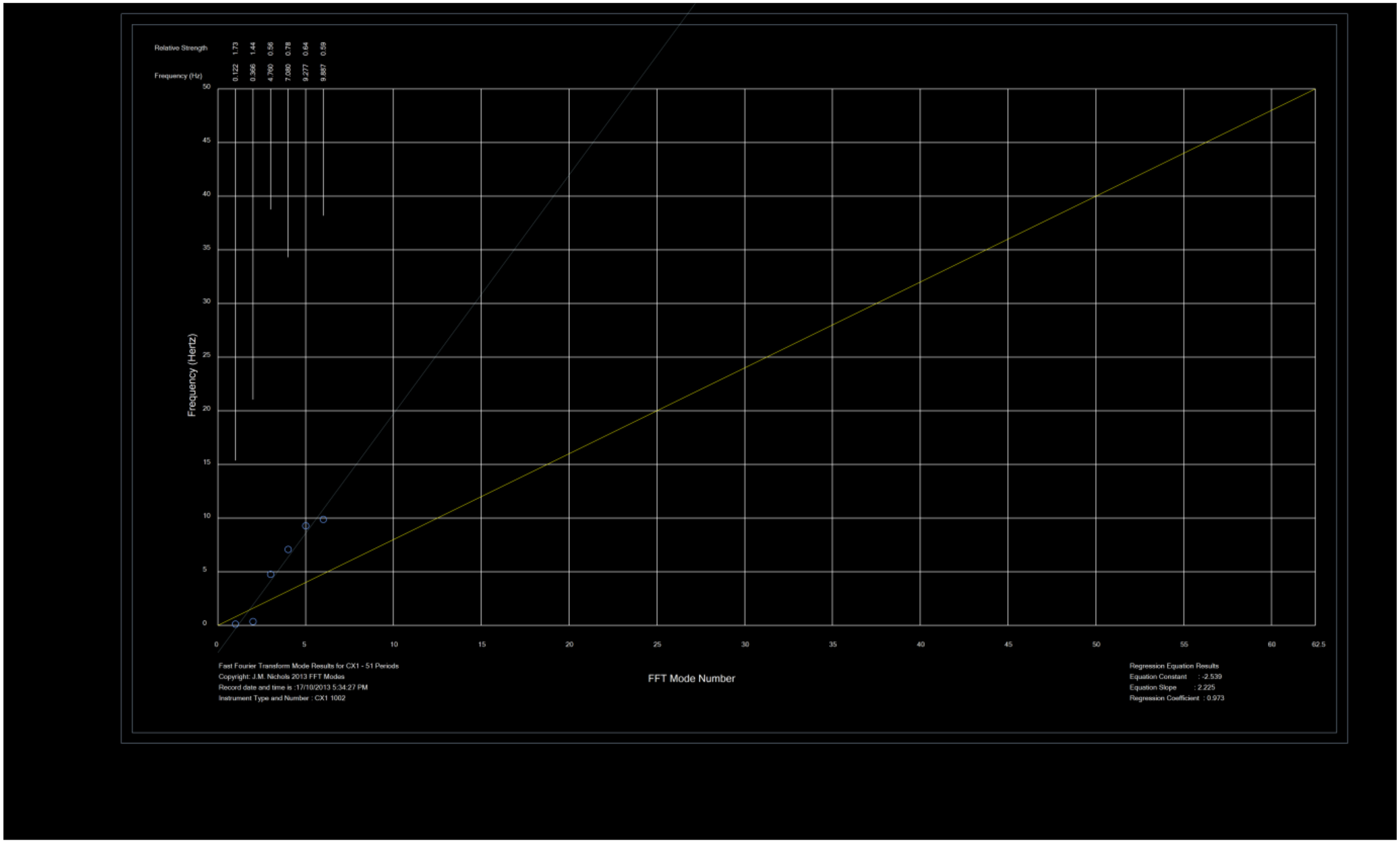

Figure 62 FFT Spectrum Modal Analysis for the 27th Data Set

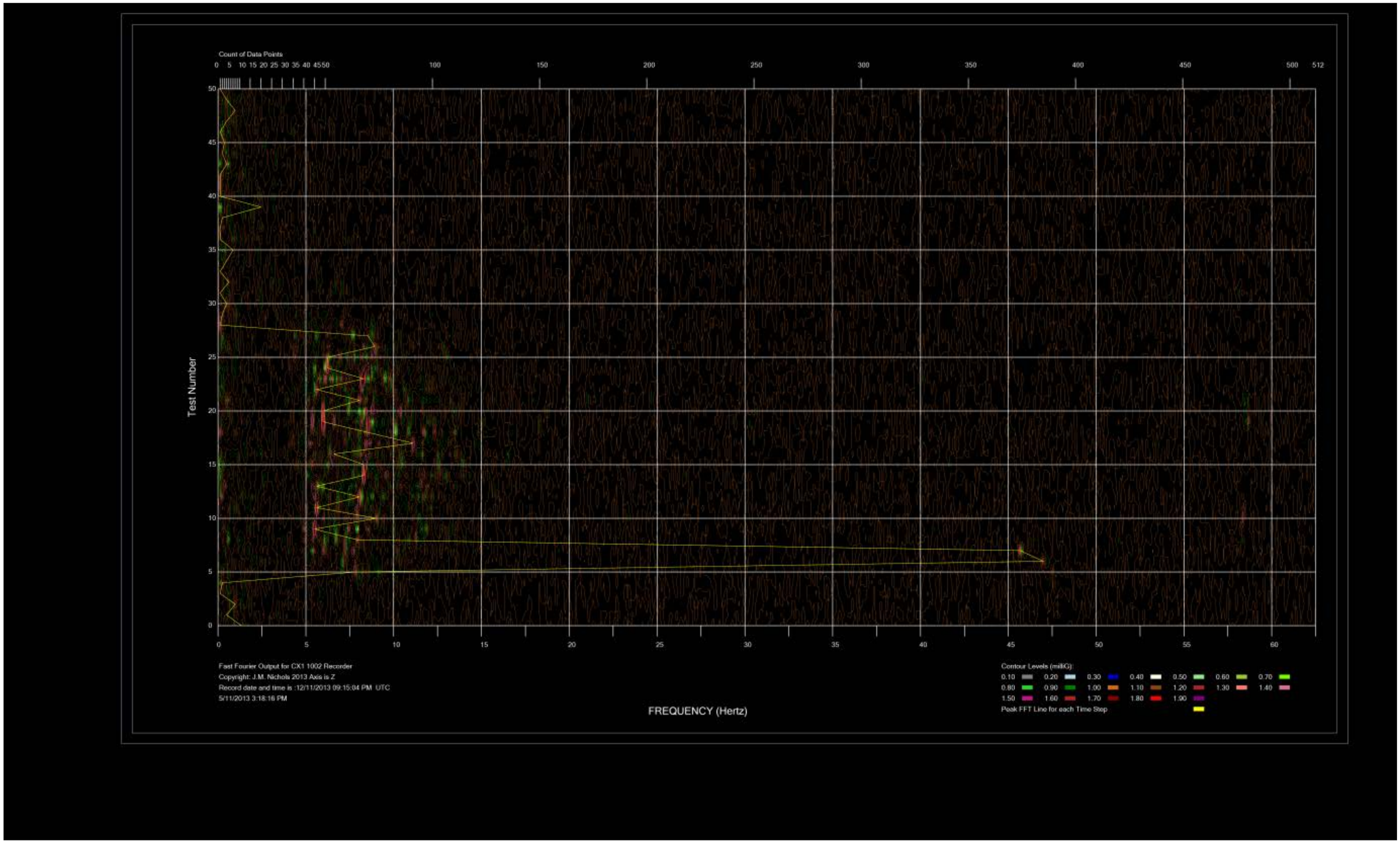

Figure 63 FFT Result 7 from Day Two, Train onto Bridge

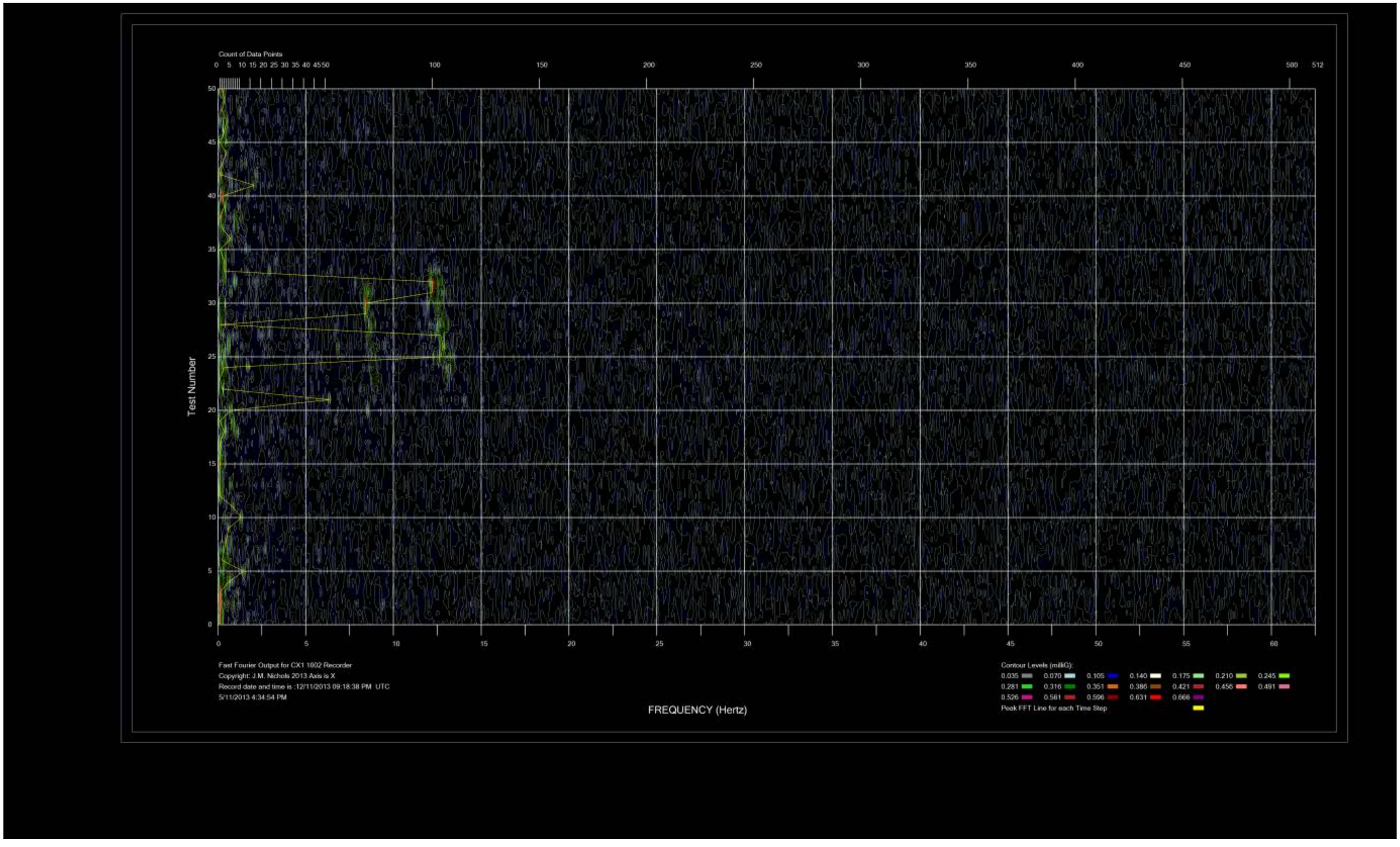

Figure 64 FFT Result 27 X Direction from Day Two, Train onto Bridge

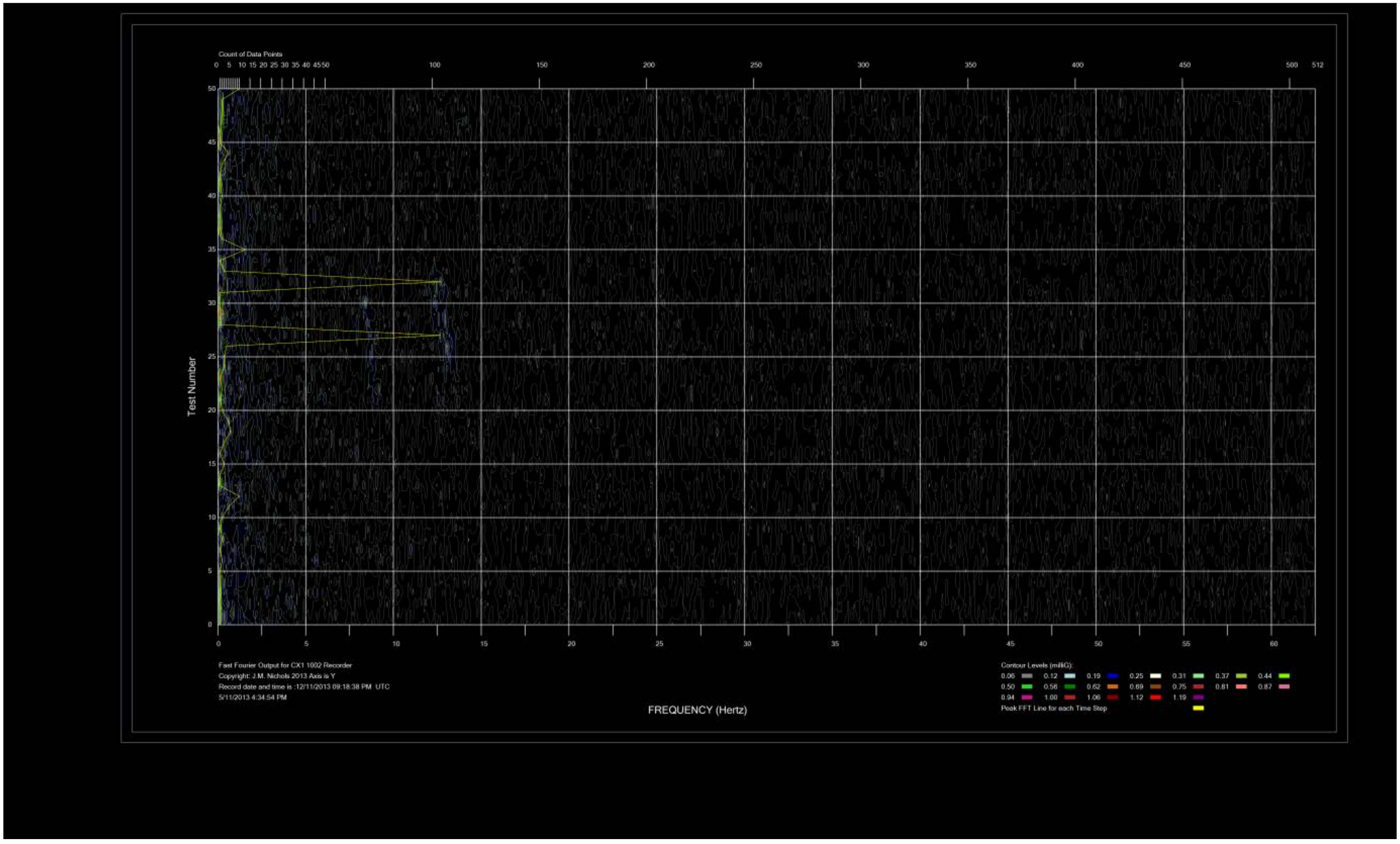

Figure 65 FFT Result 27 Y Direction from Day Two, Train onto Bridge

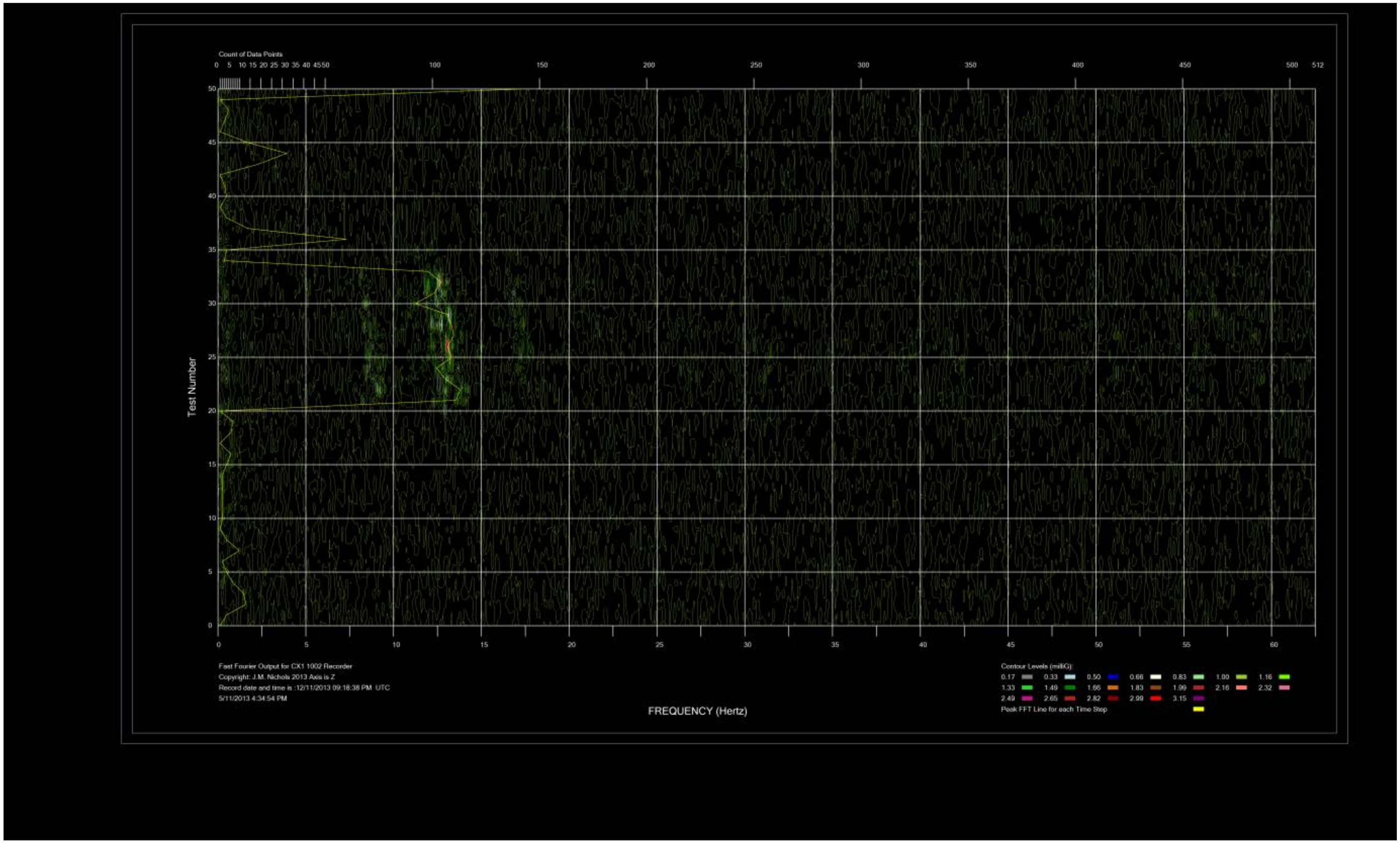

Figure 66 FFT Result 27 Z Direction from Day Two, Train onto Bridge

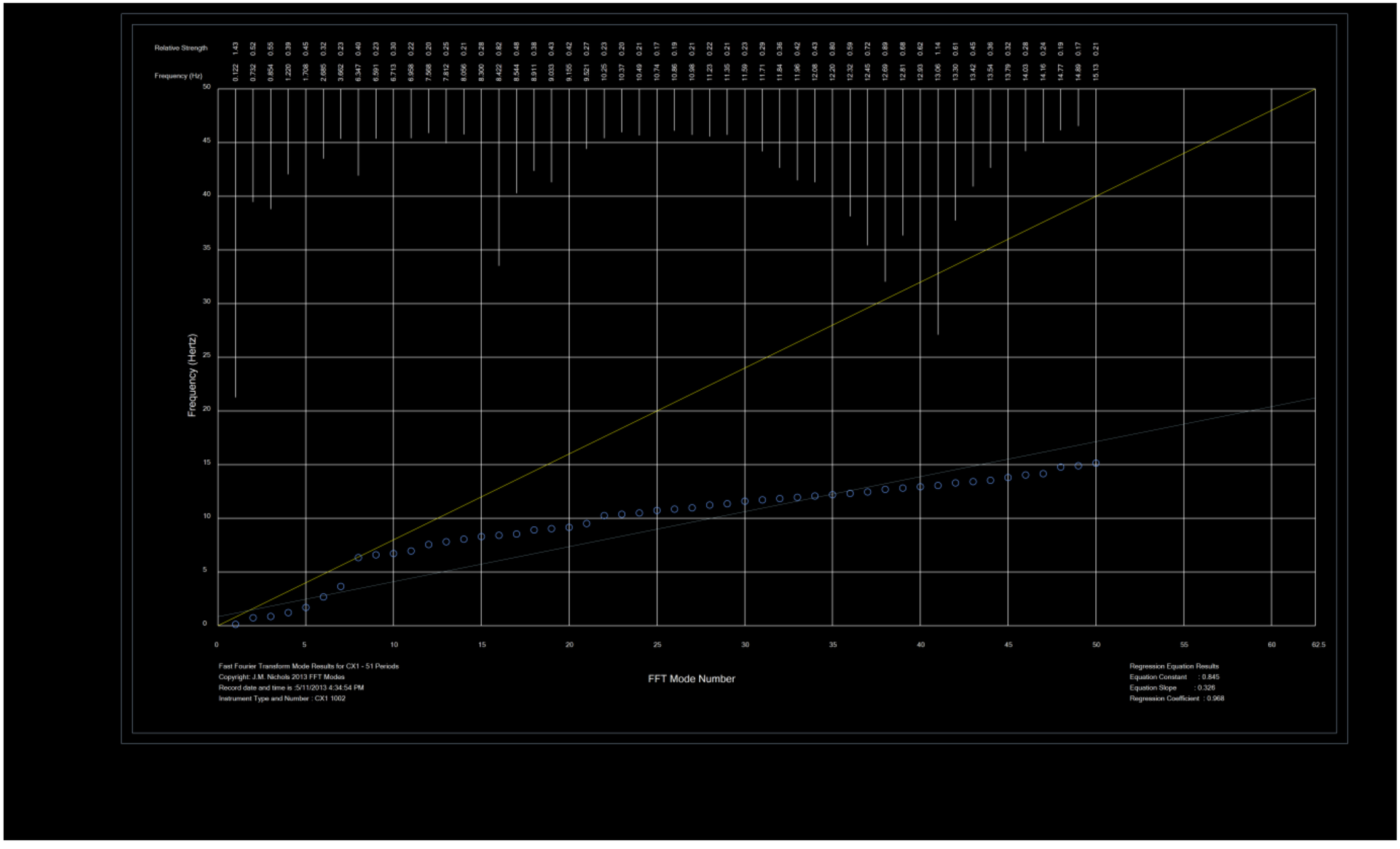

Figure 67 FFT Spectrum Modal Analysis for the 27th Data Set

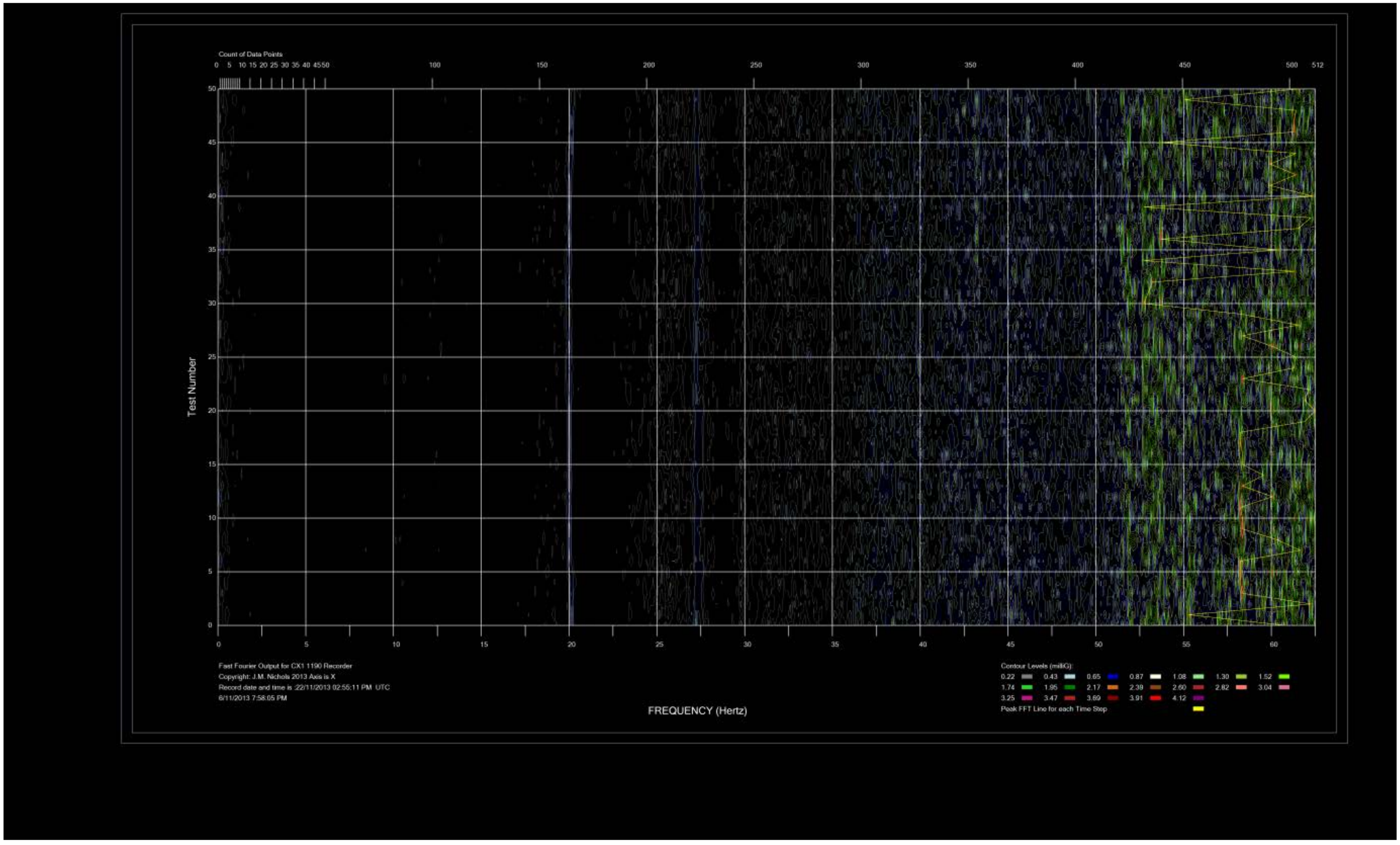

Figure 68- FFT Result 5 X Direction Ambient Study

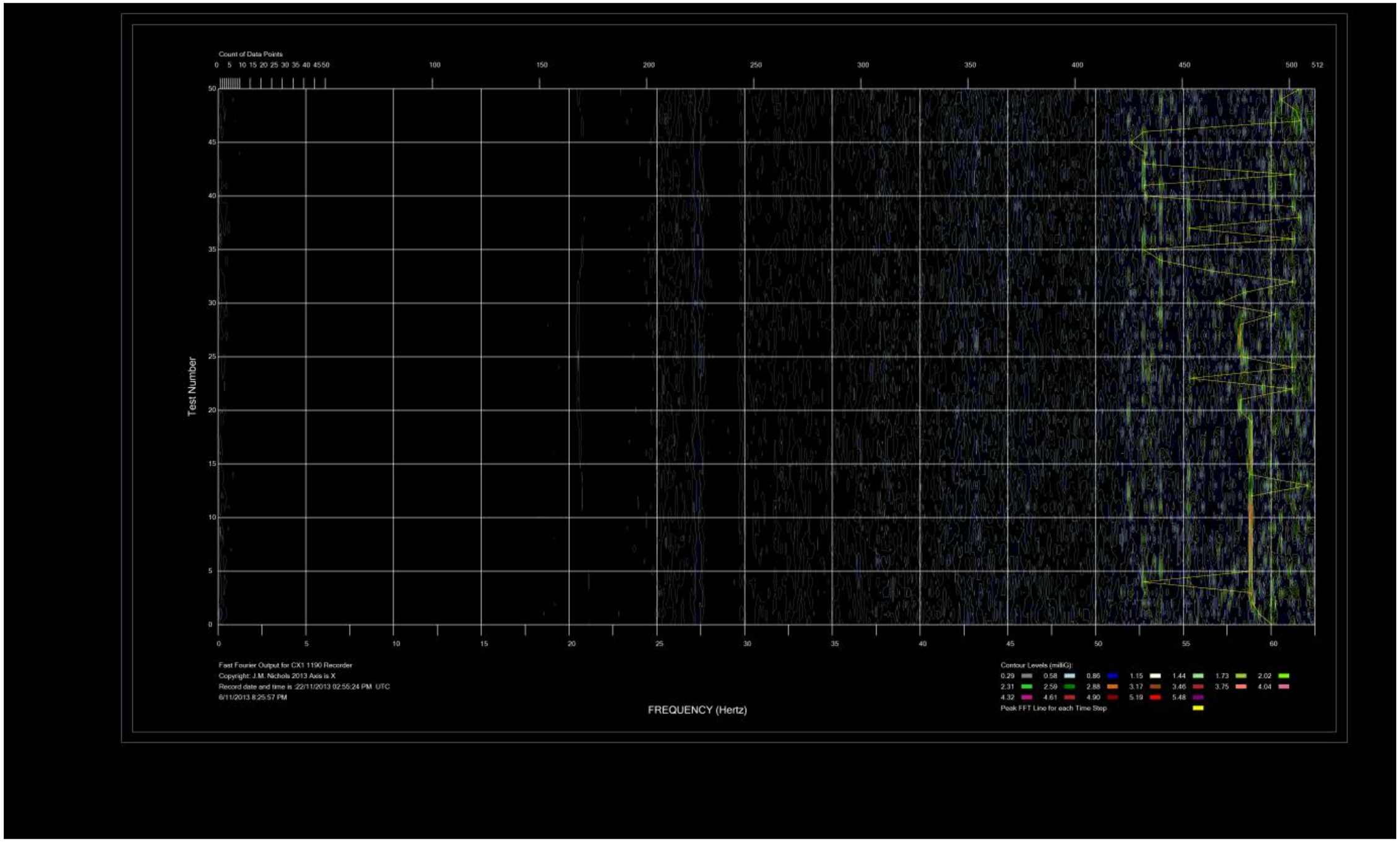

Figure 69 FFT Result 9 X Direction Ambient Study

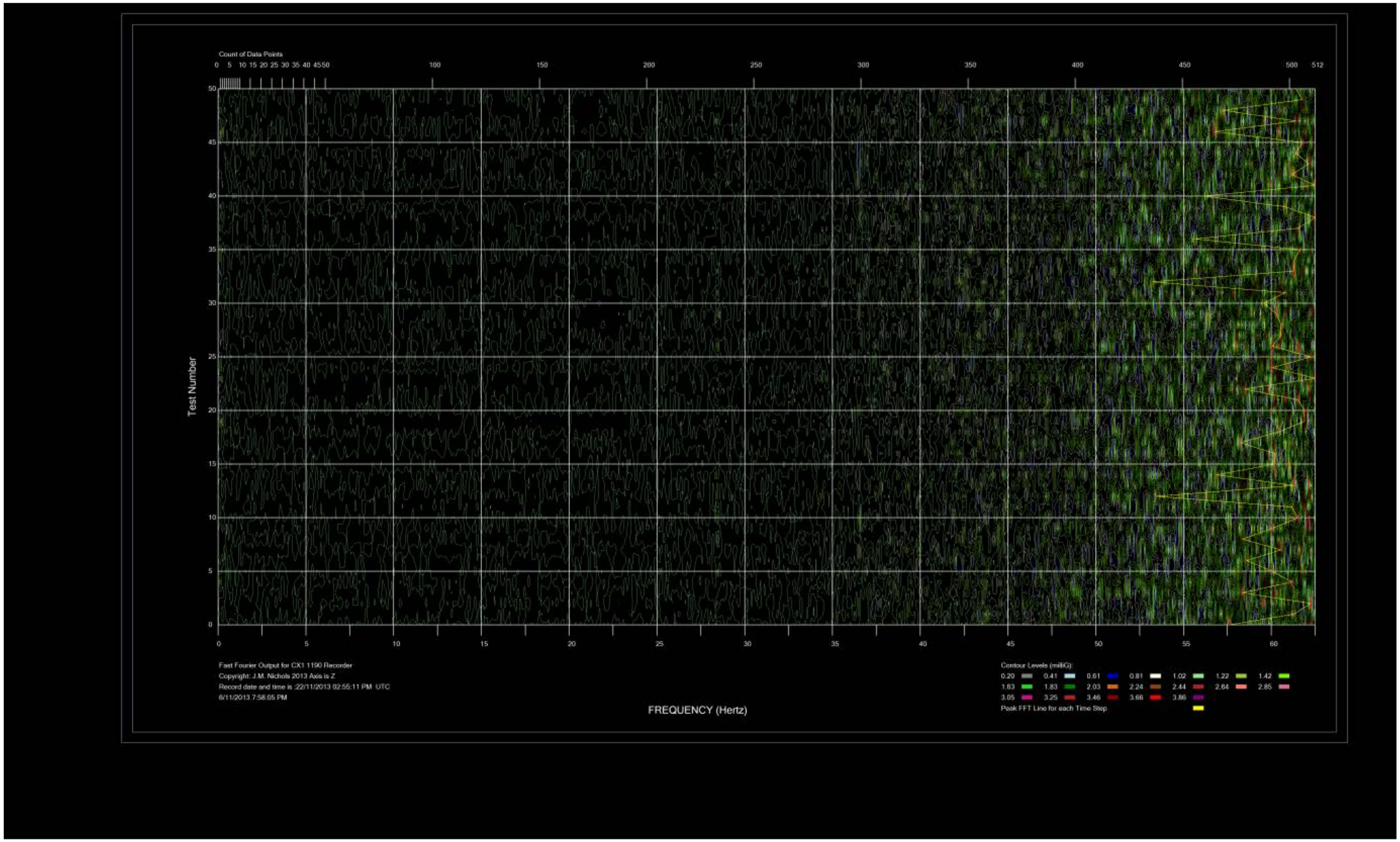

Figure 70 FFT Result 5 Z Direction Ambient Study

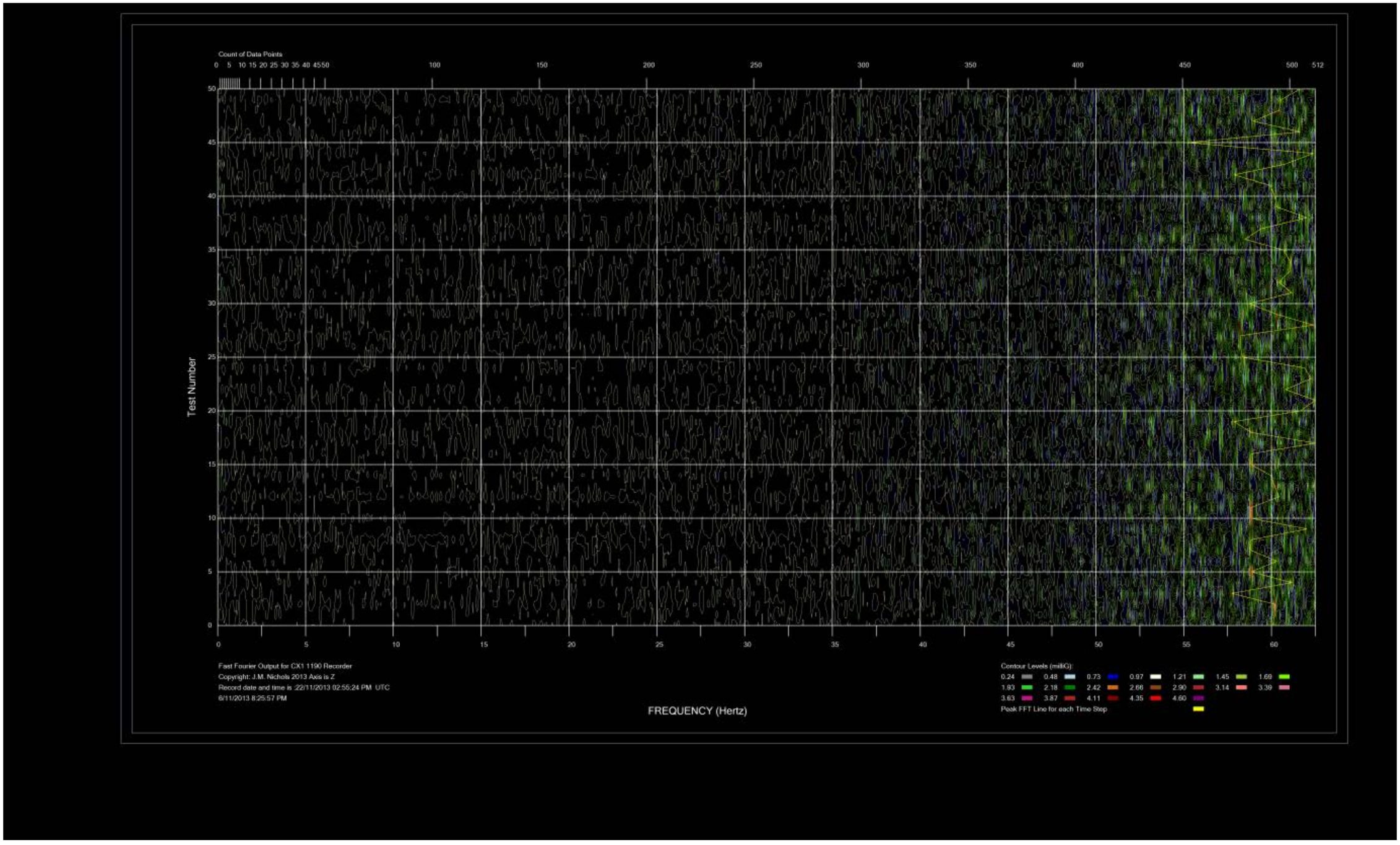

Figure 71 FFT Result 9 Z Direction Ambient Study

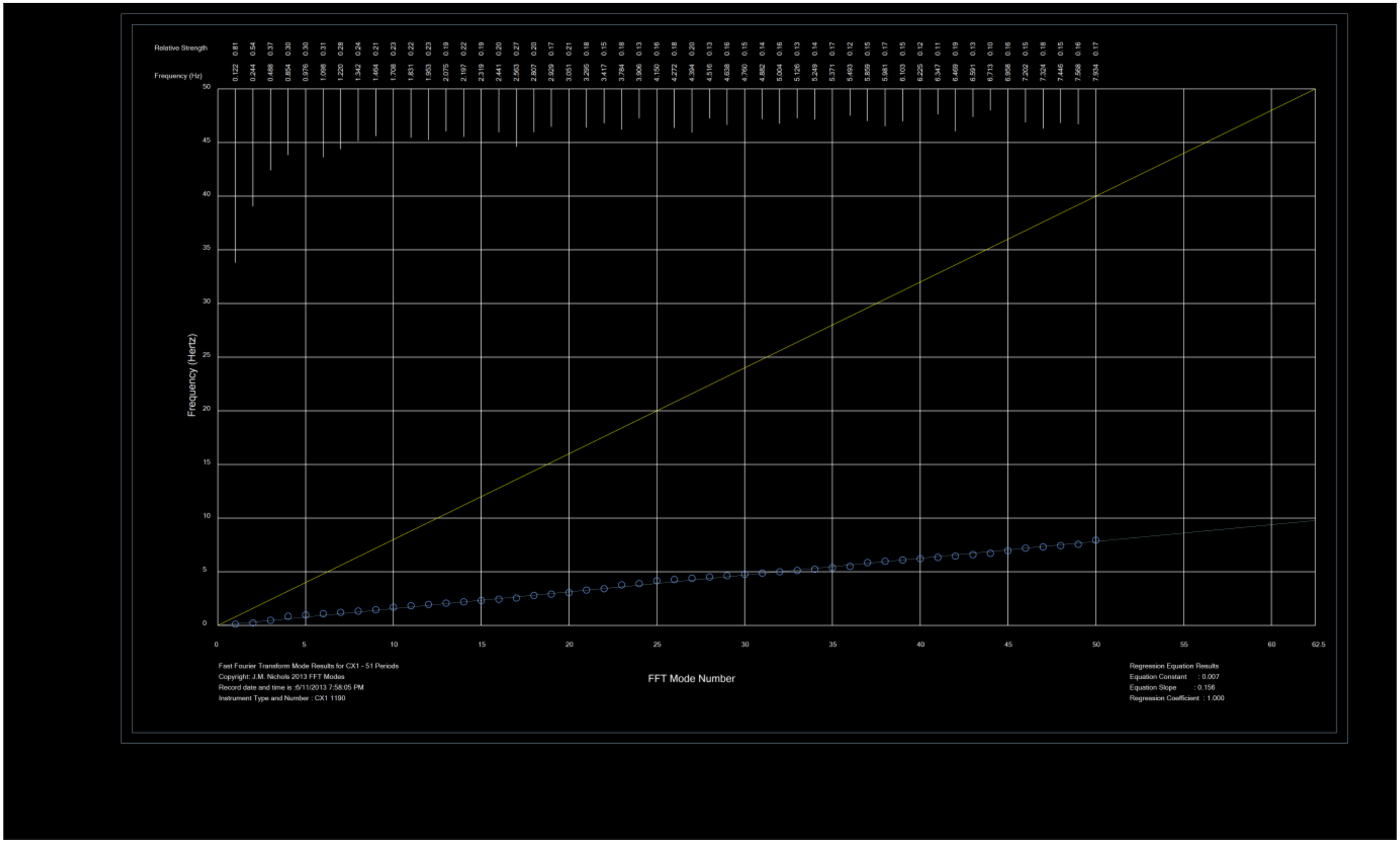

Figure 72 FFT Spectrum Modal Analysis for the 5th Data Set

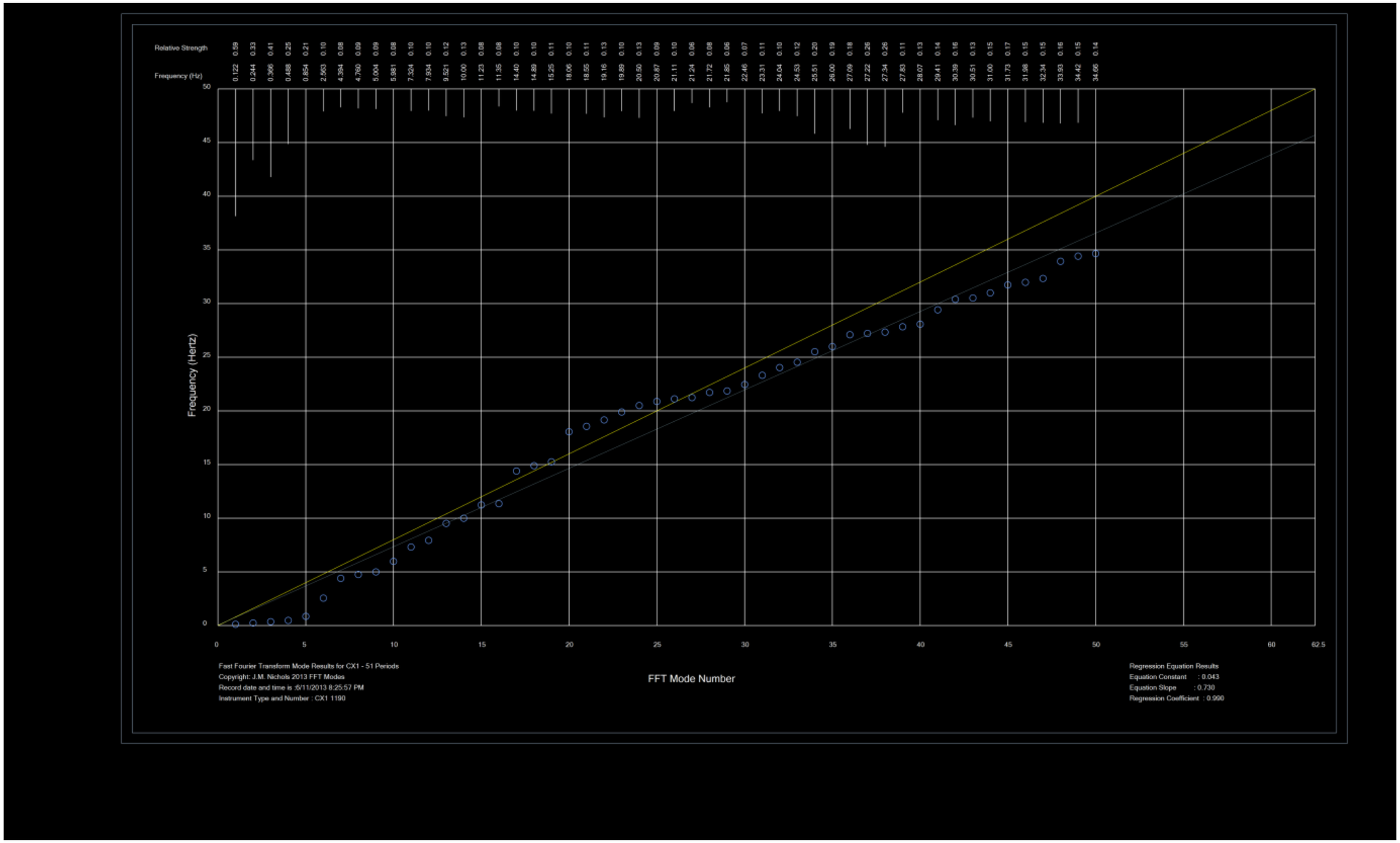

Figure 73 FFT Spectrum Modal Analysis for the 9th Data Set

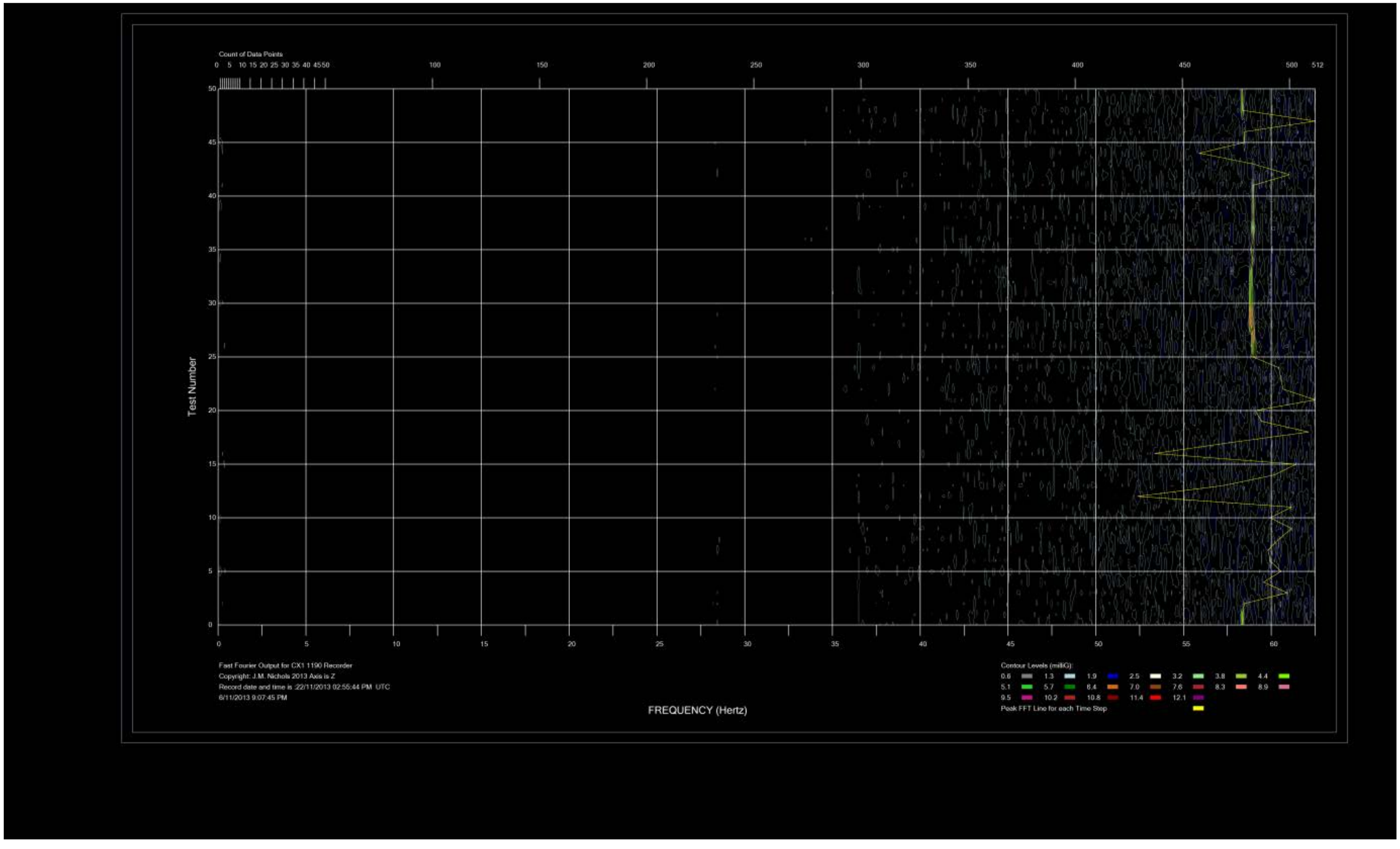

Figure 74 Contour Plan Signal at 12th Data Set - Peak Signal Z

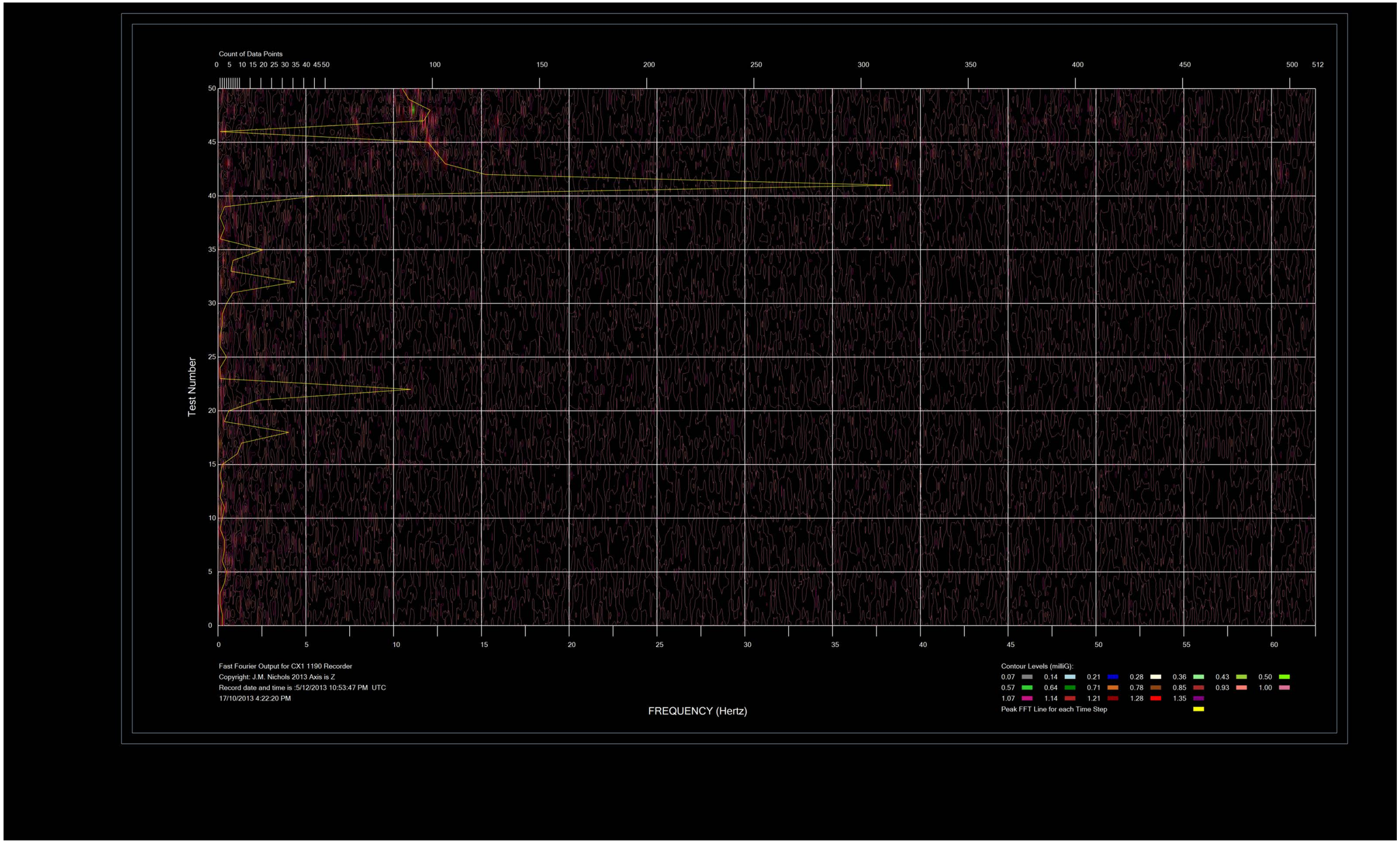

Figure 75 Day 1 CX1 1190 Train One onto Bridge Z Direction

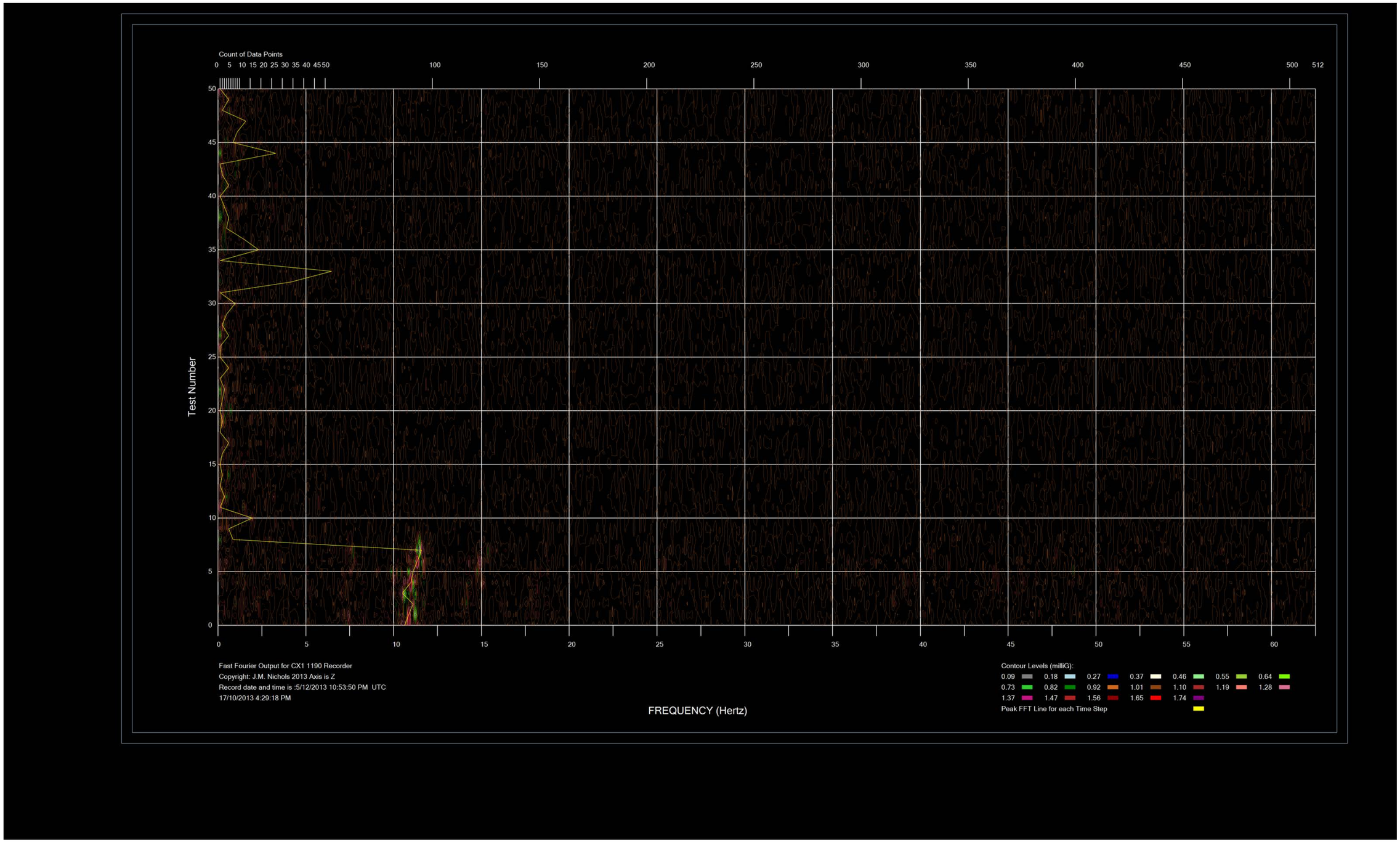

Figure 76 Day 2 CX1 1190 Train One Acceleration Contour Plan continued Z Direction

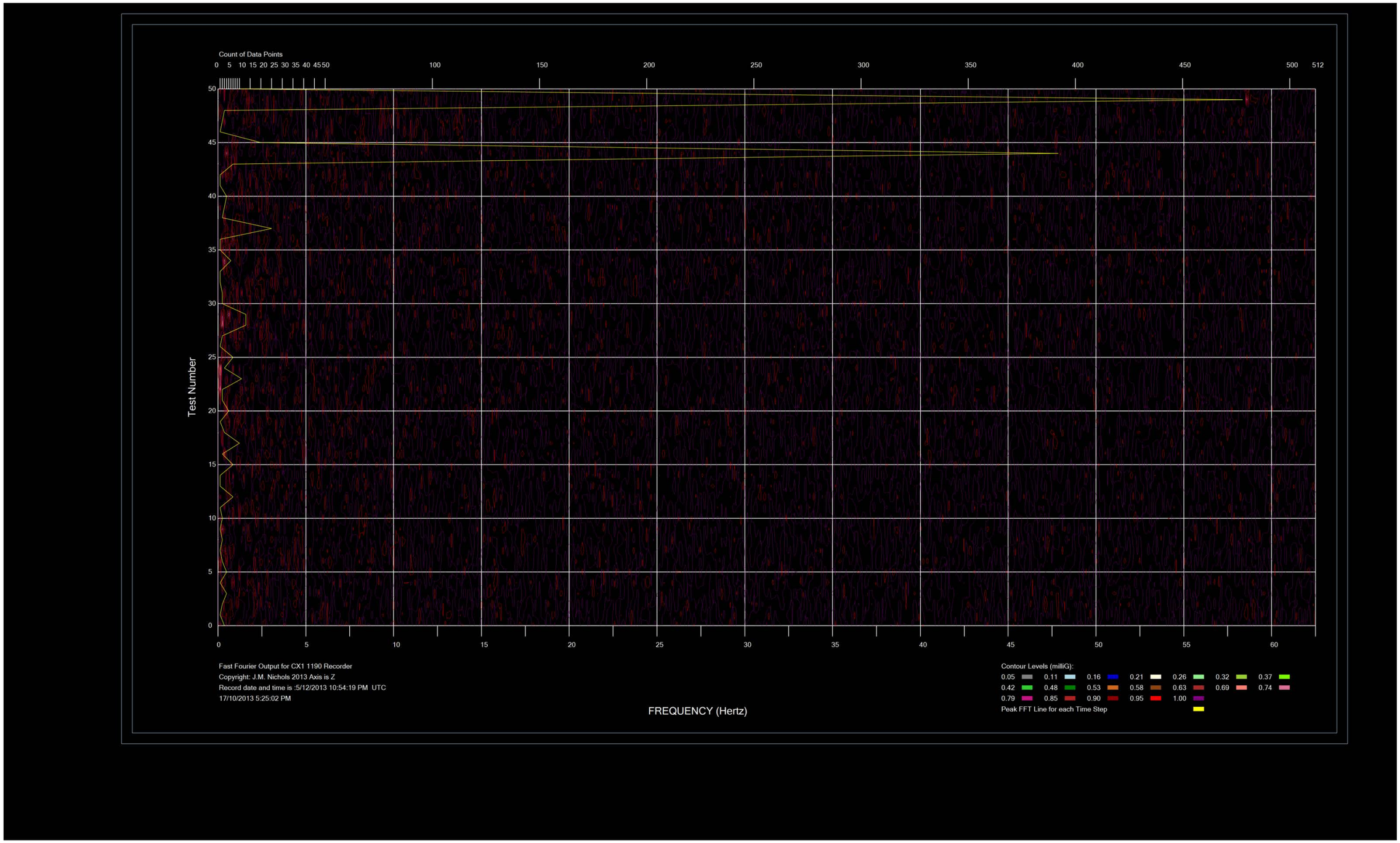

Figure 77 Day 1 CX1 1190 Train Two Z Direction

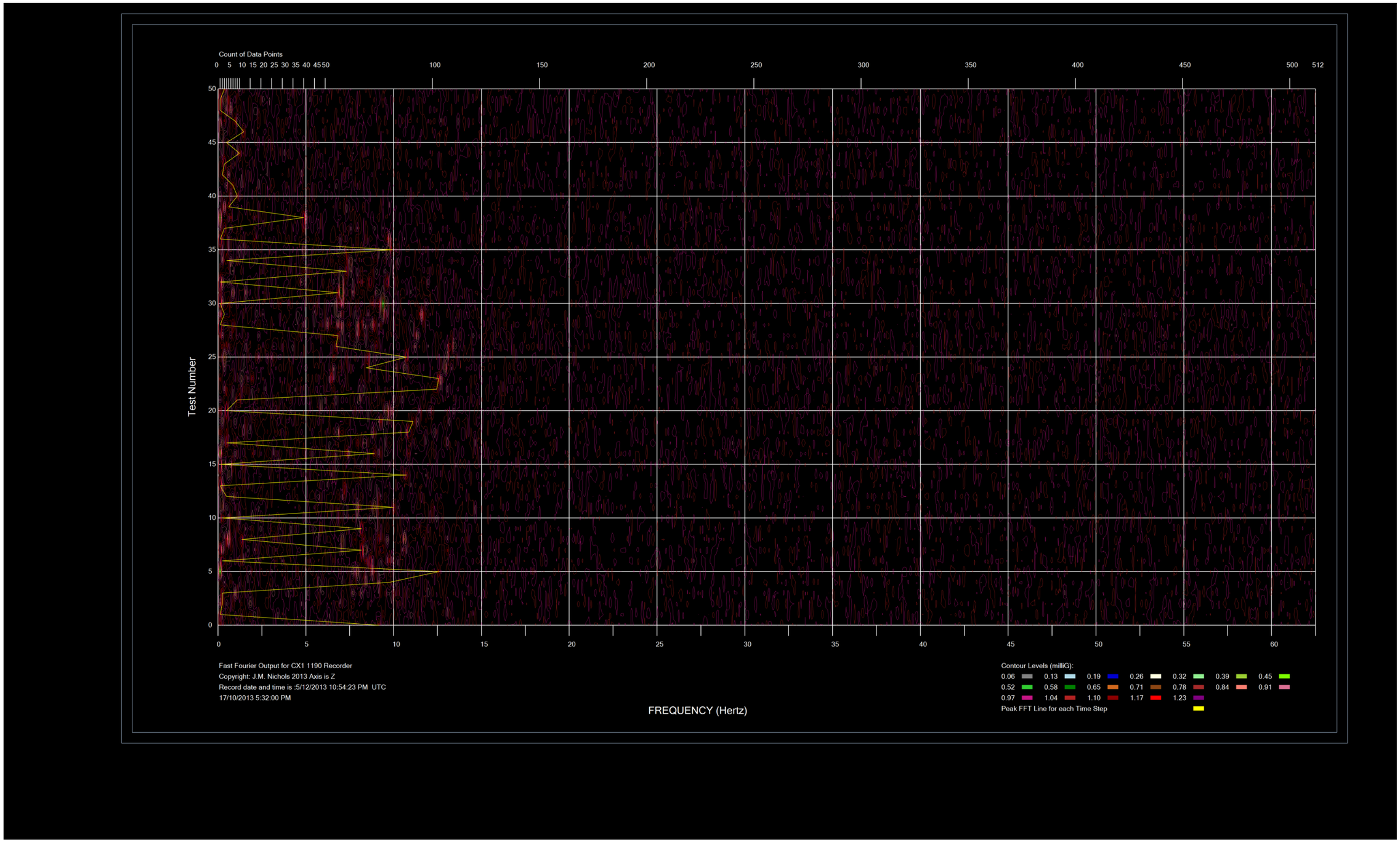

Figure 78 Day 1 CX1 1190 Train Two Continued Z Direction

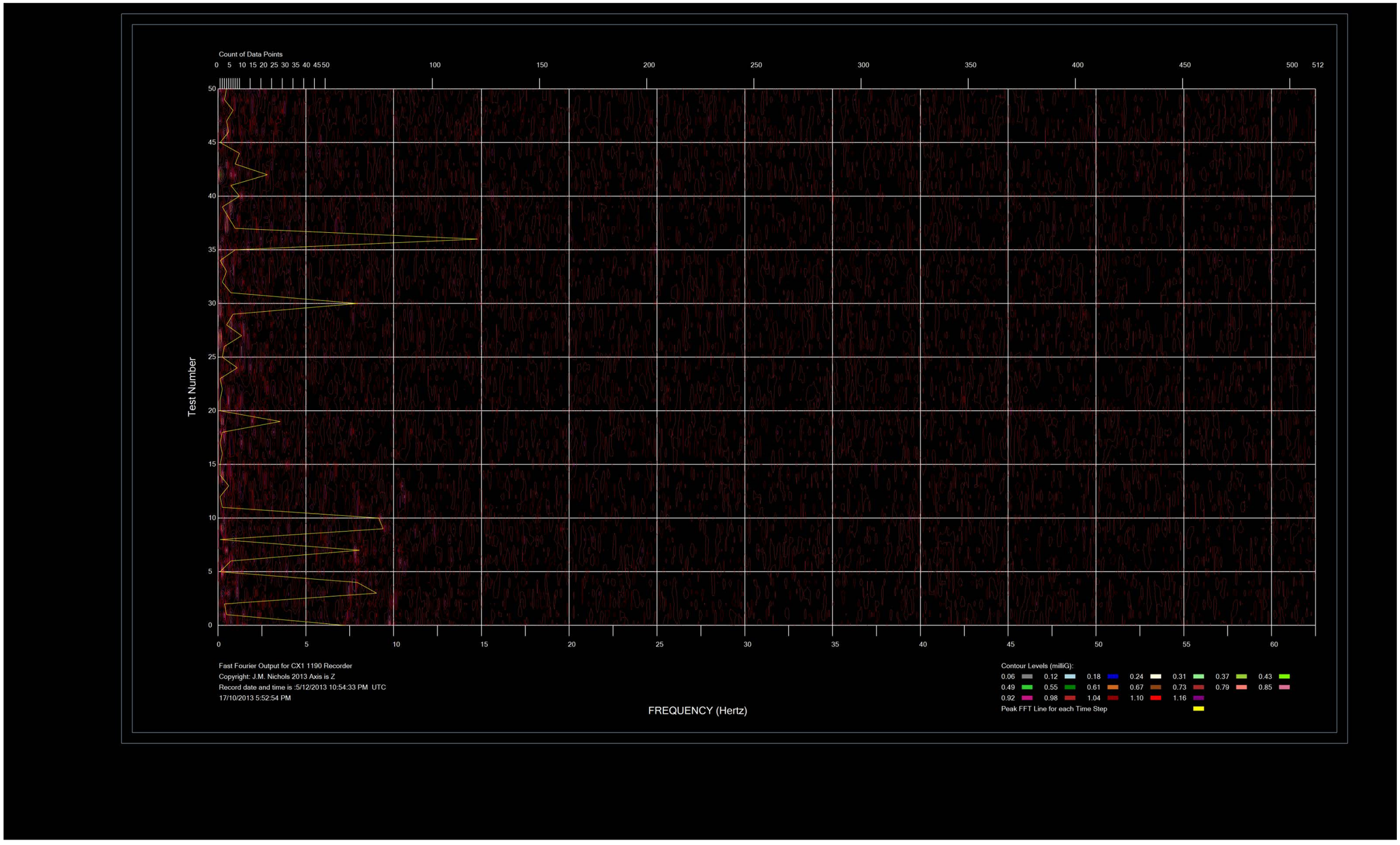

Figure 79 Day 1 CX1 1190 Train Three Z Direction

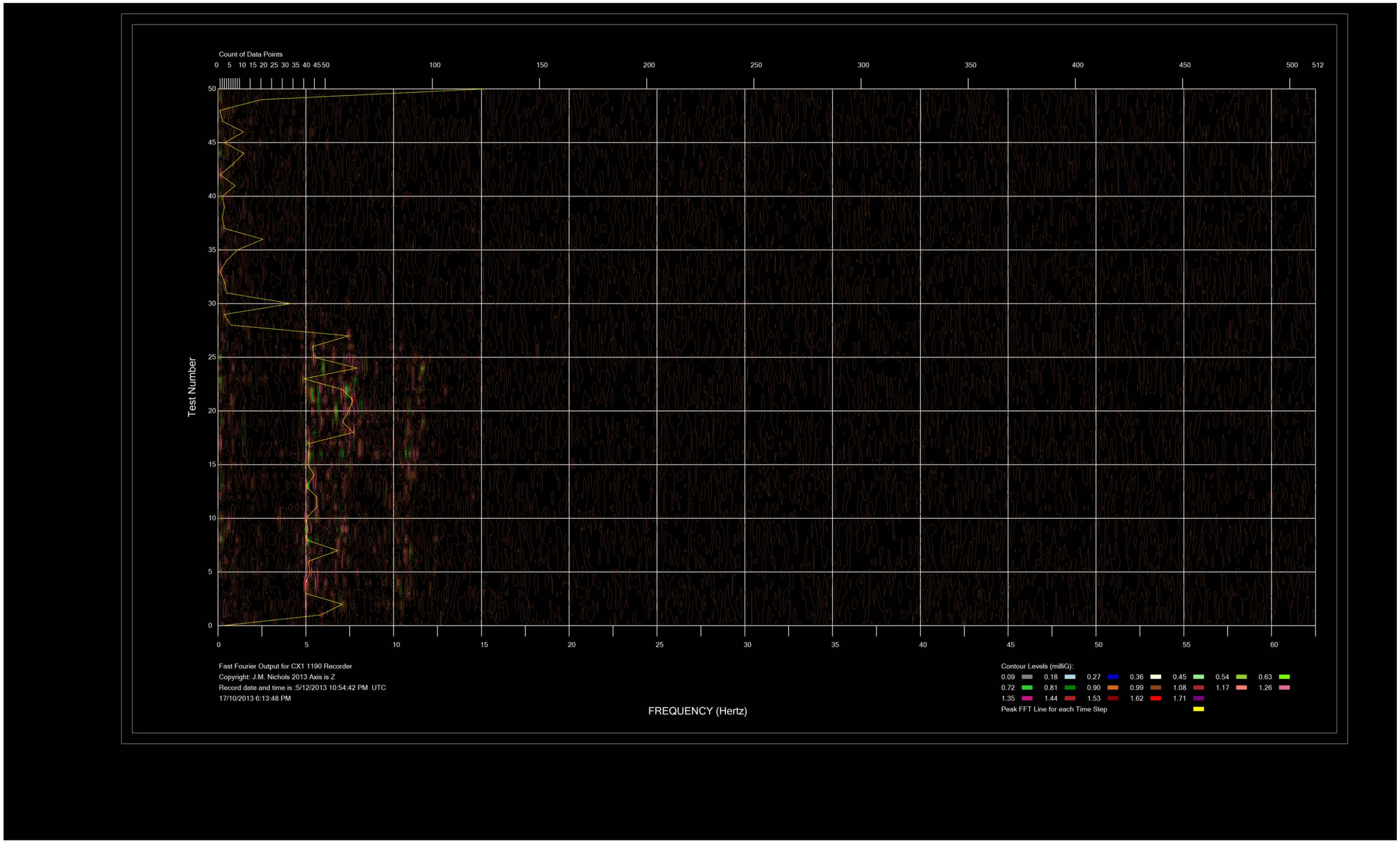

Figure 80 Day 1 CX1 1190 Train Four Z Direction

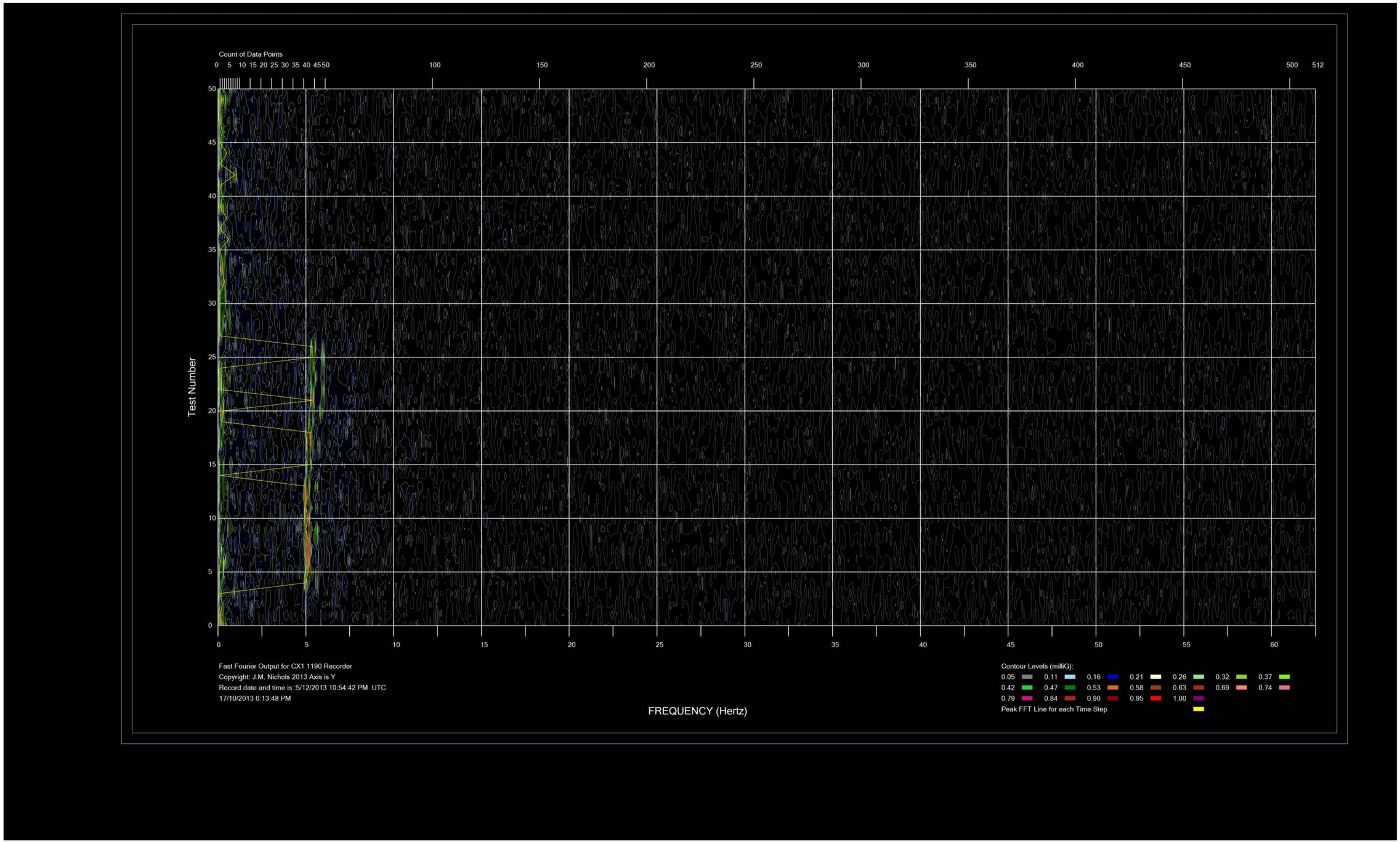

Figure 81 Day 1 CX1 1190 Train Four Y Direction

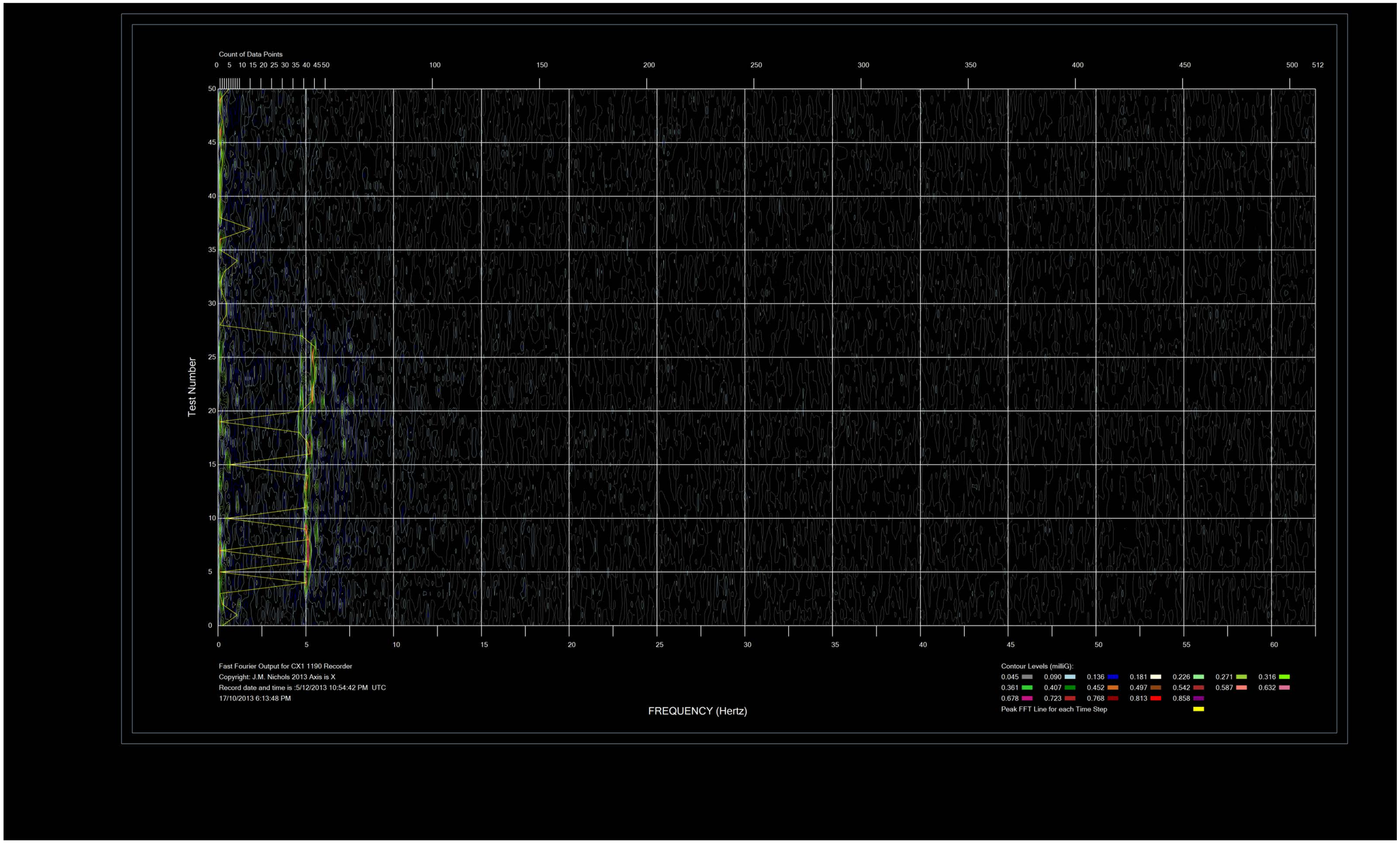

Figure 82 Day 1 CX1 1190 Train Four X Direction

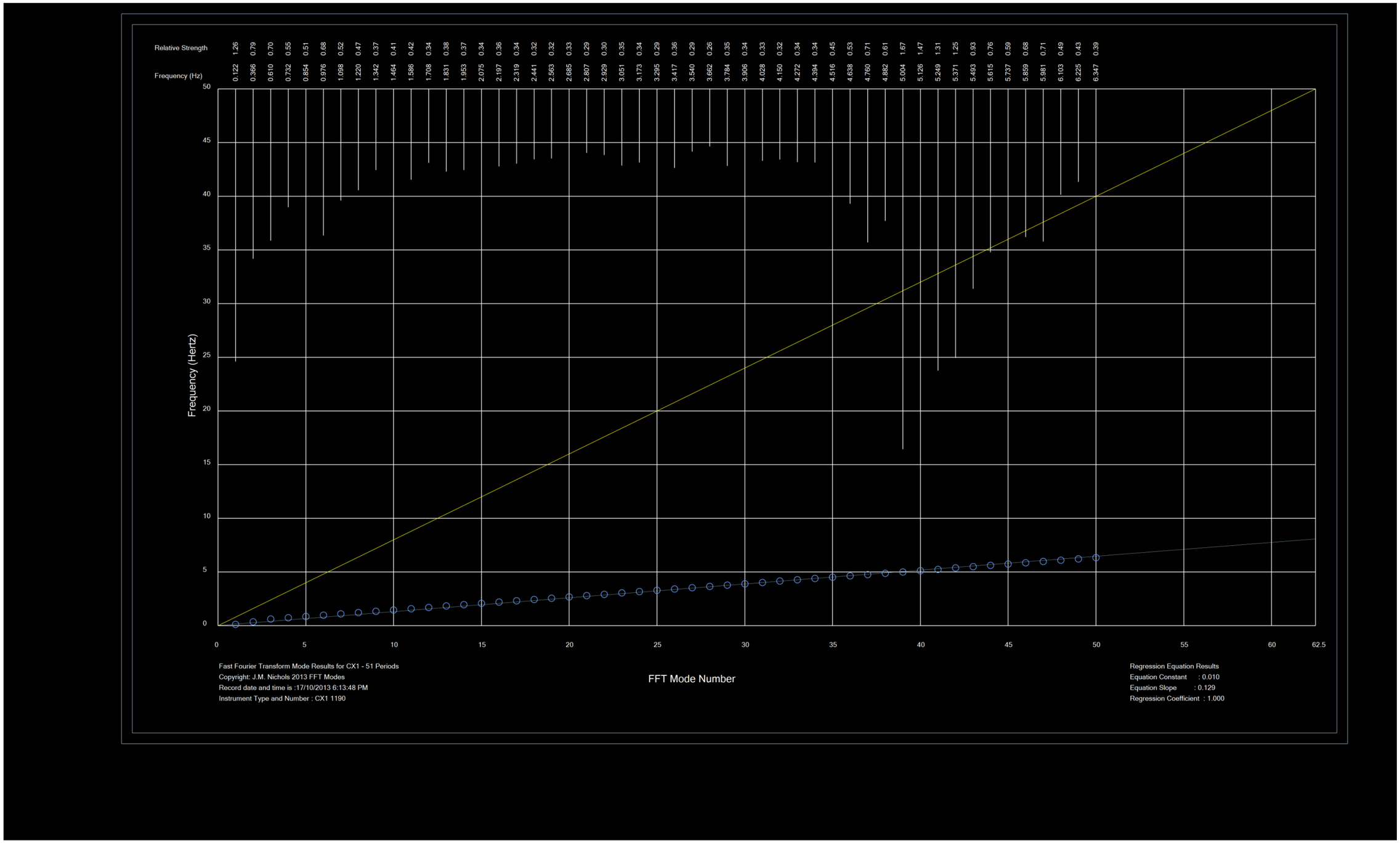

Figure 83 Day 1 CX1 1190 Train Four Spectrum Modal Data